

Envisioning the Mineral Demand *for Clean Energy Futures*



Abstract

As global energy systems undergo a rapid transformation, a decisive shift occurs from fossil-fuel intensive to one dependent on energy transition minerals (ETMs). This research expands the International Energy Agency's (IEA) Net Zero Energy Scenario from 2050 to 2075, encompassing an additional technological cycle. By comparing it to supply data from the United States Geological Survey, the study assesses how climate ambitions might affect the global ETM market, identify potential supply bottlenecks, evaluate reserve sufficiency, and examines the role of recycling in mitigating risks.

The findings indicate that while ETM supply can generally align with demand through effective resource management, efficient recycling, and substitution efforts, several ETMs require careful monitoring. Post-2050, following substantial capacity additions, it is expected that demand is mainly driven by stock turnover of clean energy technologies and demand from emerging industries, further stressing ETM supply chains. Co-mined ETMs, including those for thin-film photovoltaics, currently have limited refining capacity, necessitating upscaling to meet NZE projections. In the battery sector, the dominant chemistry will shape future ETM demand, with nickel- or manganese-intensive chemistries likely gaining traction due to ethical concerns over cobalt.

Infrastructure development is found to be highly copper-intensive, necessitating increased material efficiency and substitution efforts. Nickel, widely adopted in clean energy technologies, remains difficult to substitute. Material efficiency of wind and PV are expected to improve, while also providing a future source of secondary ETMs. While platinum-group metals are abundantly required in hydrogen technologies, it is found that with material efficiency improvements and effective utilization of outflow streams, supply bottlenecks can be mitigated. Policies incentives could further stimulate the use of less ETM-intensive technologies or encourage recycling.

Despite the IEA's lack of transparency in its assumptions and data limitations due to inconsistent regulatory standards, this research underlines the importance of enhancing recycling practices, particularly for ETMs with non-existent recycling infrastructure. Urban mining could yield greater returns than primary extraction, supporting the argument that while ETM availability should not hamper NZE targets, it must be accompanied with technological innovation, robust policies, and a focus on sustainability to ensure resource availability for current and future generations.

Contents

1. Introduction.....	1
1.1 Transitioning to a Sustainable Future: The surge of Energy Transition Minerals.....	1
1.2 Sustainable Resource Management	1
2. Methodology	3
2.1 Data Sources.....	4
2.1.1 Scenario Description	4
2.1.2 Demand.....	5
2.1.3 Supply.....	6
2.1.4 Co-mining.....	6
2.2 Extrapolation of energy trends.....	8
2.2.1 Energy Production and Capacity	8
2.2.2 Battery-Based Energy Storage (BESS)	8
2.2.3 Transport	8
2.2.4 Infrastructure	9
2.3 Dynamic Stock Flow Analysis (dMFA)	9
2.3.1 Lifetime Distribution	9
2.3.2 ETM Demand from added capacity	9
2.4 ETM Demand from Stock Replacement.....	11
2.5 End-of-Life	12
2.6 ARIMA.....	13
2.7 Supply-Demand Analysis	14
2.8 Sensitivity analysis	14
3. Technology Overview	15
3.1 PV.....	15
3.1.1 PV Production.....	15
3.1.2 Design of PV Systems.....	15
3.1.3. PV sub-technologies	15
3.2 Wind.....	16
3.2.1 Wind Electricity Production	16
3.2.2 Wind System Design.....	16
3.2.3 Wind Turbine Types.....	17
3.3 Hydrogen.....	18
3.3.1 H ₂ Production through electrolysis	18
3.3.2 Electrolyzer System Design	18
3.3.3 Electrolyzer types.....	18
3.3.4 Future Developments.....	19
3.4 Batteries.....	21
3.4.1. LIBs.....	21
3.4.2 Future Developments.....	22
3.5 Electric motors	24
3.6 Infrastructure.....	24

3.6.1 Future Developments	25
3.7 Refining of ETMs	26
4. Technology Development	27
4.1 Solar PV	27
4.2 Wind	28
4.3 H ₂ Production.....	29
4.4 BESS	30
4.5 Infrastructure.....	31
4.6 Transport.....	32
4.6.1 Light-Duty Vehicles	32
4.6.2 Heavy-duty vehicles	34
4.6.3 Two- and Three-wheelers	36
5. Supply-Demand Analysis.....	38
5.1 Cadmium.....	39
5.2 Gallium.....	40
5.3 Germanium	41
5.4 Indium	42
5.5 Tellurium & Selenium.....	43
5.6 Cobalt	45
5.7 Graphite.....	46
5.8 Lithium	47
5.9 Manganese.....	48
5.10 Nickel.....	50
5.11 Copper.....	52
5.12 PGMs.....	54
5.13 Rare Earth Elements.....	55
6. Sensitivity Analysis	56
7 Discussion.....	59
7.1 Demand comparison	59
7.2 Supply comparison.....	61
7.3 EoL	62
8. Conclusion.....	63
9. Recommendations.....	64
9.1 Policy recommendations.....	64
9.2 Further research.....	64
10. References.....	66

Supplementary Document

S.1 Compound Annual Growth Rate

S.3 Survival Functions

S.4 ARIMA Model

Defining ARIMA Parameters

Model output

S.5 Market shares for technologies

S.6 Recycling Scenarios

S.7 ETM demand for selected years

S.8 Supply Demand Analysis

Nomenclature

AEM – Anion Exchange Membrane
a-Si – Amorphous Silicon
ARIMA – Autoregressive Integrated Moving Average
ASSB – All-Solid-State Batteries
BESS – Battery Energy Storage Systems
CdTe – Cadmium-Tellurium
CISGS – Indium Gallium-Diselenide
CRMs – Critical Raw Materials
DD – Direct Drive
DFIG – Doubly-Fed Induction Generator
D_x – Distribution infrastructure
EESG – Electrically Excited Synchronous Generator
ETMS – Energy Transition Minerals
EV – Electric vehicles
FC – Fuel Cell
FCVs – Fuel Cell Vehicles
GaAs – Gallium Arsenide
GB – Gearbox
HDEV – Heavy Duty Electric Vehicle
HPMSM – High-purity Manganese Sulfate Monohydrate
HTS – High temperature superconductors
IEA – International Energy Agency
IPCC – International Panel on Climate Change
LDEV – Light Duty Electric Vehicle
LFP – Lithium iron phosphate
LIBs – Lithium-ion batteries
Li-S – Lithium Sulphur
LTES – Long term energy scenarios
MI – Material Intensity
NMC – Nickel Manganese Cobalt
NZE – Net Zero Energy Scenario
PEM – Proton Exchange Membrane
PGMs – Platinum-group metals
PMSM – Permanent Magnet Motor
PSMG – Permanent Magnet Synchronous Generator
PV – Photovoltaic
REEs – Rare Earth Elements
SCIG – Squirrel Cage Induction Generator
SOE – Solid Oxide Electrolyzer
T_x – Transmission infrastructure
STEPS – Stated Policies Scenario
VFRB – Vanadium Flow Redox Battery

1. Introduction

1.1 Transitioning to a Sustainable Future: The surge of Energy Transition Minerals

As global energy systems undergo a rapid transformation, the demand for energy transition minerals (ETMs) is experiencing an unparalleled surge, signaling a decisive shift from fossil fuel dependence to reliance on CRMs. ETMs, particularly those classified as critical raw materials (CRMs), are essential to renewable energy systems but are characterized by considerable supply risks, economic importance and strategic value (European Commission, 2023). As the backbone in the global energy transition, it raises crucial questions about the sustainability of resource availability for future generations, especially given the complex geopolitical, economic, and environmental considerations surrounding extraction and supply. Table 1 provides an overview of various ETMs used in clean energy technologies.

In this context, the International Energy Agency's (IEA) landmark report, drawing on the methodologies of the Intergovernmental Panel on Climate Change (IPCC), outlines pathways to limit global warming. The IEA's Net-Zero by 2050 (NZE) scenario, the most ambitious pathway, proposes a strategy to limit warming to 1.5°C, envisioning widespread adoption of clean energy technologies, prioritization of energy efficiency, and safeguarding energy security (IEA, 2023a). The cornerstone of this scenario is electrification, which is expected to account for 53% of total final energy consumption by 2050. This shift will drive significant increases in renewable energy sources, with wind and photovoltaic (PV) systems to have growth rates of 26% and 16% by 2030. Electric vehicles (EVs) are projected to make up 95% of market sales by 2050 (IEA, 2023a). Nonetheless, these technologies necessitate extensive infrastructure and energy storage solutions, further escalating the demand for ETMs.

The market conditions for ETMs are diverse. While some minerals have seen price stability due to market equilibrium, others face challenges beyond price fluctuations, such as geological complexity and increasingly difficult-to-mine deposits that require advanced technologies and significant investments. Moreover, the development of new mining projects often takes an average of 15.7 years from discovery to operation, creating a significant lag between market signals and increased supply (S&P Global, 2023a). Geopolitical tensions and trade restrictions further complicate ETM accessibility, underscoring the need for a comprehensive approach to ETM production and supply chain management that balances innovation, strategic investments, and international cooperation (IEA, 2024a).

ETMs are either mined directly from the Earth or extracted from parent ores and then refined to meet industrial demands. Understanding the global distribution of these minerals are distributed across our earth, for understanding potential geological scarcity and developing effective resource policies. The concept of reserves – defined as the economically extractable fraction of a mineral under current market conditions – plays a key role in this analysis. Entities such as the United States Geological Survey (USGS) monitor these deposits to forecast future supply constraints, which are essential for maintaining a resilient supply chain (USGS, n.d.). Disruptions in mining operations can trigger ETM shortages, leading to significant discrepancies in global supply chains (Castillo-Villagra & Thoben, 2022). As global efforts to decarbonize intensify, the effective management of these reserves becomes increasingly vital to ensure long-term resource availability.

1.2 Sustainable Resource Management

Sustainable resource management is a prerequisite for intergenerational resource availability – meeting the needs of a world population of ten billion for two hundred years, while keeping service levels on par with those in developed countries in 2022, at an affordable price (Henckens & Worrell, 2020). Despite extensive research for material requirements under various climate scenarios (Watari et al., 2019; Watari et al., 2019; Liang et al., 2023), there remains a lack of focus on ensuring intergenerational resource availability.

Furthermore, these studies tend to offer a limited analysis on the demand-supply dynamics, particularly how efficient EoL practices could reduce primary demand and mitigate future supply bottlenecks. Lastly, these material requirements studies often focus on specific technologies, such as mobility or electricity generation, rather than a comprehensive examination of the whole future energy system, while also keeping track of ETM demand outside the energy sector.

This research aims to determine the specific ETMs and quantities necessary to effectively implement the global energy transition envisioned under the NZE scenario, while assessing the implications of this demand for future supply. The study will analyze the complex dynamics of global ETM supply chains, consider the impact of technological advancements and substitution options, and evaluate whether the anticipated surge in demand, alongside with demand from other sectors, can be met by future supply, ensuring these critical resources are available for future generations. By focusing on the year 2075, the research narrows its scope while extending beyond typical projections to encompass an additional technological cycle, offering insights into how this cycle could be leveraged to effectively reduce ETM demand under climate scenarios.

This research aims to enhance the scientific understanding of ETM supply chains and provide insights that could shape long-term policy decisions. As it might be overambitious to estimate ETM demand and supply over a period of two hundred years, this study narrows its focus to the year 2075. Long-term energy scenarios (LTES) are instrumental for governments in designing informed strategies and selecting proper energy technologies (Gielen, 2019). Nonetheless, there is a particular need for a deeper exploration of the supply side, which has often been overlooked. By extending the analysis further into the future, this study will encompass an additional technological cycle, offering a unique opportunity to examine how this cycle could be utilized to effectively reduce ETM demand.

The study will differentiate between the Stated Policies Scenario (STEPS) and the ambitious NZE scenario, examining a range of potential outcomes and their implications for sustainable resource management. These scenarios were chosen for their broad international acceptance and because they represent different paces of transition towards electrification. The STEPS scenario, which considers only existing policies, serves as a baseline for comparison. The NZE scenario, on the other hand, outlines a pathway to achieving net-zero emissions by mid-century, highlighting an accelerated and ambitious transition. By examining these scenarios, the study aims to provide a comprehensive understanding of the future of ETM demand and supply and how sustainable resource management practices can be optimized in different contexts (IEA, 2023a).

Table 1: Selected ETMs for the investigated technologies based on IEA data (2024). Thin-film PV ETMs involve cadmium, gallium, germanium, indium, selenium and tellurium.

	PV	BESS	EVs/FCVs	Wind	Electrolyzers	Infrastructure
Thin-film PV ETMs	<input checked="" type="checkbox"/>					
Silicon	<input checked="" type="checkbox"/>					
Lithium		<input checked="" type="checkbox"/>	<input checked="" type="checkbox"/>			
Cobalt		<input checked="" type="checkbox"/>	<input checked="" type="checkbox"/>			
Manganese		<input checked="" type="checkbox"/>	<input checked="" type="checkbox"/>	<input checked="" type="checkbox"/>		
Graphite		<input checked="" type="checkbox"/>	<input checked="" type="checkbox"/>			
Nickel		<input checked="" type="checkbox"/>	<input checked="" type="checkbox"/>	<input checked="" type="checkbox"/>	<input checked="" type="checkbox"/>	
Aluminum	<input checked="" type="checkbox"/>	<input checked="" type="checkbox"/>	<input checked="" type="checkbox"/>	<input checked="" type="checkbox"/>		<input checked="" type="checkbox"/>
Copper	<input checked="" type="checkbox"/>	<input checked="" type="checkbox"/>	<input checked="" type="checkbox"/>	<input checked="" type="checkbox"/>		<input checked="" type="checkbox"/>
Platinum-Group Metals			<input checked="" type="checkbox"/>		<input checked="" type="checkbox"/>	
Rare Earth Elements			<input checked="" type="checkbox"/>	<input checked="" type="checkbox"/>	<input checked="" type="checkbox"/>	

2. Methodology

Figure 1 provides an overview of the methodology applied in this research. Initially, the data sources and the foundation of this research, the NZE scenario, will be explained. Following this, the handling of supply data will be detailed. The assumptions and techniques used in the NZE extrapolation will then be discussed. Subsequently, the mathematical framework for determining material demand along the investigated ETM, along with the chosen parameters, will be provided, including the quantification of reserves. Next, stock calculations, which were used to define the outflow, will be examined. The ARIMA model and supply extrapolation will also be analyzed. Subsequently, the EoL calculations will be presented. With all this information, the supply-demand analysis will be explained. Finally, the methodology for the sensitivity analysis of the to be determined parameters will be delineated. The calculations were done in both an excel and a python environment.

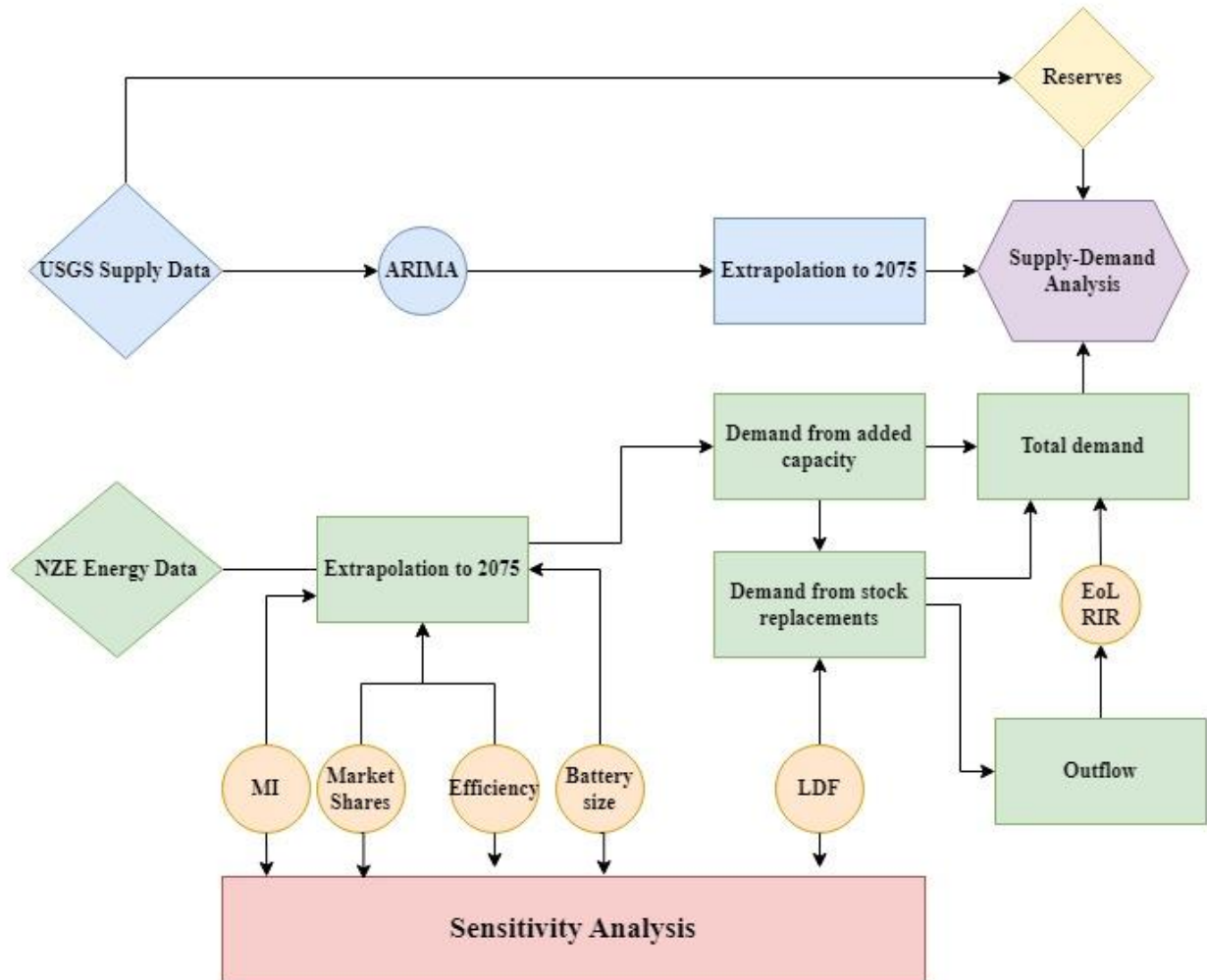


Figure 1: Flow Diagram for Methodology

2.1 Data Sources

2.1.1 Scenario Description

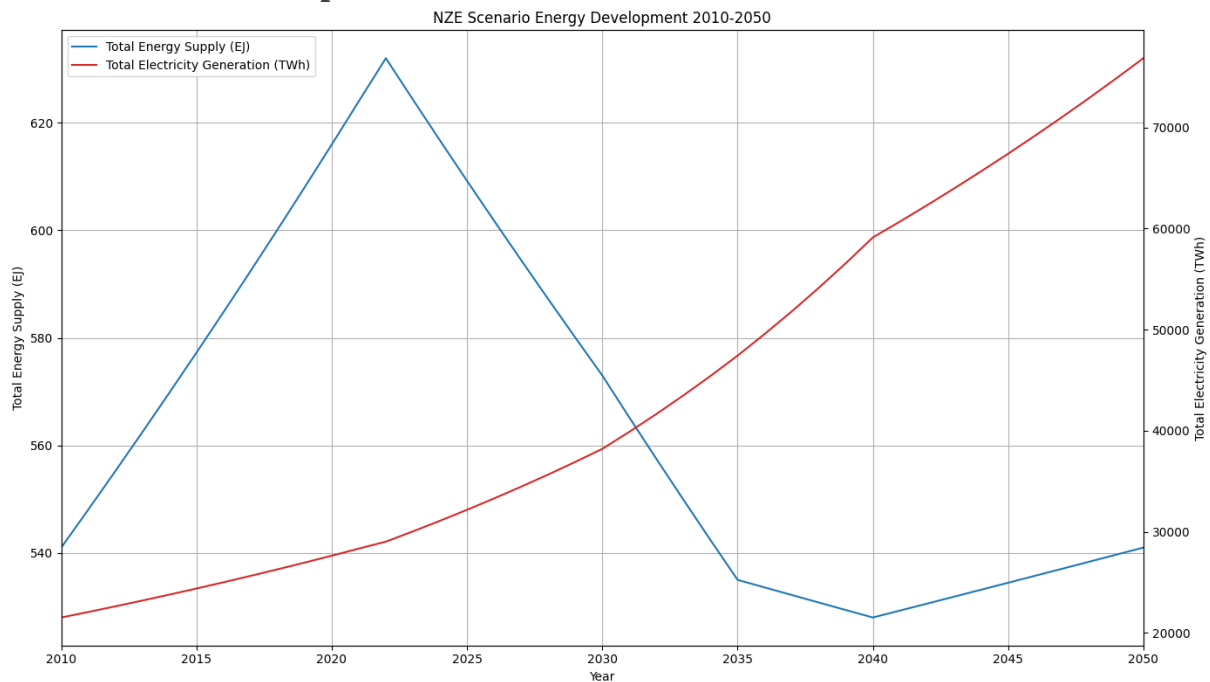


Figure 2: NZE Energy Supply Trajectories, based on IEA (2023a).

This study will differentiate between the STEPS and the NZE scenario, analyzing an array of potential outcomes and their implications for sustainable resource management. These scenarios were chosen due to their broad international acceptance and because they represent different paces of transition towards electrification.

The STEPS, which only considers specific policies that have been put into place, serves as a baseline for comparison purposes (IEA, 2023a). It provides a conservative benchmark based on a detailed analysis of the current policy landscape, reflecting the current trajectory of energy system development without ensuring that climate targets will be achieved. Thus, it does not aim for a particular outcome but reflects the current state of play.

In contrast, the NZE scenario outlines a pathway to achieving global net zero emissions by 2050, limiting global warming to 1.5°C. The NZE emphasizes the rapid deployment of clean energy technologies and energy efficiency improvements. It underscores the necessity of global collaboration to drive down clean technology costs, scale up diverse and resilient global supply chains CRMs and technologies, and ensure energy equity for emerging markets and developing economies (IEA, 2023a).

Figure 2 provides the current downward trend in energy supply. This trend is primarily driven by the increasing adoption of electrification and energy efficiency improvements. Less primary energy is required when using electricity due to fewer conversion losses compared to conventional energy carriers such as fossil fuels. This trend is expected to continue until 2040, after which only a minor increase is observed, associated with electrifying more complex sectors, such as heavy industry.

Conversely, the development of electricity is on a continuous upward trend, with a projected increase of 357% compared to the 2010 levels. This significant growth implies a substantial demand for ETMs.

In this research, the NZE was utilized to provide a comprehensive LTES analysis of ETM demand. The IEA offers a variety of energy data across various technologies, PV systems, wind energy, H₂ demand, battery energy storage systems (BESS), and infrastructure spanning the period from 2022 to 2050. The energy data obtained from the NZE dataset was employed in material intensity (MI) calculations to provide a detailed understanding of the potential impacts and requirements of a rapid transition towards clean energy technologies. This scenario outlines a pathway to limit global temperature increase to 1.5°C, emphasizing rapid deployment and development of clean energy technologies.

STEPS has been used as a conservative benchmark. This scenario is based on a detailed analysis of the current policy landscape and provides a sense of the current trajectory of energy system development without ensuring that climate targets will be achieved. Thus, it does not aim for a particular outcome but reflects the current state of play. This scenario serves a comparative function in this research, offering a contrast to the ambitious NZE and will be addressed in the discussion.

2.1.2 Demand

This research aligns closely with IEA documentation, analyzing various flagship reports such as the Critical Mineral Market Review (2024a), EV Outlook (2024b), NZE electricity grid outlook (2023b) and NZE energy outlook (2023c). Deployment rates and EV stock approximations are primarily extracted from these sources. When specific deployment rates were unavailable, the Critical Mineral Explorer database was consulted. For instance, a near-zero demands for cobalt by 2050 indicates a low cobalt intensive share in the battery chemistry mix. Another example is the high demand for gallium for PV, which indicates a high share of thin-film PV installations in the future. The data explorer was used to compare and confirm the findings. As IEA did not provide mineral intensities (except for electrolyzer material intensities) complementary literature was referred to, which will be addressed in 3. Technology Overview.

Additional parameters like battery size, and energy and material efficiency improvements were collected similarly. Battery and fuel cell lifetimes for EVs are assumed to match the vehicle lifetime, and a 3-hour load duration was assumed for BESS applications, as it was found to approximate the battery grid analyses by the IEA. Recycling rates were sourced from UNEP (2011) and will be elaborated further. Finally, to further extend the array of outcomes, multiple scenarios were formulated with varying market shares for sub-technologies, found in S.5 Market shares for technologies.

IEA suggests that for EVs, the dominant battery chemistry will be NMC₈₁₁, while there is increased attention for lithium-iron-phosphate (LFP) batteries. Therefore, both an LFP and NMC_x scenario were adopted in this research. For BESS, IEA claims that vanadium-flow batteries (VRFBs) and LFP will become the dominant battery chemistries. Two scenarios were adopted in which there was differentiated between an LFP-dominant market and a vanadium-flow dominant market. This will be further be extended in the sensitivity analysis for the other technologies. While the IEA provided data on some material demand outside clean energy technologies, this was incomplete. Therefore, other ETMs were obtained from an extensive literature review by Watari et al. (2020), which collected numerous studies focusing on future ETM demand in and outside clean energy technologies.

2.1.3 Supply

The USGS plays a crucial role in providing comprehensive data on natural resources, which is essential for sustainable development and efficient mining practices of ETMs. The USGS Mineral Resources Program offers valuable information on ore formation, mineral potential, and environmental impacts, which is pivotal for analyzing reserves, mine production, and mineral refining (USGS, 2024).

This study will utilize USGS data collected from 1975 to 2023 for various commodities to extrapolate future trends, based on the historical dataset (USGS, n.d.). Resources, in this context, refer to naturally occurring materials that are economically feasible for extraction, including both current and potential future deposits. Due to the highly aggregated nature of USGS commodity mining data, some assumptions are necessary. For simplicity, it is assumed that indicated reserves can be economically extracted in the investigated timespan.

2.1.4 Co-mining

For certain ETMs, such as PGMs and REEs, the USGS only provides total supply values or refining data. It's important to note that demand growth rates for individual commodities may significantly exceed the total growth rate. Achieving a supply-demand equilibrium would require increased production of specific elements, which is often challenging due to co-mining constraints.

Co-mining, where materials are extracted as by-products and then separated through chemical processing, limits the supply of these ETMs to the number of ore extracted and the concentration of the desired mineral. Therefore, it is impossible to increase production capacity for each separate ETM without increasing production of another (Alonso et al., 2012).

Table 2 provides the analyzed co-mined ETMs, found in thin-film PV applications. For REEs, which are extracted and refined in China, reserve estimates are not provided, due to China's non-compliance with international reporting requirements. To estimate REE reserve quantities, a reserve-resource ratio based on Carrara et al. (2023) was defined:

$$Reserves_i = \frac{Reserves}{Resources} * Resources_i \quad (1)$$

REE reserves are typically reported in oxide form, necessitating a conversion factor to metal form, as provided in S.2 Rare Earth Elements abundance and conversion factor. For PGMs, aggregate production numbers for palladium and platinum are provided. While some deposits involve co-mining of PGMs, the world's largest PGM deposit in South Africa does not follow this pattern (Mudd et al., 2018). For a full overview of the reserves, consult Table 3.

Table 2: Co-mined ETMs and their parent ores (USGS, n.d.)

ETM	Parent Ore
Cadmium	Zinc
Germanium	
Indium	
Tellurium, Selenium	Copper
Gallium	Bauxite (Aluminium), Zinc

Table 3: Global Reserves for investigated ETMs, based on literature and USGS data. The reserves for the specific REEs will be presented in the result section.

Commodity	Reserves 2024 (Kt)	Source / Comments
Aluminum (Bauxite)	30000000	USGS (2024)
Copper	1000000	
Lithium	28000	
Cobalt	11000	
Natural Graphite	280000	
Nickel	130000	
Gallium	11100	
Germanium	119	Patel & Karamaldis, 2021
Indium	312	van Allen, 2024
Cadmium	66	Based on 0.3% content in zinc deposits, USGS (2024)
Manganese	680	USGS
Silicon	NA	USGS claims that no good indication of silicon reserves is available, yet abundantly available
Tellurium	31	USGS (2024), refining data
Selenium	100	USGS (2024), refining data
Platinum-Group Metals	71	USGS (2024)
Of which Platinum	32.4	Hughes et al. (2021)
Of which Palladium	24.4	
Of which Iridium	1.53	
REEs	110000	In REE-O ₂ content, USGS (2024)

2.2 Extrapolation of energy trends

As the scenario projections of the IEA only extend to the year 2050, an additional extrapolation was performed based on the scenario projections, as well as other projections in line with the IEA methodology. As stated before, the IEA follows the standard metrics used in the IPCC reporting, therefore these will primarily be used to project energy trajectories beyond 2050. For an overview of how the compound annual growth rate (CAGR) was applied, consult S.1 Compound Annual Growth Rate.

2.2.1 Energy Production and Capacity

First, as the IEA methodology is based upon the metrics used by the IPCC, it was claimed that economic growth is the most relevant driver in per capita energy use, and in turn, renewable energy development (IPCC, 2022). Hence, the growth trajectories for population and gross domestic product (GDP) per capita and the specific renewable energy technology (2040-2050) were obtained from IEA, in which the GDP and capacity development were the dominant variables. Since significant growth patterns were observed in the remaining part of the investigated timespan, this might have provided overexaggerated results.

2.2.2 Battery-Based Energy Storage (BESS)

BESS are considered to serve a pivotal role and are imperative to support increased deployment of renewables and ensure grid reliability (IEA, 2023a). BESS provides both short- and long-term energy storage, as well as ancillary services such as grid stabilization and the deferment of new infrastructure investments. The CAGR observed in the final interval (2040-2050) was used for extrapolation. Given the unavailability of MI in terms of power (i.e., t/GW), a load duration of three hours was assumed to convert this into gigawatt-hours (GWh) of electric output, closely approximating the IEA documentation.

While the assumption that renewable capacity additions will stagnate post-2050 remains, there is uncertainty regarding whether BESS capacity will be sufficient to ensure grid stabilization and mitigate the intermittent nature of renewables. Future technological advancements are likely to enhance both electricity production efficiency from renewables and storage capacity. Additionally, BESS applications are essential in off-grid applications, providing reliable energy solutions where traditional grid infrastructure is not feasible.

2.2.3 Transport

The IEA provided some data on the expected share of EVs in the total car fleet for 2050 but did not provide clear information on the absolute values for the EV stock envisioned for that year. Furthermore, the IEA only provided car stock data until 2035 and shares in the total fleet for EVs for the NZE. This left a degree of uncertainty regarding the IEA's vision for EV stock development. To address this uncertainty, the study by Liang et al. (2023) was used as a reference. Three vehicle types were considered: light-duty EVs (LDEVs), heavy-duty EVs (HDEVs) and 2/3 wheelers.

Following the approach by Liang et al. (2023), the IEA data was supplemented with other sources. Car ownership data per one thousand capita were obtained from Modaresi et al. (2014), averaging low and medium ownership scenarios. United Nations population projections were utilized for the timespan under investigation, which were used to compute the LDEV stock in the investigated timespan.

Historical EV data, as well as projections until 2035, were obtained from the IEA's EV Outlook (2024b). A logistic fitting curve was applied to distribute the development of EV shares across the timespan. The 2050 car ownership values per one thousand capita were used to extrapolate to 2075, assuming that market saturation is achieved in the NZE by 2050. For fuel cell vehicles (FCVs), projected sales along with historic stock development were obtained, which were then used to quantify the FCV stock development for the investigated timespan.

This approach provided a more detailed and nuanced understanding of potential EV stock development, drawing on a range of reliable sources to supplement the limited and unclear data provided by the IEA.

2.2.4 Infrastructure

The IEA provided data on infrastructure requirements in million kilometers for the Announced Pledges Scenario (APS), which assumes that all climate commitments made by governments around the world are met in full and on time. It both contains the amount of additional infrastructure as well as the required replacements. Consequently, the ratio between electricity capacity and infrastructure length until 2050 was obtained:

$$L_{grid} = \frac{L_{grid,t,APS}}{Cap_{t,APS}} * Cap_t \quad (2)$$

In which L_{grid} denotes the required (additional or replaced) infrastructure length in million km, $\frac{L_{grid,t,APS}}{Cap_{t,APS}}$ the ratio between infrastructure length and electrical capacity in million km/GW for year t , and Cap_t the electricity generation capacity in year t .

2.3 Dynamic Stock Flow Analysis (dMFA)

Dynamic stock flow analysis (dMFA) serves as a robust quantitative method to track and project the flows of ETMs over a specified period. This approach is instrumental in demand analysis, as evidenced by studies such as those by Giurco et al. (2019). Watari et al. (2019) and Liang et al. (2023). The dMFA framework operates on both material and component levels, highlighting the role of efficient end-of-life (EoL) practices in minimizing primary demand. It facilitates the distribution of lifetimes across various technologies, approximating when in-use stocks reach their EoL.

2.3.1 Lifetime Distribution

The lifetime distribution of clean energy technologies is modeled using survival functions. This allowed us to quantify when material stocks require be replenished as clean energy technologies reach their EoL. For technologies like EV batteries, the weibull distribution was preferred due to its ability to accommodate the environmental impact on technology durability. The weibull distribution was defined as:

$$L(t)_i = \exp\left(-\left(\frac{t}{\lambda}\right)^k\right) \quad (3)$$

where $L(t)_i$ is the survival probability of sub-technology i at year t , λ is the scale parameter indicating the distribution's skewness, and k is the shape parameter, indicative of the maximum lifetime.

Conversely, for PV, wind, and infrastructure technologies, a normal (Gaussian) distribution was applied. This distribution is chosen for its ability to model a more frequent outflow around the mean lifetime, thus providing a better representation for these technologies. The survival function for the Gaussian distribution is:

$$L(t | \mu, \sigma) = 1 - \Phi\left(\frac{t-\mu}{\sigma}\right) \quad (4, \text{Sreevalsan-Nair, 2022})$$

Here, t represents time, μ the mean lifetime, σ the standard deviation reflecting lifetime variability, and Φ the cumulative density function. For comprehensive details on all lifetime distributions, parameters, and sources used, please refer to.

2.3.2 ETM Demand from added capacity

In this section, the mathematical framework for demand calculations from added capacity are addressed. For a complete overview of the utilized market shares, consult S.5 Market shares for technologies..

2.3.2.1 PV, Wind and BESS

A material-based approach as depicted was utilized for determining ETM demand. MI per unit of power (i.e., t/GW) were obtained from various literature and the IEA. Leveraging the established energy development trajectories from the investigated scenarios, the research aimed to ascertain the ETM demand necessitated by the added capacity each year (t).

Based on this equation, the material demand from added capacity for PV, wind and BESS was computed with the following equation:

$$Demand_{\Delta Cap,x,t} = \sum_{i=1}^n (Share_{j,t} * MI_{x,i,t} * \Delta Cap_{i,t}) \quad (5)$$

In which $Demand_{\Delta Cap,i,x,t}$ denoted the sum of ETM x in year t in kiloton (kt), $Share_{j,t}$ the share of each sub-technology, $MI_{x,j,t}$ the material intensity for sub-technology i for ETM j and $\Delta Cap_{i,t}$ the added capacity in that year. For wind and PV, material intensity improvements are considered based on Liang et al. (2023).

2.3.2.2 Hydrogen

For H₂ production, a similar approach was adopted. The computation was done based on the H₂ demand in year t as projected by the NZE scenario, resulting in the following mathematical expression:

$$D_{H_2,x,t} = \sum_{i=1}^n (Share_{i,t} * MI_{x,i,t} * \eta_{i,t} * D_{H_2,t}) \quad (6)$$

In which $D_{H_2,x,t}$ denotes the ETM x demand in kt in year t , $Share_{i,t}$ represents the share of sub-technology i in year t , $MI_{x,i,t}$ the ETM intensity in kt/GW for each electrolyzer type, $\eta_{i,t}$ denoted the efficiency of the electrolyser sub-technology, and $D_{H_2,t}$ represents the H₂ demand in Mt in year t (Greenwald et al., 2024). Efficiency and lifetime improvements were incorporated into the calculation based on IRENA (2020).

2.3.2.3 Infrastructure

For infrastructure, a distinction was made between transmission (Tx) and distribution lines (Dx). Tx lines involve high-voltage cabling (>100 kV), while Dx encapsulates medium- (MV, 100–1 kV) and low-voltage (>1 kV). Moreover, a distinction is made between underground and overhead cabling. Other infrastructure equipment including transformers and substations were considered as well. The distribution of various cable types were based on the comprehensive analysis on ETM demand for the electricity grid by Deetman et al. (2021) and are provided in Table 4. The ETM demand for infrastructure was then quantified with the following expression:

$$D_{grid,x,t} = \sum_{i=1}^n L_{grid,i,t} (Share_{i,k} * MI_{x,i,j}) + L_{grid,i,t} (n_{equipment,i,j} * MI_{x,i,j}) \quad (7)$$

In which $D_{grid,i,t}$ is the annual ETM demand in year t for ETM x in kt, $L_{grid,i,t}$ the additional infrastructure requirements, $Share_{i,k}$ is the distribution of underground and overhead cables for D_x and T_x respectively, $MI_{x,i,k}$ is the ETM intensity for each cable type, $n_{equipment,i,k}$ the amount of transformers and substations required based on type and amount of infrastructure and $MI_{x,i,k}$ the material intensities for equipment based on the cable type, denoted in Table 5. Note that the MI has been kept constant over time.

Table 4: Cable types distribution based on Deetman et al. (2021)

Transmission	
Underground	7%
Overhead	93%
Distribution	
Underground	60%
Overhead	40%
LV	32%
MV	68%

Table 5: Equipment requirements for distinct types of power lines in units/km based on Deetman et al. (2021).

Equipment units/km	HV [Transmission]	MV [Distribution]	LV [Distribution]
Transformers	0.0532	0.103	1.107
Substations	0.0002	0.085	1.107

2.3.3.4 Transportation

For transportation, a component-based modelling approach was adopted. This approach is more suitable as the vehicle is collected during the EoL instead of each separate ETM. With the total stock of EVs in place for the investigated timespan based on IEA projections, ETM demand was quantified for the 3 considered vehicle types. Eq. (5) was then used to determine the ETM demand:

$$D_{EV,t} = \sum_{i=1}^n (EV_{Sales,i,t} * Share_{j,t} * Share_{k,t} * Cap_{x,t} * MI_{y,t}) \quad (8)$$

In which $D_{EV,t}$ is the ETM demand of all vehicle types in year t , $Share_{j,t}$ the share of the battery chemistry in year t , $Share_{k,t}$ the share of battery-EV (BEV) and plug-in hybrid vehicle (PHEV), and $MI_{y,t}$ the specific ETM demand for battery chemistry j . $Cap_{x,t}$ denotes the battery size for vehicle type x at time t . Battery size developments was based on the analysis by Junne et al. (2020) and are provided in Table 6. Since the amount of PHEV by 2035 in heavy applications was neglectable (6% in total HDEV shares) it has been excluded from this research.

Table 6: Battery size developments based on Junne et al. (2020)

Battery Size (kWh)	Technology	2020	2025	2030	2035	2040	2045	2050
LDEV	PHEV	6	8	10	12	13	14	15
	BEV	40	43	48	52	57	60	62
TWEV	BEV	4	4.1	4.75	5.5	6.25	7	7.5
HDEV	BEV	210	250	312.5	345	370	395	420

2.4 ETM Demand from Stock Replacement

Stock replacement was determined by the outflow of stock, which is affected by the lifetime distribution of the technologies in use. The lifetime distribution function is pivotal in calculating the outflow, as it provides the probability of a technology reaching its EoL in any given year.

To calculate the outflow of stock in year (t), the lifetime distribution function was applied to estimate the proportion of the stock that has reached its EoL. This is represented mathematically as:

$$S_{x,out}(t) = \sum_{i=0}^t (1 - L_{i,k}) * Cohort_i \quad (9)$$

Here, $S_{x,out}(t)$ denotes the outflow of stock of material x in year t , $(1 - L_{i,k})$ is the survival function specific to the technology. The in-use stock $S_{x,t}$ is then quantified by subtracting the outflow and adding the demand from added capacity:

$$S_{x,t} = S_{x,t-1} + D_{x,t} - S_{x,t,out} \quad (10)$$

Ensuring that both the stock replacement demand and demand from added capacity are used to compute the final ETM demand for a specific commodity. The limitation of this approach is that it is assumed that the stock replacement equals the EoL. This limitation will be comprehensively addressed further on.

2.5 End-of-Life

From a resource perspective, it is most interesting to define how much primary mining has been avoided with the utilization of outflow, now referred to as secondary materials. Figure 3 denotes a typical value chain of an ETM. While not all minerals are going through all process steps (i.e., fabrication is only done for alloys and various sheet metals), it shows that many process steps generate outflow which are used again in primary production. As the main goal of efficient EoL practices is to reduce primary demand, the choice was made to use the EoL Recycling Input Rate (EoL RIR).

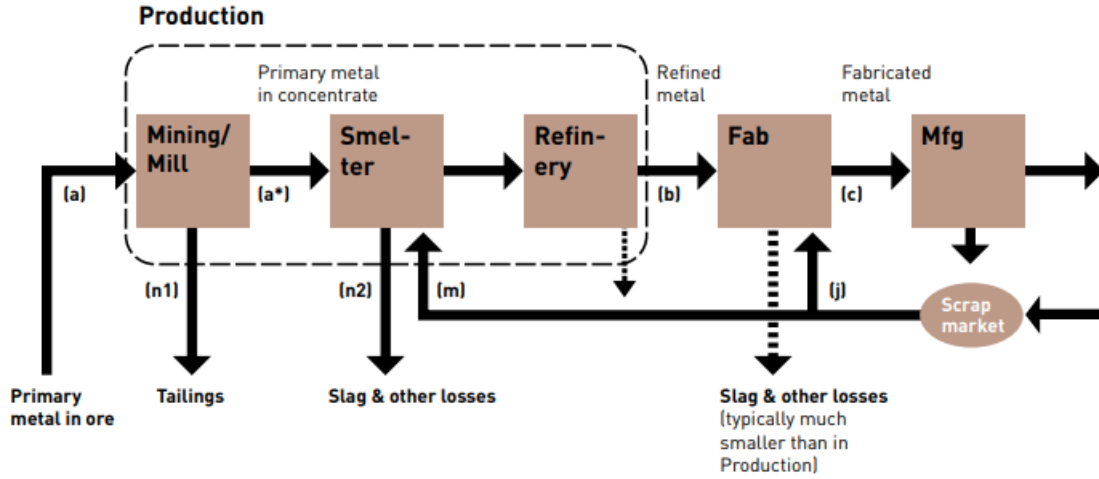


Figure 3: Supply chain of an ETM, UNEP (2011)

EoL RIR is the combination of both primary and secondary material input, in which the primary material input is the metal content in the processed ore. Therefore, the EoL RIR is computed by the following expression:

$$EoL RIR (\%) = \frac{(j+m)}{(a+j+m)} \quad (11, UNEP, 2011)$$

In which j , m and a denote outflows from ETM refining, fabrication and manufacturing as depicted in Figure 3. As the EoL RIR does not require any input on data from imported metals, it is suitable to be applied in a global analysis. Furthermore, it encompasses the full value chain of ETMs and relates to ETM extraction. Another remark about the EoL RIR is that it never can reach 100%, as dissipation and losses in each supply chain step are occurring. All values for EoL RIR are provided in the supplementary document.

Finally, having all parameters in place, the final ETM demand in year t could be quantified:

$$Demand_{x,t} = \sum_{n=1}^i (Demand_{\Delta cap,j,x,t} + S_{x,t,out} - (S_{x,out}(t) * EoL RIR_{j,x})) \quad (12)$$

In which $Demand_{x,t}$ denotes the total demand in year t of ETM x , $Demand_{\Delta cap,x,t}$ the demand from added capacity from technology j , $S_{x,t,out}$ the demand due to stack replacement, and $(S_{i,out}(t) * EoL RIR_{i,k})$ the share of outflow that is recycled and used in primary production for scenario k . A low and high recycling scenario were established, to define to what extent recycling requires to be to avoid eventual supply bottlenecks. For a full overview of the recycling scenarios, consult S.6 Recycling Scenarios

2.6 ARIMA

The Autoregressive Integrated Moving Average (ARIMA) model stands out among various forecasting methodologies for its application in time series analysis, including in the mining sector. Notable studies such as Rachidi et al. (2021) for cobalt supply, Saadat et al. (2021) for fossil fuels, and Mutele & Caranza (2024) for South-African gold deposits have demonstrated its utility. This chapter explores the ARIMA methodology, its application in this research, and its contribution to forecasting in the mining industry.

Historical data on the production and refinement of ETMs from 1975 to 2023 were sourced from the USGS. For lithium, mining data was only obtainable from two thousand on. For some commodities, i.e., tellurium and selenium, only refining data was provided as these are by-products from other commodity mining such as copper. ARIMA provided insights on how production might develop, at what point in time cumulative production exceeds the reserve threshold, and if mining and refinement can ramp up in line with incremental demand.

When ARIMA is applied to the mining sector, it does not operate in isolation from economic realities. The cumulative supply curve is a theoretical concept that reflects how total cumulative availability could vary over time in relation to extraction costs. Cumulative supply is therefore fixed by the amount of ETMs that can be economically extracted (Henckens et al., 2016). ARIMA can capture the complex interplay of factors that shaped historical price trends, and thus the amount of ETMs extracted historically. This includes the influence of geopolitical events, monopolistic market control, the proportion of minerals obtained as by-products, and operationalization times for new deposits, all of which contribute to the observed mining developments over time.

Conversely, ARIMA primarily relies on past data to make predictions and may not fully account for changes in economic drivers and future developments. While it can model historical trends effectively, the future extrapolations based on these trends might differ significantly if there are substantial changes in key economic factors. These could include market shifts, technological advancements, new environmental regulations, or unexpected geopolitical events that could alter the dynamics of the mining sector in ways not captured by historical data. While ARIMA provides valuable insights into historical patterns for forecasting, it is important to consider its limitations in predicting future changes driven by evolving macroeconomic conditions.

As a result, ARIMA can be explained as mathematical representation to forecast production trends over time, accounting for patterns that persist and adjusts for shifts that could lead to inaccurate prediction if left unaddressed, resulting in Eq. (1):

$$ARIMA = (1 - \sum_{i=1}^{\rho} \theta_i L^i)(1 - L)^d X^t = (1 + \sum_{i=1}^q \theta_i L^i) \varepsilon_t \quad (13, \text{Prabhakaran, n.d.})$$

- L denotes the lag operator, shifting the time series back by one period. This was set to 20 for data series ranging from 1975-2023, and to ten for data series with lower data points (i.e., lithium).
- ρ denotes the number of autoregressive terms, determining the extent to which past values influence future production.
- d denotes the degree of differencing required to make the series stationary, required to remove trends in the data so that variations are constant over time.
- q denotes the number of moving average terms, capturing the relationship between current and residual errors from previous predictions.
- θ_i denotes the coefficients for the moving average term.
- ε_t is the error term at time t , representing random fluctuations in production that cannot be predicted by the model.
- X_t is the new forecasted production value in year t .

Due to the high uncertainty, both a lower and upper confidence interval were modelled, indicating a high and low supply supply scenario. As the ARIMA model analyses the historic time series, lead time for operationalizing mines is already considered. For a detailed description of the determination of the ARIMA parameters, data transformation and model validity, consult S.4 ARIMA Model.

2.7 Supply-Demand Analysis

Identifying potential future ETM bottlenecks or risk of reserve depletion will be done by comparing the obtained supply and demand trajectories for each investigated ETM. A few conditions may imply that a future bottleneck might occur in the future. For battery chemistries of EV and BESS, the highest computed demand combination (i.e., NMC_x and flow) will be used in the determination of the cumulative demand.

The first condition for potential risk of reserve depletion is that the cumulative demand for ETM i exceeds the determined reserves in 2023:

$$\sum_{i=0}^t Demand_i - EoL_i \geq Reserves_{2022,i} \quad (14)$$

Secondly, a potential supply bottleneck may occur if cumulative mining or refining exceed the determined reserves:

$$\sum_{i=0}^t Supply_i \geq Reserves_{2022,i} \quad (15)$$

Finally, a bottleneck may occur if cumulative demand exceeds the cumulative supply or the demand in year t is higher than supply in year t :

$$\sum_{i=0}^t Demand_i \geq \sum_{i=0}^t Supply_i \quad (16)$$

$$Demand_i - EoL_i \geq Supply_{i,t} \quad (17)$$

With these conditions in mind, the obtained results will be combined and plotted over the investigated timespan. Furthermore, it could be that the scenario with high recycling rates mitigate the potential risk; this will indicate similarly. If these conditions are met, mitigation and potential substitution options will be addressed.

2.8 Sensitivity analysis

To assess the robustness of our baseline scenario and explore the impact of a range of factors on the cumulative demand for battery materials, a comprehensive sensitivity analysis was conducted. This analysis will help identify which parameters have the most significant influence on the results and provide insights into potential trade-offs within the deployment of clean energy technologies. It will be determined how these parameters would influence the percentual change in the total cumulative demand, based on the obtained values in the baseline scenario. Parameters may include recycling rates, MI development and lifetime. Furthermore, potential substitution options will be analyzed, and particular emphasis will be put on potential trade-offs in ETM use. While an ETM could be eliminated, it may cause a surge in demand for another ETM.

3. Technology Overview

This chapter will delve into the investigated clean energy technologies incorporated in this research. The fundamentals of each (sub)technology will be addressed, while putting emphasis on what ETMs are used in various technologies, as well as their function, substitution potential and efficiency improvements.

3.1 PV

3.1.1 PV Production

PV panels capture energy through a photoelectric effect. Semiconductors, such as silicon, are crystalline solids with specific electron energy levels and an energy gap between the valence band and conduction band. Doping is a process to increase conductivity, which introduces impurities with different valence electrons, resulting in p-type or n-type semiconductors. A p-n junction is formed by combining these, creating an electric field in both the junction area and the depletion zone. The depletion zone's electric field separates these pairs, causing movement of electrons to the n-region and holes to the p-region, generating a potential difference. Connecting this to an external circuit will allow electricity to flow (Hernandez-Callejo et al, 2019; Usman et al., 2020).

3.1.2 Design of PV Systems

To increase the output, PV cells are connected in series (to raise voltage), parallel (to raise current), or both (to meet specific voltage and current requirements), forming a PV panel or module. PV cells consist of wafers, thin slices of crystal that constitute the cell's structure, produced from a purified ingot, either from one crystal (monocrystalline) or multiple (polycrystalline) (Chen & Gao, 2024; Preet & Smith, 2024).

PV panels can be assembled into a PV array to fulfill the system's needs. Most systems include an inverter to convert the DC electricity from the panels into AC for residential use. Optionally, a battery may be installed for energy storage or backup power, managed by a charge controller to regulate voltage and current. Cu is integral to PV systems, as this is the primary material used in wiring and components for its superior electrical conductivity, connecting all the system's components. Depending on the system requirements, three types of PV system exist: stand-alone, hybrid or grid-connected (Alhousni et al., 2022).

3.1.3. PV sub-technologies

Since the PV market started to emerge, many developments have been made in order to optimize the system's performance. These include a wide array of structures and materials. In today's market, three main technologies emerge:

First-generation PV: made from crystalline silicon, (c-Si) and currently accounting for 95% of the market share. Monocrystalline has the highest efficiency amongst all PV panel types, but excessive costs, while polycrystalline is cheaper but has lower performance (Lubon et al., 2017).

Second generation PV: also known as thin-film PV, which uses a lower amount of semiconductor materials. Moreover, the manufacturing process is less complex, making it less energy intensive. Thin-film modules are usually comprised of cadmium telluride (CdTe), indium gallium-diselenide (CIGS) and amorphous silicon (a-Si). The thin-film market share has been increasing, reaching to around 5% according to IEA (2022). Gallium-arsenide thin-film (Ga-As) are a promising innovation in the thin-film market. Although gallium is co-mined at low concentrations, GaAs panels have higher efficiencies than their thin-film counterparts due to their good light adsorption capabilities (Shah et al., 2020).

Third generation PV: Solution-based, semiconducting technologies including dye-sensitized solar cells (DSSCs), quantum dot-sensitized solar cells (QDSCCs), and perovskite solar cells (PSC). PV cells classified as third generation are those that can achieve high power conversion efficiency at a cheap cost of manufacture. Methylammonium lead iodide ($\text{CH}_3\text{NH}_3\text{PbI}_3$) are the typical adsorption layers used in perovskite, which may reduce the need for crucial ETMs in PV panel applications. A major implication is that lead-based perovskites use toxic materials, but this can be avoided with substitution of materials (Azizman et al., 2023). Third-generation PV panels have a lot of promise, even though they still need to be commercialized (Shah et al., 2023).

For some materials, such as silicon, major reductions have been realized. In 2004, the intensity of Si in mono- and polycrystalline was over 16 t/GW and this has been reduced to 4 t/GW by 2019. This trend is assumed to continue to drop to 3 t/GW by 2028. Nonetheless, it is difficult to determine the mineral intensity of various thin-film panels and third-generation PV, as there is low transparency regarding material composition in the supply chain (Carrara et al., 2020). Table 7 provides the material intensities for the selected technologies utilized in this research.

Table 7: PV ETM intensities in t/GW for with material efficiency improvements over investigated timespan for the selected technologies based on Liang et al. (2023) & Carrara et al. (2020)

PV Technology	ETM	2022	2030	2040	2050
All	Aluminium	7500	7200	7000	6800
	Copper	4600	4500	4300	4200
C-Si	Silicon	4	3	2	1.5
a-Si		15	10	8	6
CdTe	Cadmium	50	27	20	12
	Tellurium	52	27	21	15
CISGS	Copper	22	15	12	10.5
	Indium	15	10	8	6
	Gallium	4	2.5	2	1.5
	Selenium	35	20	16	12
a-Si	Germanium	48	27	21	15
GaAs	Indium	NA	15	15	15
	Gallium	NA	52	52	52

3.2 Wind

3.2.1 Wind Electricity Production

Wind energy conversion is a process that transforms the kinetic energy present in wind into electrical energy. The wind imparts both lift and drag forces on the turbine blades, generating the necessary torque to rotate the rotor. This mechanical motion is transferred to a generator, where it's converted into electricity. The generated electricity can then be used for local demand or fed into the grid at various voltages through a transformer.

Wind turbines typically operate at either a fixed or variable speed. In a fixed-speed system, the rotor supports a constant speed determined by the grid's frequency and the gear ratio. Variable-speed systems, on the other hand, adjust the generator's speed to maximize wind energy extraction, maintaining a constant generator torque (Devashish & Thakur, 2017).

2.2.2 Wind System Design

The design of a wind turbine includes three blades mounted on a hub at the nacelle's front. These blades are driven by wind to rotate a shaft connected to the generator. A gearbox may be present to align the rotational speeds of the turbine and the generator. The pitch mechanism adjusts the blades' angles to control power output and optimize wind interaction. The tower, which is primarily made of steel, elevates the turbine to higher altitudes to access stronger winds. In some designs, a transformer is installed to manage the voltage for grid connection (Stavrakakis, 2012)

Materials such as copper, aluminum and REEs like neodymium, dysprosium, terbium and praseodymium are integral to the construction and functionality of wind turbines. Copper is used in wiring and the generator, while aluminum is utilized for its resistance and lightweight properties in the nacelle. High-purity manganese is primarily used in steel components in the tower, nacelle, and gearbox, improving strength and toughness, essential for the moving components of a wind turbine. Ni has a similar function while nickel also protects the system from corrosion. REE use is significant in permanent magnet configurations within the generator and are also used in the tower construction (Carrara et al., 2020).

3.2.3 Wind Turbine Types

Wind turbines can be coupled to the grid using either a direct-drive (DD) or a gearbox (GB) configuration. DD systems, which are commonly associated with permanent magnet synchronous generators (PSMG) or electrically excited synchronous generators (EESG), have fewer components, resulting in lower losses and simplified maintenance. Nonetheless, they require substantial amounts of REEs. Gearbox-driven configurations, typically used with squirrel cage induction (SCIG) and doubly fed induction generators (DFIG), are smaller in size and less costly (van de Kaa, 2020).

While the absolute material demand for wind turbines has increased with capacity, the relative material use per unit of capacity has decreased. This trend indicates an improvement in material efficiency, with the potential for even lighter materials to be used in the future to reduce costs while maintaining power output. High-temperature superconductors (HTS) represent a promising technology that could further improve efficiency by eliminating parts of the magnetic circuit in generators. Yet, HTS technology is not commercialized and requires a cooling system, which may impact overall system efficiency and increase costs (Pan & Gu, 2016; Carrara et al., 2020). The material intensities for the investigated technologies are provided in Table 8.

Table 8: Wind ETM intensities in t/GW for with material efficiency improvements over investigated timespan for the selected configurations based on Liang et al. (2023) & Carrara et al. (2020)

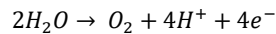
ETM	Technology	2022	2030	2040	2050
Dyprosium	GB-SCIG	2	1.8	1.6	1.4
	DD-EESG	6	5.4	4.8	4.2
	DD-PSMG	17	16	15	14
	GB-PSMG	17	16	15	14
	GB-DFIG	2	1.8	1.6	1.4
Neodymium	GB-SCIG	12	10.8	9.6	8.4
	DD-EESG	28	25.2	22.4	19.6
	DD-PSMG	180	162	144	126
	GB-PSMG	51	46	41	36
	GB-DFIG	12	10.8	9.6	8.4
Praseodymium	GB-SCIG	0	0	0	0
	DD-EESG	9	9	9	9
	DD-PSMG	35	31.5	28	24.5
	GB-PSMG	4	4	4	4
	GB-DFIG	0	0	0	0
Terbium	GB-SCIG	0	0	0	0
	DD-EESG	1	1	1	1
	DD-PSMG	7	7	7	7
	GB-PSMG	1	1	1	1
	GB-DFIG	0	0	0	0
Aluminium	GB-SCIG	1400	1300	1200	1120
	DD-EESG	700	650	600	560
	DD-PSMG	500	450	425	400
	GB-PSMG	1600	1450	1340	1280
	GB-DFIG	1400	1300	1200	1120
Copper	GB-SCIG	1400	1300	1200	1120
	DD-EESG	5000	4750	4250	4000
	DD-PSMG	3000	2800	2600	2400
	GB-PSMG	950	875	825	760
	GB-DFIG	1400	1300	1200	1120
Manganese	GB-SCIG	780	730	680	624
	DD-EESG	790	725	675	632
	DD-PSMG	790	720	700	632
	GB-PSMG	800	750	700	640
	GB-DFIG	780	720	670	624
Nickel	GB-SCIG	430	400	370	344
	DD-EESG	340	310	290	272
	DD-PSMG	240	220	205	192
	GB-PSMG	440	410	380	352
	GB-DFIG	430	400	365	344

3.3 Hydrogen

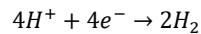
3.3.1 H₂ Production through electrolysis

H₂ production through water electrolysis represents a sustainable alternative to conventional carbon-intensive hydrogen production methods like steam methane reforming. Water electrolysis is an electrochemical process that splits water (H₂O) into its constituent elements—hydrogen (H₂) and oxygen (O₂)—using electricity. This process is facilitated by an electrolyzer, which consists of two electrodes (an anode and a cathode) submerged in an electrolyte, often referred to as the electrolyzer stack.

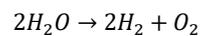
At the anode, the oxidation reaction occurs, where water molecules lose electrons to form O₂ positively charged H⁺ ions (protons). The half-reaction at the anode can be represented as:



At the cathode, the reduction reaction takes place, where H⁺ ions gain electrons to form H₂. The half-reaction at the cathode is:



The overall water electrolysis reaction is thus:



This process is considered zero-emission when powered by renewable energy sources, as it does not directly emit greenhouse gases, although it does perturb the distribution of ozone in the troposphere (Derwent et al., 2006). The objective is to produce high-purity H₂ as these ensure that H₂-based technologies operate optimally, while also causing less degradation. The efficiency of water electrolysis is influenced by factors such as the electrolyte type, electrode materials, and operating conditions (Cavaliere, 2023).

3.3.2 Electrolyzer System Design

An electrolyzer requires renewable power from i.e., a solar and wind farm to produce green H₂. While it can operate as a stand-alone system, installations with multiple stacks are referred to as electrolyzer plants. Within these plants, gas-liquid from the anode and cathode reactions are cooled and stored in two gas separators downstream. The electrolyte from the gas separators is collected in a small buffer tank. Additional water is added to the buffer tank to replenish the water level. The outlet flow is then pumped and cooled in a shared heat exchanger and is returned to the electrolyzer stack (Rizwan et al., 2021).

Bipolar plates and the catalyst-coated membrane are used to facilitate the electrolysis reaction, but often use coatings containing CRMs such as iridium and platinum. While the plant's lifetime is usually up to 20 years, stacks require to be replaced more often depending on the electrolyzer type and the environmental conditions (i.e., higher temperature will cause faster degradation of the stack) (Bareiß et al., 2019). Significant material improvements are expected in the future, especially on the costly catalyst-coated membrane and bipolar plates (IRENA, 2020).

3.3.3 Electrolyzer types

There are currently 3 main electrolyzer types in the market, although anion-exchange membrane electrolyzer (AEM) is gaining attention. For now, the electrolyzer as depicted in Figure 4 are considered. The preferred choice is based on a range of factors such as type of application, operating conditions, cost, environmental considerations, type of energy supply and commercial availability.

Historically, alkaline electrolyzers have been the preferred system choice and therefore this technology has matured the most. As the name implies, the alkaline electrolyzer uses an aqueous alkaline solution (i.e., potassium hydroxide) as an electrolyte operating at a temperature of 65–100°C. The cathodes are commonly made of steel mesh such as nickel coated low carbon steel. For the anode, materials could include cobalt, iridium, nickel, zirconium and PGMs. While alkaline electrolyzers have relatively low capital costs, long-term operational feasibility and tolerance to utilize raw water instead of purified water, there are some implications such as low partial load range, low operating current density and a risk that low-purified H₂ is produced due to the porous separator diaphragm commonly used in such a system (Dincer & Al Zahrani, 2018).

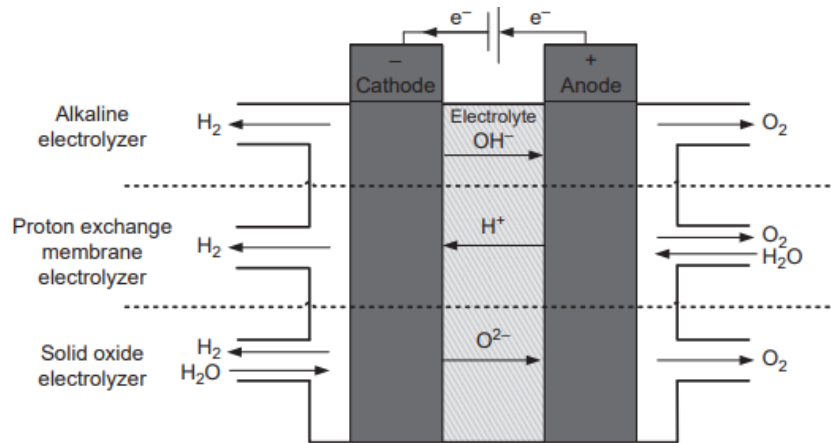


Figure 4: H₂ production process in various electrolyzer types (El-Shafie, 2023).

Proton Exchange Membrane (PEM) electrolyzers can produce high-quality H₂ at lower temperature ranges compared to their alkaline counterpart (70–90°C). Iridium and Platinum are used at anode and cathode. Moreover, PGMs and REEs (such as lanthanum) are used as a catalyst. Yttrium is used in advanced designs for H₂ storage in metal hydrides. Due to the material choices, the reaction kinetics in PEM are quickly induced, making it a safer option compared to alkaline electrolysis, while being able to operate at atmospheric pressures (El-Shafie, 2023). The major challenge for PEM is upscaling, due to the criticality and costs of iridium and platinum. Increasing the scale of such an electrolyzer increases the mechanical stress, which enhances component degradation (Zhang et al., 2022). While substitution efforts are made for platinum, iridium is found to be difficult to substitute, due to its high corrosion resistance while featuring sufficient electrochemical activity (Kiemel et al., 2021)

Solid-Oxide electrolyzer (SOEs) operate at high temperatures (900–1000 °C). Commonly, the cell electrodes are made from Ni, and less electricity is required due to the high operating temperatures. Contrarily, this also results in faster degradation of the cell's stack, with IRENA (2020) implying that current SOEs need to be replaced every 4 years. Moreover, it has not been commercialized up to MW range (El-Shafie, 2023). Table 9 provides the MI for selected ETMs.

Contrarily, FCs are an energy conversion device that converts chemical energy in a fuel into electrical energy, under the condition that both are available. It exhibits various advantages exceeding conventional combustion techniques, one of them being FC demonstrate a 60% conversion efficiency. Basically, FCs perform the opposite process of what an electrolyzer, undergoing an oxidation reaction which dissects H₂ into H⁺ ions and electrons, which migrate from the cathode through the electrolyte and the free electrons travel through an electric circuit, generating an electric current (Fan et al., 2021). FCs appear in the same forms as their electrolyzer counterparts, albeit PEMFCs being prioritized due to their low operating temperature and high efficiency (Mo et al., 2023).

3.3.4 Future Developments

Many developments have been made to decrease the intensity of various valuable minerals, i.e., the costly coating with PGMs of bipolar plates. Since these bipolar plates require excellent thermal conductivity, low permeability, and high shock durability, it is extremely challenging. IRENA (2020) addresses that this is currently unrealizable, but materials such as tantalum might be a preferred option with future developments. Current loadings of platinum and iridium equal 0.5 g/kW and 5 g/kW, and it is estimated that this may decrease to 0.1 g/kW and 0.2 g/kW by 2050, respectively. Other technological advancements may imply thinner diaphragms, or more surface area for the electrodes to enhance H₂ output. Another promising technology is the AEM electrolyzer, which uses non-noble catalysts, but limited catalyst activity and lower conductivity is still a significant obstacle for commercialization (Al-Shafie, 2023).

Table 9: Levelized demand for selected electrolyzer types based on 5000-hour load time, IEA (2022)

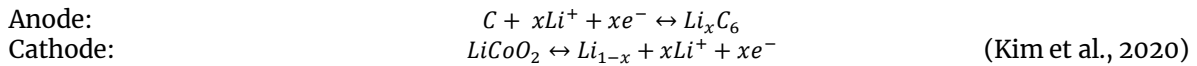
ETM	Electrolyzer Type	ETM Demand (kg/GWh)
Nickel	Alkaline	8.93
	SOFC	1.36
Lanthanum	PEM	0.2
Yttrium	SOFC	0.025
Platinum	PEM	0.002
Iridium	PEM	0.008

3.4 Batteries

3.4.1. LIBs

Among the rechargeable batteries in the current technology mix, Lithium-ion (LIBs) batteries have revolutionized the EV and BESS markets. Li-ion are analyzed extensively for optimization and discover new and more advanced battery chemistries. IEA claims battery demand rose 65% (550 GWh) in 2022 compared to 2021 (330 GWh), an increase of 65%. Li-ion batteries have advantages such as high energy and power density, lack of memory effect, lower self-discharge, and higher lifetime (Chen et al., 2021).

LIBs consist of a positive and a negative electrode separated by an electrolyte solution containing dissociated salts, which allow ion transfer between the two electrodes. A Lithium ion from the cathode material then diffuses into the electrolyte to the anode material. Electrons move in opposite directions through achieving neutrality. During discharging the opposite occurs:



A wide array of battery chemistries is available in today's EV market, such as the nickel-manganese-cobalt (NMC_x), nickel-manganese-aluminum (NCA) and lithium iron phosphate (LFP). As significant advancements are being made, promising technologies such as all-solid-state batteries (ASSB) and vanadium-flow batteries will be addressed as well.

NMC are currently the dominant cathode chemistry in the EV market, representing 60% of the market share according to the IEA. Itani & De Bernardinis (2023) claim that this will continue to grow to 90% in 2030. NMC is the preferred option due to its good performance in terms of specific power, lifetime and safety. Currently, NMC₁₁₁ and NMC₆₂₂ (the subscript denotes the molar ratio over the materials) have the most significant market shares. High nickel batteries NMC₈₁₁ and NMC_{9.5.5} are expected to gain market share due to their increased capacity and lower material costs.

High-nickel batteries still suffer from implications such as high safety concerns and substantial capacity fade. The specific metal used in NMC batteries is NiSO₄. Cobalt is required to be refined and used in oxidized form (LiCoO₂) to be applied in battery-grade applications. Similarly, Manganese requires to be refined into high-purity manganese sulfate monohydrate (HPMSM). According to S&P Global (2024), only 1% of manganese is currently refined to HPMSM.

LFP exhibits a lower cell voltage compared to resulting in a 20% lower specific energy (Hesse et al., 2017). Due to this reason, it is expected that LFP batteries are found less frequent in automotive applications, despite having excellent lifetime. This does bring potential for BESS applications as battery size and weight are less of a crucial factor compared to EV application.

Graphite is either synthetic and graphitized from a carbon precursor, or natural and mined from an ore. Graphite anodes typically consist of both, sometimes with some silicon included. However, natural graphite has lower performance than its synthetic counterparts, due to inconsistent purity. Moreover, natural graphite is unequally distributed, and graphite mining has significant environmental impact. Nonetheless, synthetic graphite has higher efficiency, but more than double the emissions (4.8-13.8 kgCO₂-eq/kg, Barre et al., 2024).

Graphite is the preferred anode option in LIBs for distinct reasons. It has a high theoretical capacity. It also exhibits excellent electrical conductivity, enabling efficient charge and discharge cycles. Additionally, graphite's layered structure facilitates the intercalation and deintercalation of lithium ions, contributing to a long cycle life and good rate capability. Its stable electrochemical potential ensures safe operation over a wide range of conditions. Low cost and abundance are other factors considered (Goodenough & Kim, 2010; Nitta et al., 2015). Table 10 provides the MI for the investigated ETMs for selected battery chemistries.

3.4.2 Future Developments

There are other interesting developments in the LIB market, including ASSBs, such as Li-S, and Li-Air batteries, with energy densities of 2600 Wh/kg and 3500–5500 Wh/kg (compared to 500–800 Wh/kg) for conventional batteries. A typical Li-S battery uses solid sulfur as its cathode material; in Li-air, air is the storage material due to the versatility of O_2 redox reactions (Bandyopadhyay & Nandan, 2022; Liu et al., 2020). However, due to its complex designs and drawbacks, both are not yet commercialized. Li-S batteries have high interfacial resistance between the electrolyte and cathode and limited conductivity; Li-Air requires steady inflow of uncontaminated air, and the formation of dendrites by the reaction between Li and O_2 has severe safety implications (Bruce et al., 2011; Janek & Weier, 2016).

Other interesting BESS applications include VRFBs. Major advantages include the electrolyte being recyclable, regeneration of ion crossover and improved safety. A big distinction that is made between VRFBs and their counterparts is the method of electrolyte storage: as shown in Figure 5: electrolytes are stored in external tanks away from the battery center. Two tanks are used, with vanadium ions in four oxidation states, so that a separate redox couple is present in each. Electrolytes are channeled through distinct half-cells within the battery before being cycled back to storage tanks for recirculation. Each half-cell encompasses an electrode paired with a bipolar plate. The half-cells are partitioned by a selective membrane that facilitates ion exchange. This configuration forms a single cell. To create a stack, cells are interconnected by a shared bipolar plate. Multiple stacks can be connected for an increase in scale. However, high capital costs, limited energy density and degradation are yet obstacles to overcome (Choi et al., 2017; Lourenssen et al., 2019). Vanadium is geologically abundant with current demand, making it an interesting option (USGS, 2023).

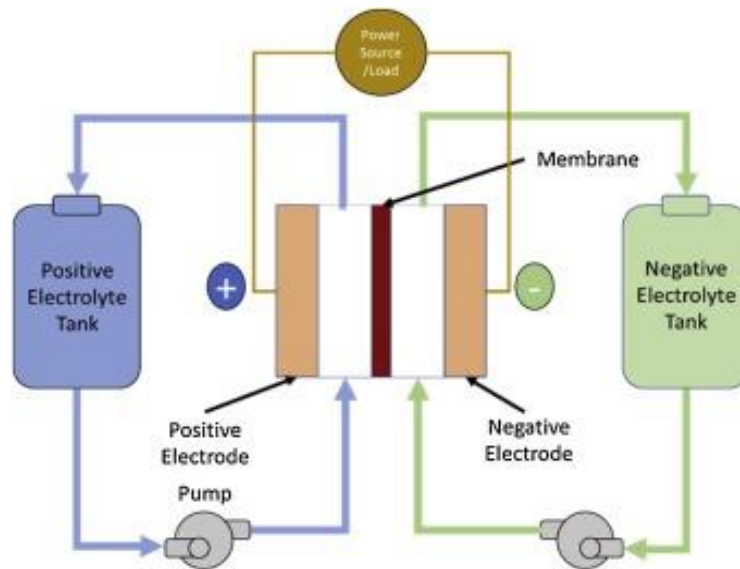


Figure 5: Flow battery principle (Lourenssen et al., 2019)

Table 10: Battery intensities in kg/kWh for various chemistries, based on Olivetti et al. (2017), &Dunn et al. (2022) and Liang et al. (2023). * Indicates an assumption due to data unavailability.

Battery Chemistry	ETM Intensity
Lithium	
NCA	0.150
NCM111	0.145
NCM532	0.143
NCM622	0.135
NCM822/955	0.112
LFP	0.103
ASSB	0.261
Cobalt	
NCA	0.135
NCM111	0.273
NCM532	0.329
NCM622	0.175
NCM822/955	0.085
Nickel	
NCA	0.716
NCM111	0.371
NCM532	0.434
NCM622	0.575
NCM822/955	0.675
Manganese	
NCM111	0.349
NCM532	0.322
NCM622	0.183
NCM811/955	0.08
Graphite	
NCA	0.97
NCM111	0.978
NCM532	0.981
NCM622	0.96
NCM822/955	0.978
LFP	1.085
ASSB *	1.085
VRFB *	1.085
Aluminium	
ASSB	2.92
NCM111	3.11
NCM532	3.07
NCM622	3.01
NCM822/955	2.92
LFP	3.5
ASSB	3.5
Copper	
NCA	0.564
NCM111	0.677
NCM532	0.66
NCM622	0.605
NCM822/955	0.549
LFP	0.946

3.5 Electric motors

Apart from a battery in an EV, it requires an electric motor to generate the necessary propulsion force. This rotational energy is applied to the vehicle wheels which causes movement. Commonly, a permanent magnet motor (PMM) is applied due to their great efficiency at variable speeds and compact sizing (Rimpas et al., 2023). PMMs use a variety of REE such as neodymium, praseodymium and Terbium, due to their unique magnetic properties. Dysprosium is used for its ability to withstand demagnetization. Nonetheless, the production of these REEs is centralized in China, and a significant cost component in EVs (Widmer et al., 2015).

Substitution options are induction motors, widely used in industrial applications. Tesla claims to use such motors in their models as well. Induction motors contain no permanent magnetic material, instead operating at inducing currents in the motor's rotor, and thus creating torque, similar to the DD of a wind turbine. However, rotor losses are higher, requiring the need for a power restriction system. Yet, induction motors are often designed with copper rotor bars (Bilgin et al., 2019).

Table 11: REE use in electric motors, based on Watari et al. (2019); Calvo et al. (2019) and Liang et al. (2023)

REE (g/vehicle)	2022	2030	2040	2050
Dysprosium	117.6	111.8	105.9	94.1
Neodymium	617.9	586.9	556.1	494.3
Praseodymium	86.6	82.2	77.9	69.2
Terbium	15.0	14.0	14.0	14.0

3.6 Infrastructure

The electricity grid has significantly expanded over the past few decades, growing at an approximate rate of 1 million km per year. Additionally, as infrastructure has an approximate lifetime of 40–50 years, meaning that a significant share will be required to be replaced in the near future (Shiomi et al., 2019). This growth has occurred within distribution grids (D_x), which now account for 93% of the grid's total length. D_x grids primarily composed of low-voltage (>1 kV) and medium-voltage (1–100 kV) lines, whereas high-voltage (>100 kV) lines are reserved for transmission grids (T_x) (IEA, 2023b). A typical electricity cable consists of:

- Conductor: typically made from copper or aluminum, carrying electric current.
- Insulation: surround the conductor to prevent shocks and short circuits.
- Metallic shield: a protective layer of copper or aluminum protecting against electromagnetic interference.
- Jacket: the encapsulating layer that protects the cable from moisture and physical damage (IEEE, 2007).

For renewable integration, various infrastructure components need to be put in place. Inter-array grids, export transmission lines, and transformers and substations must be established. Inter-array grids gather electricity from individual wind turbines and PV panels. Export transmission lines then carry this power to the main grids at designated interconnection points. Transformers and substations within these systems ensure voltage regulation for efficient electricity transmission (Chen et al., 2022).

To minimize power loss, high-quality transmission conductors with excellent electrical and thermal conductivity and minimal resistance are essential. Aluminum and copper are the primary materials used in various alloys, favored for overhead transmission lines due to their cost-effectiveness and lightweight properties. Conversely, copper, known for its lower resistivity and enhanced durability, is preferred for underground cables and distribution grids (Kgoete et al., 2024).

3.6.1 Future Developments

The integration of high-voltage direct current (HVDC) systems is increasingly recognized for their efficiency in long-distance power transmission, offering reduced losses and material requirements compared to traditional AC systems. A HVDC line uses significantly less metals; 5/kg/MW/km of Al for overhead and 29 kg/MW/km of Cu for underground (underground cabling requires 101 kg/MW/km of Al for transmission, overhead 11/kg/MW/km) (IEA, 2022d).

One of the most promising developments for loss reductions is the high-temperature superconductors (HTS). HTS are characterized by their extremely low resistive losses and compact structure, utilize a cryostat—typically liquid nitrogen—to maintain the superconducting state, with HTS wires coiled around a copper core (Shaked & Holdengreber, 2022; Yazdin-Asrami et al., 2022). Other major advantages include minimal land requirements, no heat emittance and the ability for it to be directly buried (meaning that no tunnels nor pipes are required). Nonetheless, until this day HTS are still costly and still use various ETMs such as copper and REEs and are more applicable in niche applications where performance is much more important than the costs (Hassenzahl, 2013). The ETM requirements for various power line types, as well as the corresponding necessary equipment and its ETM requirements, are provided in Table 12.

Table 12: ETM Intensities for power lines, including towers/poles in kg/km line based on Deetman et al. (2020).

Infrastructure Type	Aluminium	Copper
HV-overhead [T _x]	12883	-
HV-underground [T _x]	-	11650
MV-overhead [D _x]	-	1448
MV-underground [D _x]	824	663
LV-overhead [D _x]	981	-
LV-underground [D _x]	531	-

3.7 Refining of ETMs

For some ETMs used in clean energy technologies, an additional refining step is required. Furthermore, for some commodities, USGS only provides data on refining output. One example is the ETMs used in battery technologies. After mining, these materials undergo several refining processes to achieve the purity needed for battery-grade or industrial applications (usually close to 99.99%). Here is an overview of the considered ETMs and their refining steps:

- **Battery-grade materials:** including manganese, lithium, cobalt and graphite. These materials undergo concentration through crushing, flotation, and leaching.
 - Further purification involves chemical treatment, precipitation, and filtration. For lithium this results in lithium carbonate or lithium hydroxide.
 - To use cobalt and manganese in battery applications, high-purity sulfates (i.e., high-purity manganese sulfate monohydrate, HPMSM) or dioxides are produced.
 - For graphite, additional thermal or chemical purification is necessary to achieve battery-grade quality (Mudd, 2010; Vikström et al., 2013; Olsson et al., 2014; Chehreh et al., 2021).
- **Copper:** the production of refined copper is often done in a multiple step process, including smelting, fire refining, and electrorefining, eventually using electrochemical or hydrometallurgical process to produce high-purity copper (Moats et al., 2021).
- **Nickel:** Refining involves concentration via crushing and flotation, followed by smelting or high-pressure acid leaching. Other purification steps include solvent extraction and electrowinning to produce high-purity nickel suitable for batteries, wind turbines, and electrolyzers (Dalvi et al., 2004).
- **Tellurium, Gallium and Germanium:** These metals are typically obtained as by-products of copper, aluminum, and zinc processing. Refining involves leaching, solvent extraction, and electrolytic refining to achieve the high purity required for use in PV cells (Lokanc et al., 2015;).
- **Cadmium and indium:** These metals are typically by-products of zinc refining. The process includes roasting, leaching, and electrolytic refining to produce high-purity indium and cadmium, essential for thin-film PV panels and batteries (Tolcin, 2012).
- **Silicon:** Silicon refining involves carbothermic reduction of quartz in electric arc furnaces, followed by purification through chemical vapor deposition or the Siemens process to produce solar-grade or electronic-grade silicon (Frischknecht et al., 2012).
- **Rare Earth Elements (REEs):** REEs are extracted from various ores and refined through beneficiation, leaching, solvent extraction, and multiple stages of precipitation and calcination to separate and purify individual rare earth oxides or metals (Jordens et al., 2013).
- **Platinum-Group Metals (PGMs):** Refining PGMs involves crushing, grinding, flotation, smelting, and chemical separation to produce pure metals used in catalytic converters and fuel cells (Tang et al., 2023).

The importance of refining capacity cannot be overstated. While mining capacity might be in place, the ability to refine these materials to the necessary purity levels for clean energy technologies and other industrial applications may lag behind. This analysis considers refining capacity to ensure that the transition to clean energy technologies is not hindered by shortages in high-purity materials. This information helps to explain the complex supply chains of ETMs.

4. Technology Development

First, the extrapolation results for the NZE scenario for wind, PV, H₂ infrastructure and BESS applications under NZE projections from 2022 until 2075 are provided. Stock development for EVs are provided as well, along with dedicated car sales and outflow.

4.1 Solar PV

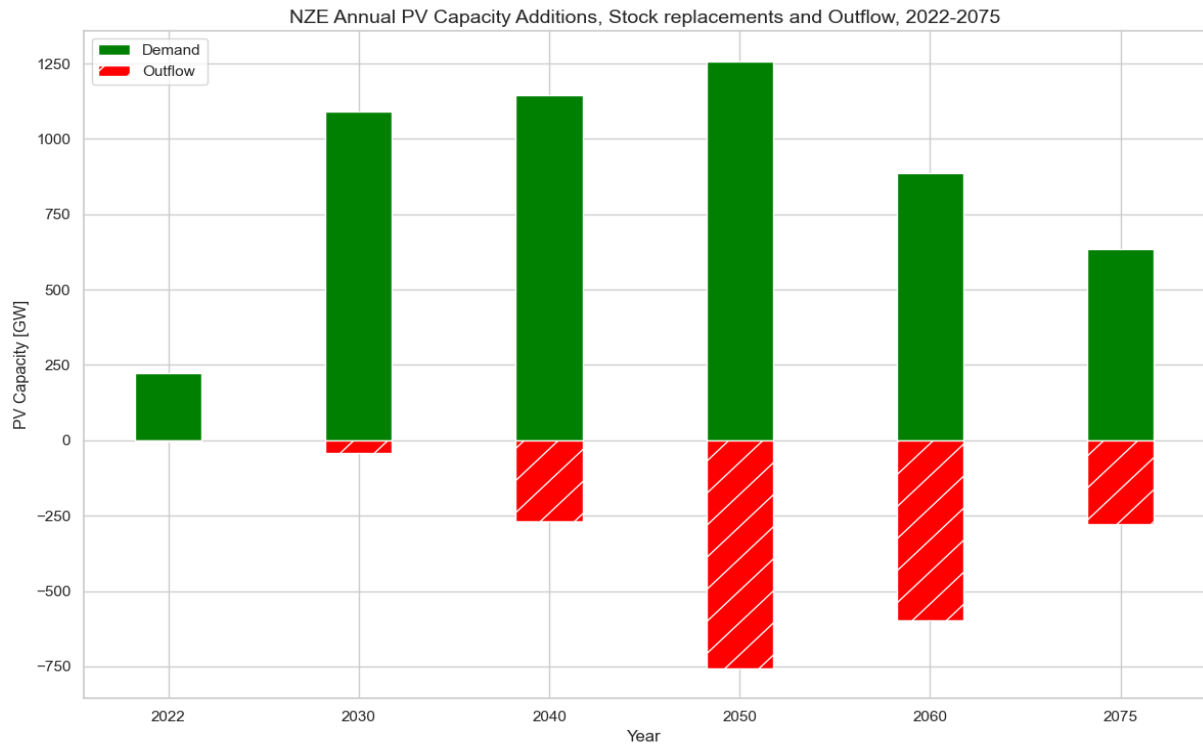


Figure 6: PV annual capacity development and outflow development in the NZE Scenario for selected years. Outflow indicates the annual amount of PV capacity that reached its EoL.

Under NZE projections, solar PV capacity is projected to experience substantial growth, as shown in Figure 6. By 2030, annual additions are expected to reach 1,048 GW, leading to a total capacity of 6,100 GW. This rapid expansion will continue, with annual additions peaking around 2035 at approximately 1,060 GW. By 2050, the total PV capacity is forecasted to rise to 18,750 GW, although the rate of new additions will decline to 501 GW annually. This increase in capacity will be accompanied by the significant rise in stock turnover.

During this period, the expansion of PV capacity will be driven by both new installations and the initial phase of stock replacements. By 2040, a turning point will be reached, as the annual outflow of EoL PV panels is expected to surpass the rate of new capacity additions. In 2044, the total outflow will exceed the new additions, meaning that recycling infrastructure should be on-scale now.

Between 2051 and 2053, the outflow will peak, reaching between 755 and 808 GW annually. 75% of the primary demand could be met by efficient utilization of this outflow. Consequently, a stabilization of annual additions and stock turnover is projected, with total PV capacity increasing to 26 TW by 2075. Despite this stabilization, ETM demand will be substantial due to the stock turnover and moderate additions.

The anticipated increase in PV outflow underscores the need for enhanced resource management and recycling processes. Currently, only 3.7% of PV panels are collected, significantly less than the EU's target of 85% (Bosnjakovic et al., 2023). Table 7 highlights that significant material efficiency improvements will be made in future developments, therefore the demand by stock turnover could be significantly lower. Additionally, as energy efficiency improves, the need for new PV installations may decrease, which could influence ETM demand (Shah et al., 2023). Policymakers should focus on developing effective EoL management systems and encouraging technological advancements that improve material efficiency and reduce dependence on primary ETM extraction.

4.2 Wind

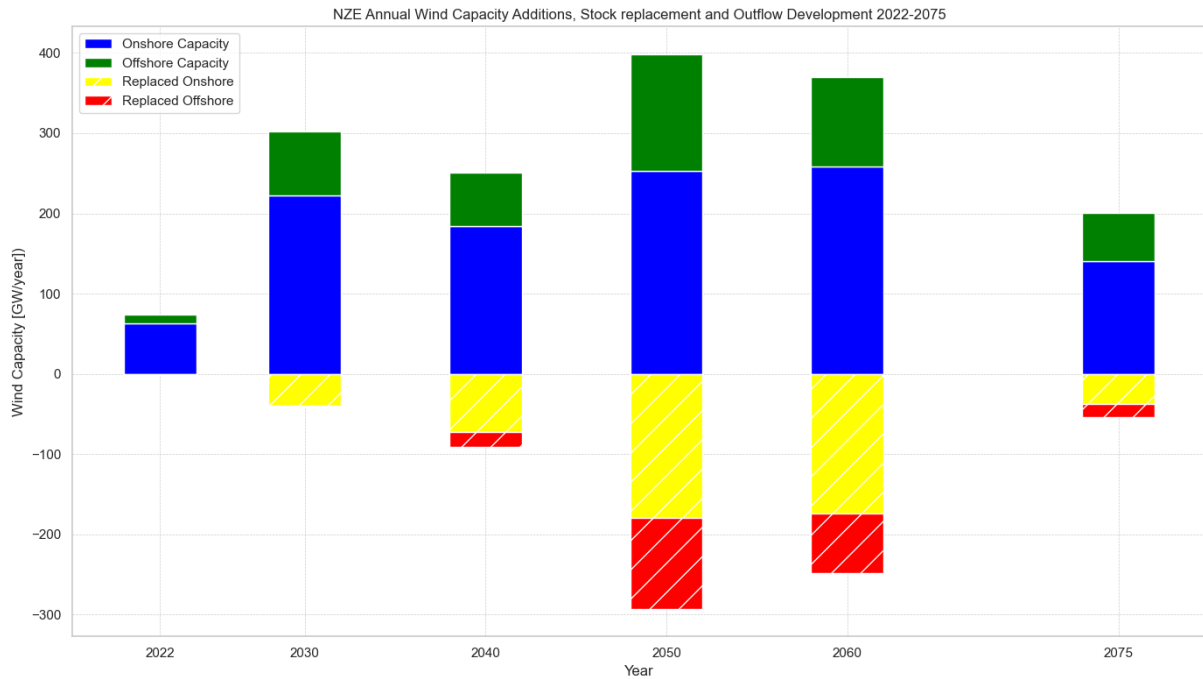


Figure 7: Annual onshore and offshore wind capacity additions, stock replacements and outflow development in the NZE Scenario for selected years. Outflow indicates the amount of wind capacity that reaches its EoL, based on a 25-year lifetime.

Figure 7 presents a detailed analysis of the annual capacity additions and outflows over the investigated period. A significant surge can be observed between 2022 and 2030, with onshore and onshore additions projected to reach 311 and 176 GW/year. The peak for offshore wind occurs in 2030, driven by major stock replacements from existing onshore configurations, which further increases demand. The overall peak in capacity additions is observed in 2035, with a total of 261 GW/year. Post-2030, however, the rate of new wind capacity is expected to slightly decline, as indicated by the NZE scenario projections.

By 2050, stock replacements will play a key role, accounting for 58% of the projected demand. The total deployed capacity of onshore wind is anticipated to triple from 2022 levels, reaching 5,331 GW. By 2075, the total wind capacity is projected to reach 10.7 TW. Like PV, a lower growth rate is expected compared to previous trends.

Although onshore wind remains the dominant technology, offshore wind configurations, which tend to be more ETM-intensive, may offer better prospects from a resource perspective. Desalegn et al. (2023) suggest that offshore wind turbines could achieve capacity factors of 60% by 2050, compared to 55% for onshore turbines. This improvement is attributed to design choices and superior wind resources, which could lead to lower ETM intensities over time. Thus, investing in offshore wind capacity might result in a more efficient use of ETMs and lower overall demand for resources related to stock turnover.

4.3 H₂ Production

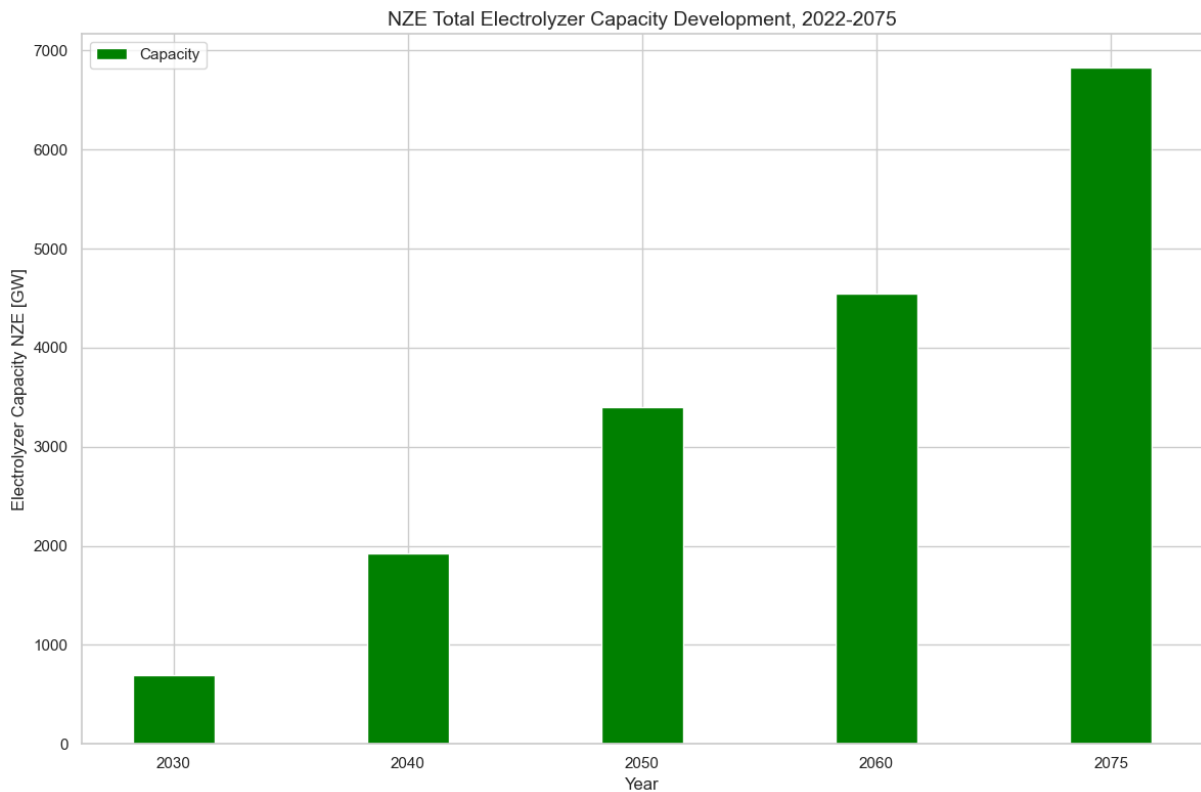


Figure 8: Total Installed Electrolyzer Capacity in the NZE Scenario for selected years. Note that outflow has not been included due to the varying lifetimes of various electrolyzer technologies.

Figure 8 illustrates the NZE projection for total installed electrolyzer capacity. In 2030, the installed capacity is expected to reach 590 GW, a considerable increase from the approximately 1 GW installed in 2022. This rapid growth is projected to continue between 2030 and 2035, with capacity surging to 1,340 GW. This surge is primarily driven by demand from heavy industry in which low-carbon H₂ is used in the production of i.e., ammonia and methanol, and to a lesser extent, in transportation (IEA, 2023e).

The anticipated decrease in the levelized cost of hydrogen production through renewables plays a pivotal role in this expansion. Currently, the cost of producing 1 kg H₂ from PV electricity ranges from USD 11.50 to USD 4/kg H₂. However, this cost is expected to drop to around USD 1.60/kg H₂ by 2030 in regions with optimal PV conditions. Combining wind and PV sources could further reduce hydrogen production costs (IEA, 2023e)

By 2050, the installed electrolyzer capacity is expected to reach 3,300 GW, with a demand for 327 Mt of hydrogen production through electrolysis. Additionally, there is growing interest in long-term underground hydrogen storage, with 1,200 TWh capacity expected to be installed by 2050. This combination of applications is anticipated to further develop hydrogen demand post-2050, as hydrogen becomes more financially viable and remains a key decarbonization option for high-temperature processes in heavy industry. By 2075, the installed electrolyzer capacity is projected to reach 6,825 GW.

4.4 BESS

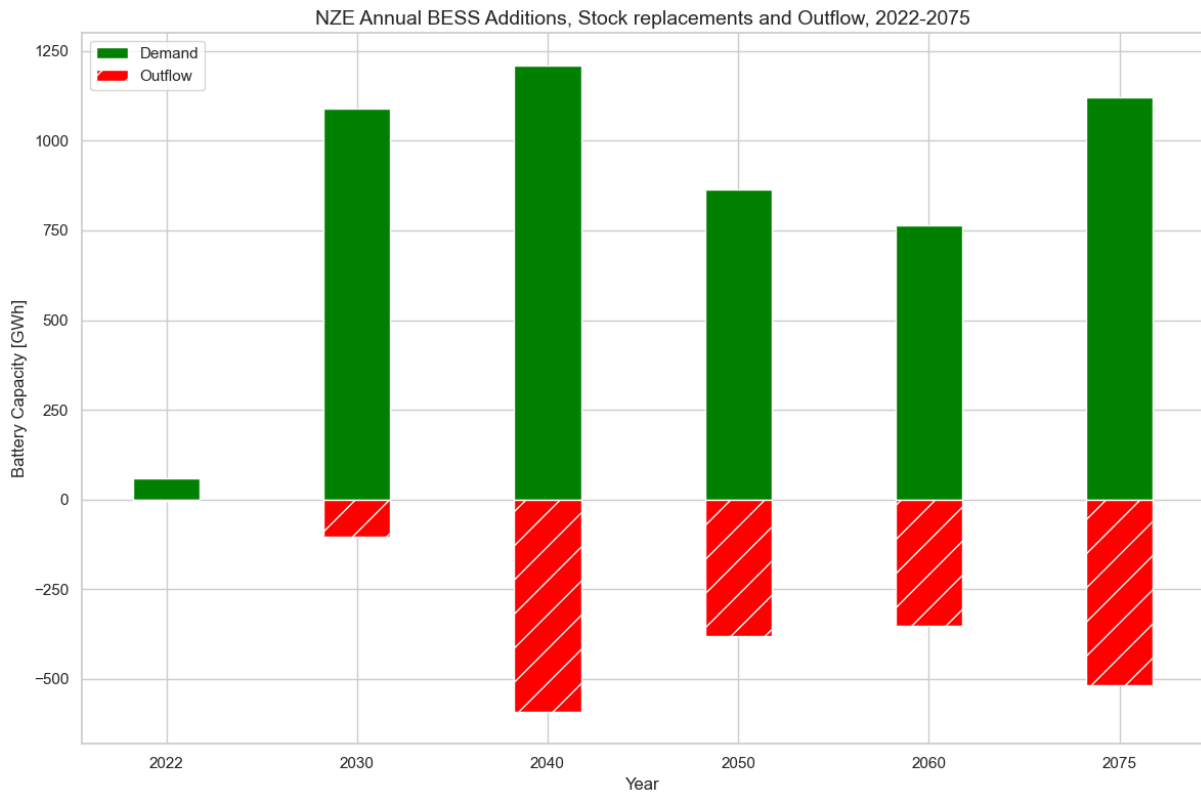


Figure 9: BESS capacity additions, stock replacements and outflow for selected years in the NZE scenario, in GWh/year.

Figure 9 provides the projections for BESS developments, showcasing a significant increase in capacity between 2022 and 2030, with installed capacity growing 20-fold to 104 GWh. Unlike solar PV and wind, BESS exhibits significant outflow by 2030 due to its shorter 8-year lifespan. IEA (2023a) claims that BESS should be an integral part of long-term energy planning and should be developed aligned with PV and wind deployment and grid capacity expansion. Therefore, it is safe to assume that BESS applications continue to grow post-2050, like PV and wind, whilst at a higher rate, due to more demand for its auxiliary functions such as grid stabilization.

BESS capacity additions peak in 2040 at 1210 GWh, driven by new installations and replacements. By 2060, new additions and stock replenishment reach equilibrium, allowing outflow to meet demand. Another peak occurs in 2075, with 1120 GWh total demand, 46% attributed to stock turnover. It is assumed that new capacity additions will further increase post-2050, as demand for short-term energy storage increases.

The early and substantial outflow of BESS materials, compared to PV and wind technologies, underscores the critical need to develop efficient recycling chains. Establishing robust recycling infrastructure for BESS components will be essential to reduce raw material demand and enhance sustainability as the technology scales up rapidly in the coming decades. Moreover, the possibility of repurposing EoL batteries should be considered, as this can drastically reduce the amount of ETMs required for BESS applications, while also slicing costs (Colarullo & Thakur, 2022).

4.5 Infrastructure

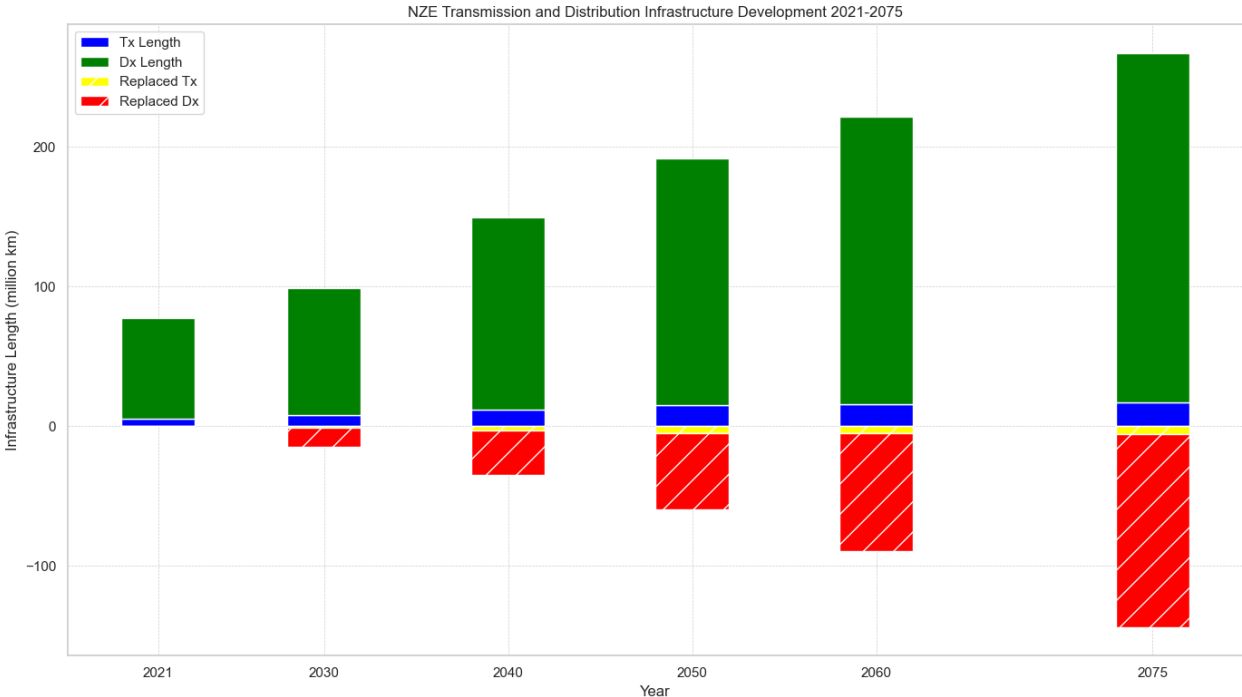


Figure 10: NZE Projected infrastructure length in million km. Both the total length and the replaced length are indicated, based on 50-year lifetime.

In 2020, the lengths of the T_x and D_x infrastructures were approximately 5.3 million km and 72 million km respectively, as illustrated in Figure 10. By 2030, a large share of both T_x and D_x will need to be replaced, primarily in advanced economies.

By 2040, the length of T_x is projected to double, while D_x will expand to 138 million km. This expansion will be accompanied by an increasing trend in replacement requirements. High collection rates can be achieved during these replacements, implying that the demand for stock turnover could be entirely met through efficient EoL practices.

Post-2050, the total length of the electricity infrastructure is expected to reach approximately 192 million km, with over a quarter of the total grid needing replacement. This trend is projected to progress until 2075, when the grid will extend to 266 million kilometers. At this point, more than half of the infrastructure will require replacement.

Improvements in material efficiency could further reduce the demand for stock turnover. Combined with high collection rates, additional demand could also be partially met through efficient EoL practices. However, the expansion of the grid will inevitably lead to significant demand for Cu and Al, both now and in the distant future. Innovative technologies such as HTS and HVDC could significantly reduce the amount of infrastructure needed to distribute a similar capacity (IEA, 2023b; Yazdin-Asrima, et al., 2023). This could potentially alter the landscape of material demand and stock turnover in the future.

4.6 Transport

4.6.1 Light-Duty Vehicles

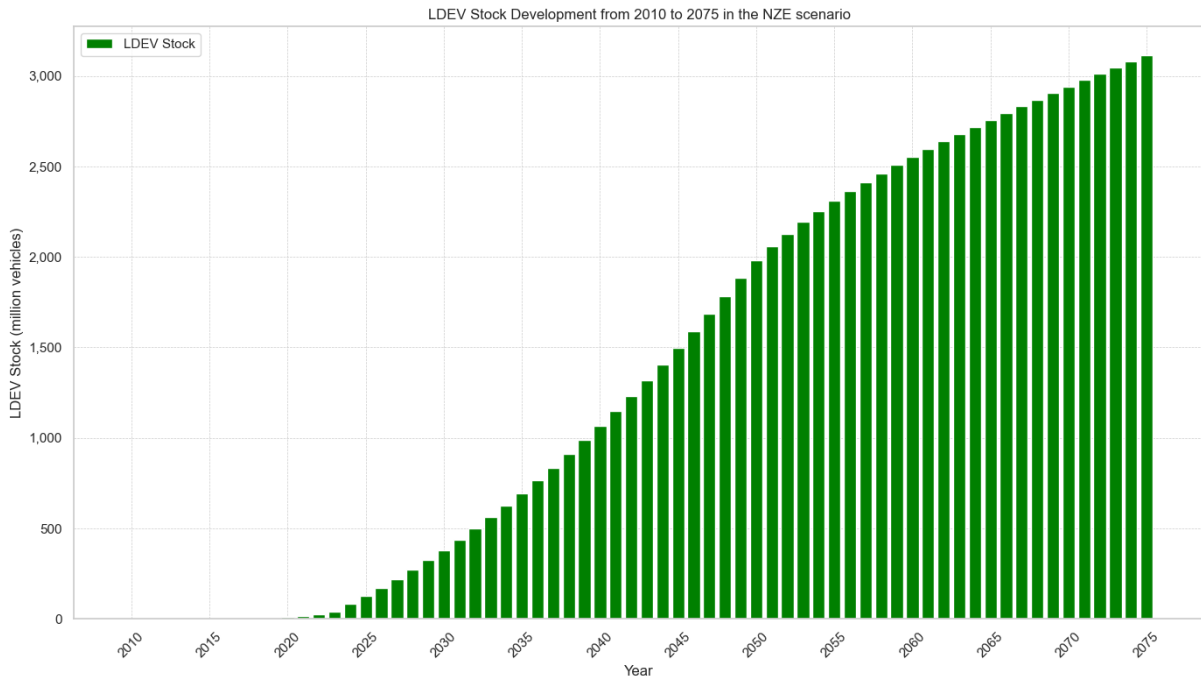


Figure 11: Stock development for LDEV and FCs under the NZE and STEPS scenario, 2010–2075.

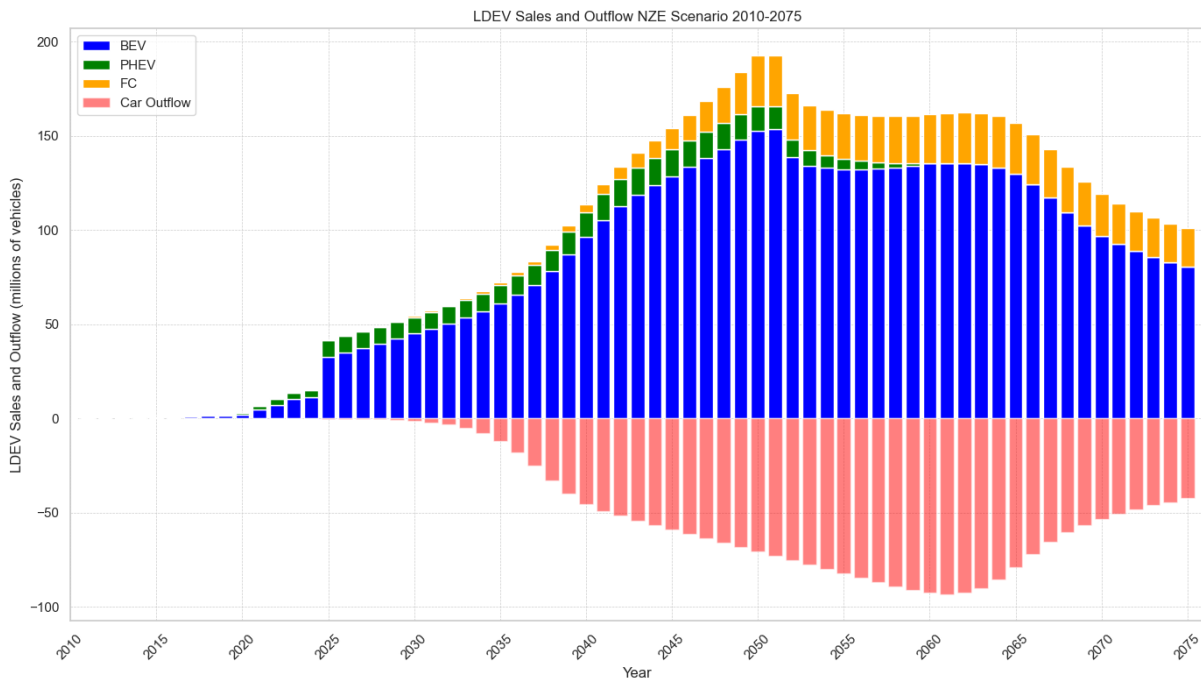


Figure 12: Sales and outflow development for LDEVs under the NZE scenario, 2010–2075.

Figure 11 depicts the projected development of LDEVs. LDEVs represent a small fraction of the global vehicle fleet. However, by the mid-21st century, the LDEV stock is expected to reach approximately 2 billion units. By 2075, LDEVs are projected to constitute about 95% of the total car fleet, resulting in an estimated 3 billion LDEVs on the road.

Figure 12 provides insight into the anticipated sales trajectory for LDEVs. The initial growth in LDEV sales is driven primarily by the substitution of combustion vehicles with EVs. To achieve the car stock levels envisioned under the NZE scenario, a substantial increase in sales is necessary. Specifically, LDEV sales need to surge from 13.8 million units in 2023 to approximately 42 million units in 2024. This sales ramp-up is crucial to align with NZE targets but contrasts with current reported sales figures. Following

this initial increase, a gradual rise in sales is expected until 2050, during which PHEVs will still hold a significant market share. However, PHEVs are anticipated to gradually phase out by 2060. For FCs, these begin to gain market share around 2040, comprising approximately 4% of the total car sales, reaching 2.7 million vehicles being sold. Over the coming decade, it overtakes PHEV sales and becomes a significant share in the total car fleet.

As the market progresses, the growth trajectory reflects a shift from replacing combustion vehicles with LDEVs to replacing existing LDEVs. The peak in LDEV sales is projected for 2050, with an estimated 165 million units sold. This peak results from a combination of extensive stock replenishment and high demand. After 2050, the market is expected to reach saturation, leading to a decline in new LDEV additions. Despite this, stock turnover will continue to drive significant demand for new LDEVs in the subsequent years.

As the projection extends further into the future, a similar vehicle replacement pattern is anticipated. EoL LDEV flows will become increasingly significant around 2035, representing 16% of the total demand. This flow is expected to grow steadily, peaking around 2060. At this peak, if 100% of the outflow is successfully collected, recycled, and reintegrated into vehicle production, it could cover up to 86% of the demand for new LDEVs. This underscores the importance of effective recycling systems in managing EoL vehicles and ensuring the sustainability of the LDEV market.

4.6.2 Heavy-duty vehicles

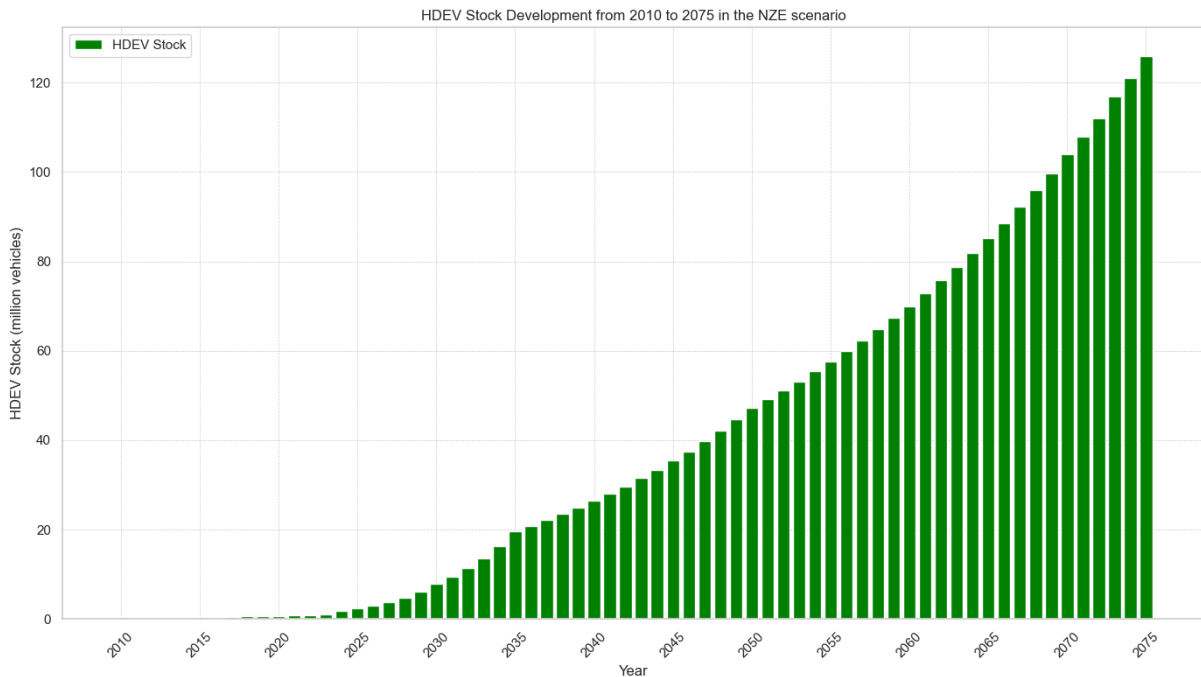


Figure 13: HDEV Stock Development under the NZE scenario, 2010–2075.

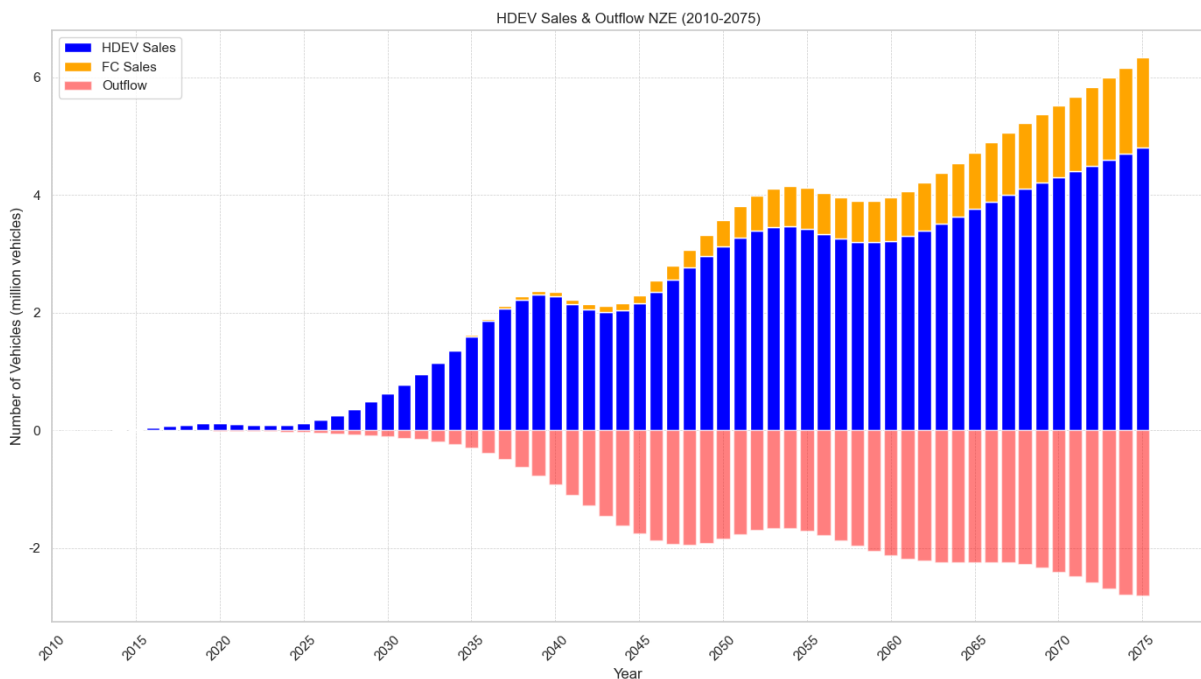


Figure 14: HDEV and FC Sales, stock turnover and outflow in the NZE scenario, 2010–2075.

Figure 13 illustrates the projected development of HDEVs. Currently, the HDEV stock is predominantly composed of electrified buses. However, as depicted in Figure 14, the electrification of trucks is anticipated to accelerate significantly in the coming years. Similar to the historic sales observed for LDEVs, a substantial increase in sales is necessary to meet the NZE targets, as historical sales data up to 2023 fall short of these objectives.

The peak in HDEV sales in 2035 reflects both the rapid turnover of existing vehicles and the ambitious targets set by the NZE scenario, which projects a demand for approximately 2.5 million HDEVs. Following this peak, a notable increase in the outflow of HDEVs is anticipated, which will continue to rise until around 2050. At this point, a sales peak of 3.6 million HDEVs is expected. This is also where FC vehicles begin to gain market momentum, with approximately 650,000 units sold by 2050.

Post-2050, while sales decrease slightly (except for FC vehicles), these are expected to stabilize at levels similar to those observed in earlier years. As technology matures and a larger proportion of the HDEV stock reaches the end of its lifecycle, a stock turnover will drive further growth. This increased replacement demand, combined with ongoing technological advancements, will lead to a significant rise in sales and overall stock. Different from LDEVs, the sales peak for HDEVs are expected in 2075.

By 2075, the total HDEV stock is projected to reach 126 million units. This growth trajectory underscores not only the expanding adoption of HDEVs but also the critical need for effective recycling and disposal strategies to manage the increasing volume of retired HDEVs. Ensuring that end-of-life HDEVs are efficiently recycled will be essential to sustain the environmental benefits of electrification and to support the long-term viability of the industry.

4.6.3 Two- and Three-wheelers

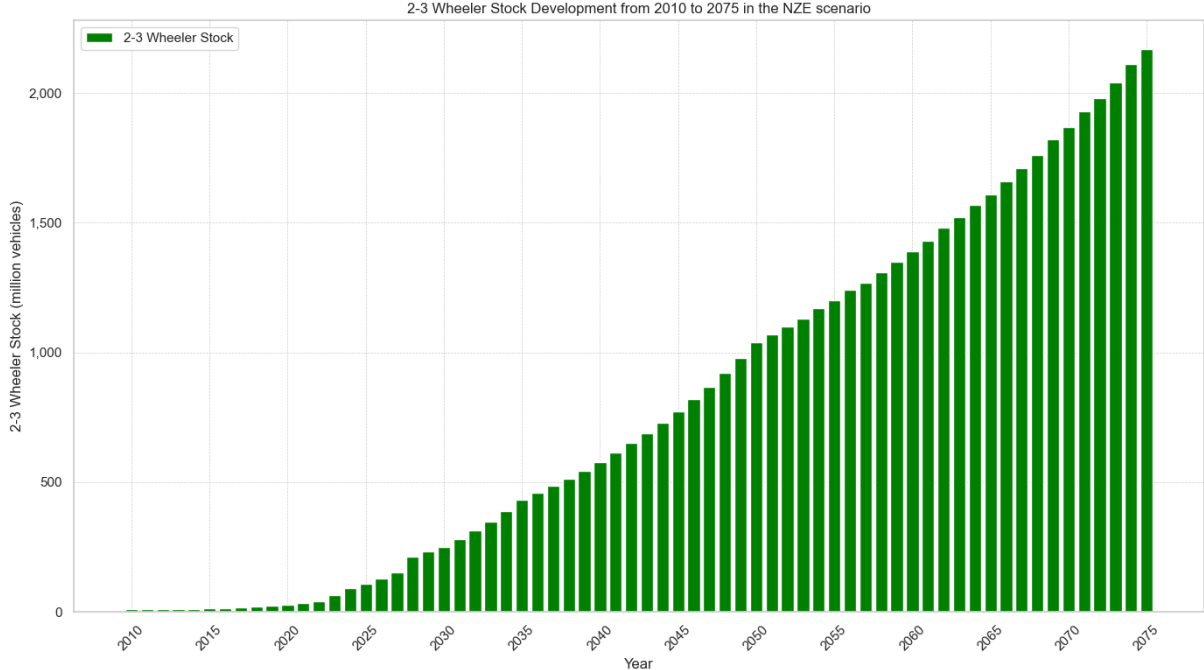


Figure 15: Stock development for 2-3 wheelers under the NZE scenario, 2010-2075.

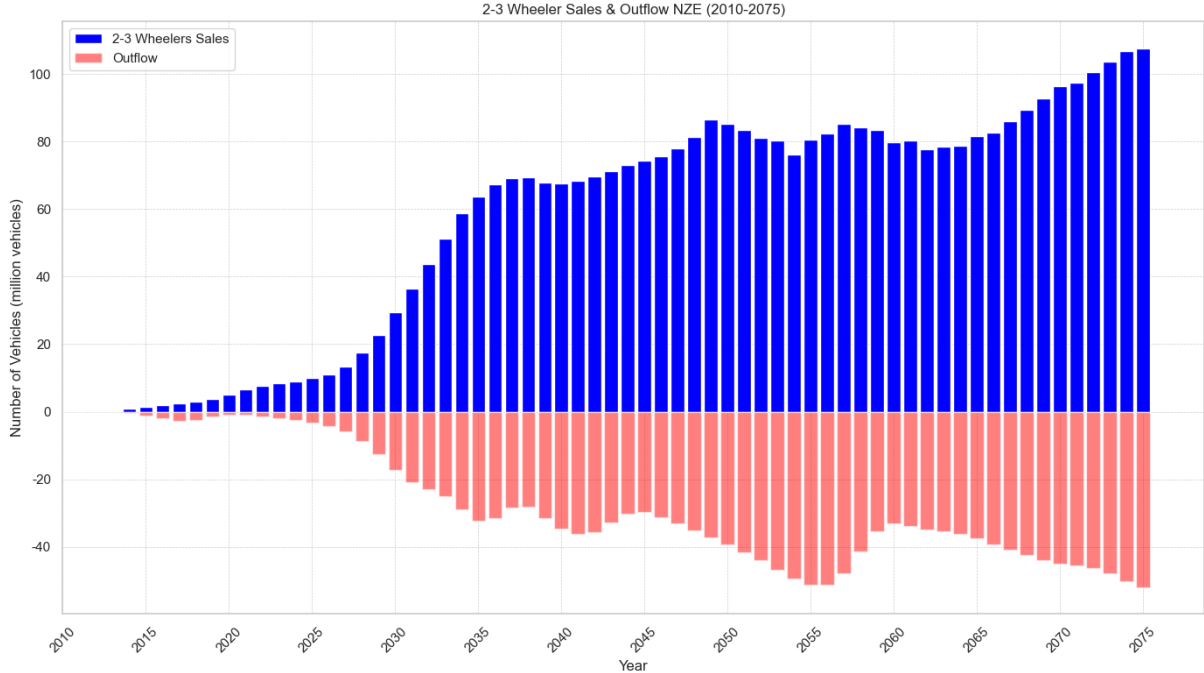


Figure 16: Sales and outflow development for 2-3 wheelers under the NZE scenario, 2010-2075.

Figure 15 illustrates the projected development of two- and three-wheelers in the NZE. According to the IEA (2024b), the electrification of these vehicle types is relatively straightforward compared to other vehicle categories and does not present significant challenges. Currently, 8% of the total 2-3-wheeler stock has been electrified. The initial phase of electrification will see a shift from fossil-fuel-powered two- and three-wheelers to electric models. By 2050, it is expected that the entire vehicle fleet in this category will be predominantly electrified. However, due to substantial vehicle outflow post-2050, demand for new vehicles is anticipated to rise, with the fleet size growing significantly from 102 million in 2022 to over 1 billion by 2050. This number will more than double by 2075, reaching approximately 2.17 billion vehicles on the road.

Figure 16 depicts the sales trajectory for these vehicles. Unlike LDEVs and HDEVs, historical sales align with IEA targets. An observable feature of this trajectory is the significant outflow early in the cycle, which is driven by the relatively short average vehicle lifetime of 8 years. This high turnover rate contributes to the fluctuating nature of outflow and sales patterns.

By 2030, nearly half of the vehicle demand could be fulfilled through the efficient management of outflow streams, highlighting the importance of robust EoL practices. The impact of EoL practices is particularly pronounced, with a significant peak in 2054 when 65% of the total demand could be met through effective recycling and disposal methods.

The relatively easier electrification of two- and three-wheelers compared to other vehicle types, given the light weight and limited driving distance, while also being financially attractive, drives the observed trends. However, no global initiatives have emerged to further accelerate this electrification, meaning that it is uncertain whether NZE targets will be attained (IEA, 2024b).

In conclusion, the NZE targets for EV deployment are ambitious. For LDEVs and HDEVs, historic sales numbers are not aligned with NZE targets. Two and three-wheelers do show that NZE targets can be attained and provide an opportunity for short-term utilization of outflow. For LDEVs, it is shown that the sales peak in 2050. This allows market maturity and easier electrification of HDEVs. The first outflow peak observed for 2/3 wheelers are expected by 2035, meaning that recycling infrastructure should be developed accordingly.

5. Supply-Demand Analysis

This section will delve into the complex dynamics of ETM supply and demand under NZE projections in the investigated timespan. Based on the overview as shown in Table 13, focus will be put on those ETMS in which there were observable risks of reserve depletion or potential supply bottlenecks, and to define whether NZE projections are feasible within current supply dynamics. Additionally, it has been indicated which ETMs have to find to have more future demand in other applications, used for selection in the upcoming sensitivity analysis. For a complete overview of the primary demand for each investigated ETM for each technology, please consult S.7 ETM demand for selected years.

Following this assessment, potential improvements in the supply chain will be explored that could alleviate these risks. This includes examining strategies for material efficiency, better EoL practices, and exploring viable substitution options. By addressing these factors, a comprehensive understanding of the challenges and opportunities associated with ensuring a sustainable and reliable supply of these essential ETMs will be explored.

Table 13: Overview of potential supply bottlenecks or risk of reserve depletion for the investigated ETMs. Green indicates that no supply bottlenecks have been found, therefore these will not be addressed in this section.

ETM	Risk of Reserve Depletion	Potential Supply Bottlenecks	Mitigated by Recycling	Higher demand outside clean energy technologies	Comments
Cadmium	☑	☑	☑	☑	High demand for outside clean energy, while CdTe demand is high under NZE projections. High recycling rates crucial but insufficient.
Gallium	☒	☑	☑	☒	Increasing demand for high-end applications. Future EoL flows may prove a valuable source of gallium.
Germanium	☒	☑	☒	☑	Minor role in clean energy. Significant demand in microelectronics.
Indium	☒	☑	☑	☑	Critical for PV configurations. Improved extraction and recycling needed.
Silicon	☒	☒	☑	☒	Abundant reserves. Significant material efficiency improvements over time. Supply trends show no implications. See S.8 Supply Demand Analysis.
Selenium	☑	☑	☒	☑	Co-mined from copper. Limited adoption reduces future demand.
Tellurium	☑	☑	☒	☑	Co-mined from copper. Demand for CdTe panels significant under NZE projections.
Cobalt	☑	☒	☒	☒	High demand for batteries. Ethical concerns and shift to less cobalt-intensive batteries.
Graphite	☒	☑	☑	☑	Sufficient reserves. Potential bottlenecks around 2050.
Lithium	☑	☒	☑	☒	Surging demand from EV market. New deposits and extraction techniques may help.
Manganese	☒	☑	☒	☑	Abundant reserves. Limited refining capacity for high purity manganese, potential short-term refining bottlenecks.
Nickel	☑	☑	☑	☒	Crucial for batteries. Demand surge expected. Recycling economically feasible and essential.
Aluminum	☒	☒	☒	☒	Vast demand and supply. Ideal for copper substitution in infrastructure. See S.8 Supply Demand Analysis
Copper	☑	☒	☑	☒	Essential for electrification. Reserve depletion a concern. Efficient EoL practices and recycling crucial.
PGMs	☑	☒	☑	☑	Significant demand driven by automotive and later, clean energy technologies. High recycling rates and material efficiency improvements can mitigate reserve depletion risk.
REEs	☒	☑	☒	☒	Wide use in permanent magnet applications. Since REE supply data for individual commodities is unavailable, difficult to make define whether demand for each REE can be met.

5.1 Cadmium

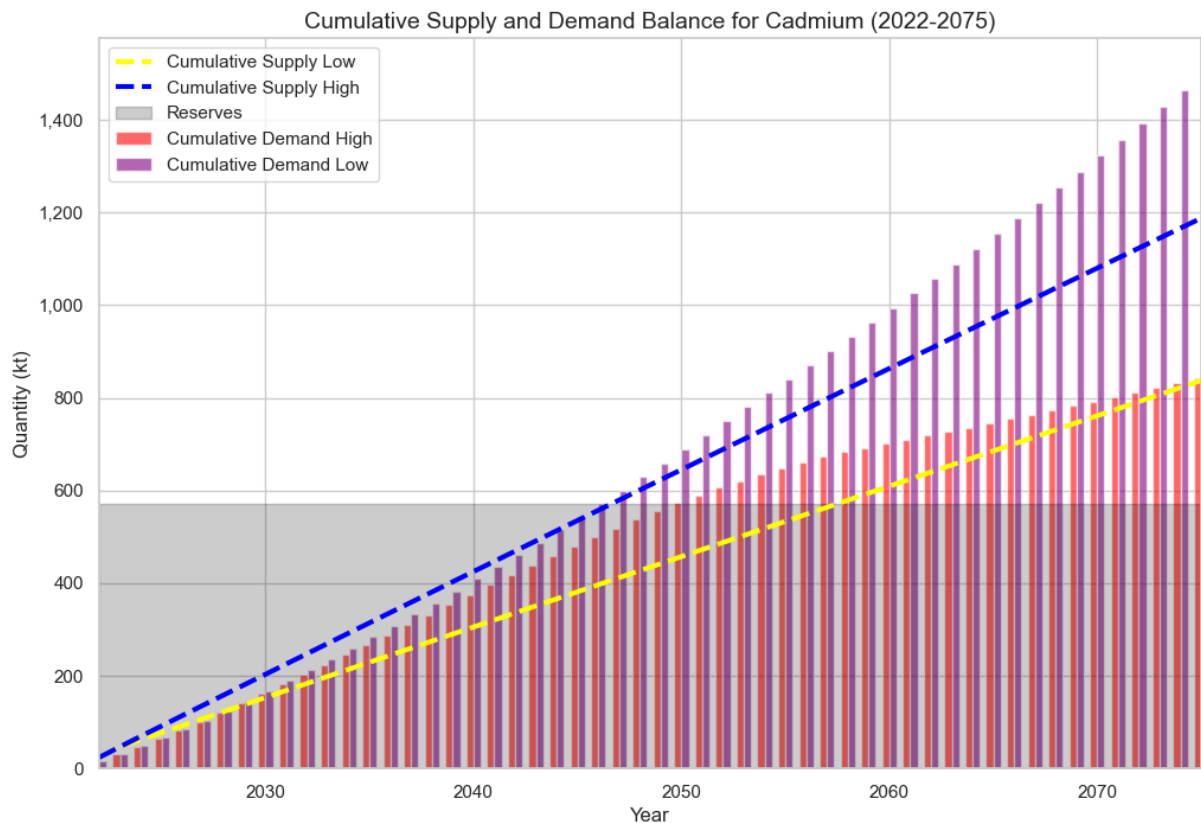


Figure 17: Cumulative Supply Demand Balance for Cadmium under NZE projections in kt, 2022-2075.

Figure 17 illustrates the supply–demand balance for cadmium. The bar chart in the visual shows the cumulative demand for cadmium from both PV applications and external demand, under both low and high recycling scenarios. The grey area represents the total measured reserves as reported by the USGS. Additionally, two dashed lines indicate the extrapolated supply data predicted by the ARIMA model, based on historic USGS data.

Cadmium demand for PV applications is expected to peak around 2030, driven by the increasing adoption of CdTe PV configurations, with demand surging to approximately 1 kt/year due to additional CdTe capacity. Post-2030, demand stabilizes as CdTe market share plateaus. By 2050, material efficiency improvements (as shown in Table 7), are projected to reduce demand to about 0.75 kt/year, largely due to stock turnover.

Nonetheless, the most significant demand for cadmium comes from the industrial sector, according to Watari et al. (2020). By 2050, demand for cadmium in applications such as alloys, pigments and alkaline batteries is estimated to reach 4.9 kt/year. This substantial external demand presents a major risk of reserve depletion and supply bottlenecks, underscoring that clean energy technologies will not be the primary driver of cadmium demand in the NZE.

Under a low -recycling scenario, there is a supply demand gap observable. Cadmium recycling is relatively high at 25% (as per UNEP, 2011), mitigating any supply bottlenecks in the high scenario. Nonetheless, demand exceeds the current determined reserves around 2050, underlining the importance of discovering new sources of cadmium. Given the importance of cadmium in various industrial processes, focusing on deployment of CdTe PV might not be feasible from a resource perspective.

5.2 Gallium

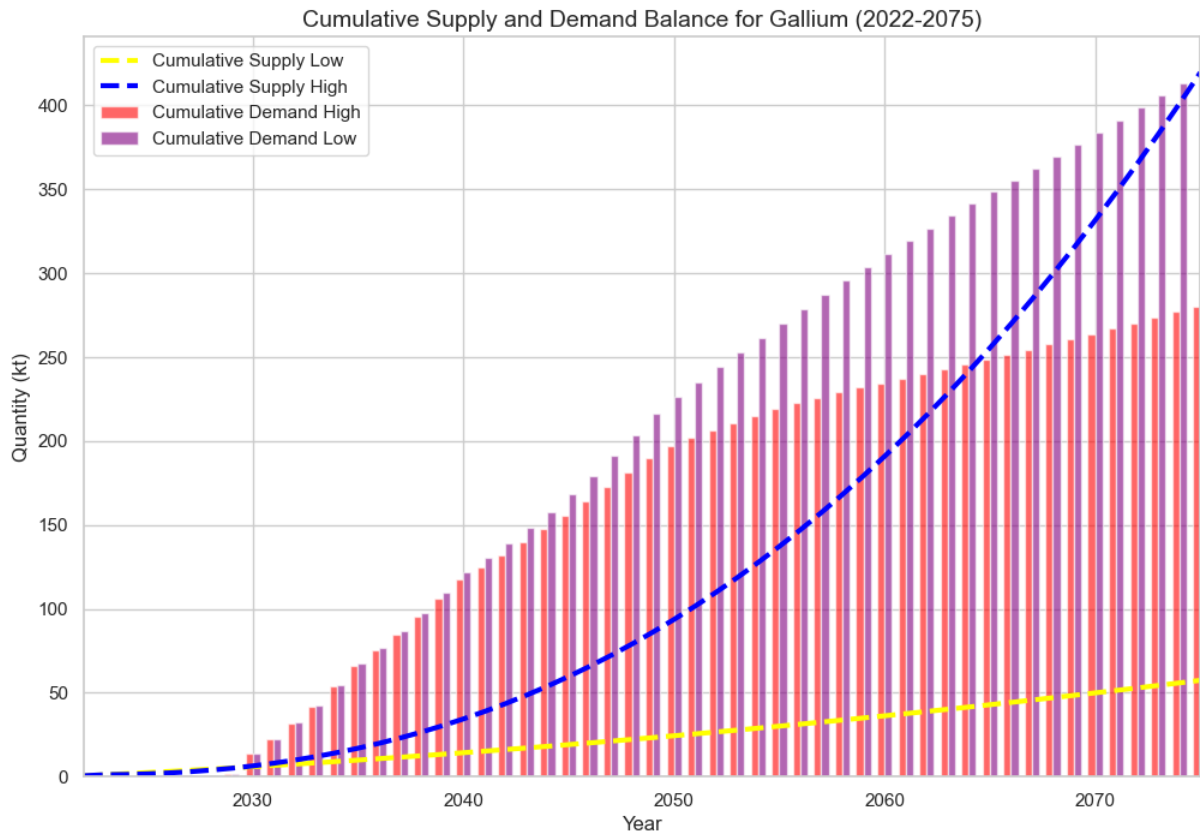


Figure 18: Cumulative Gallium Demand and Supply Balance under NZE projections in kt, 2022-2075.

As Figure 18 indicates, a significant increase of gallium content requires to be mined in order to meet future incremental demand. It was found in literature that gallium reserves are abundant, compared to the quantified cumulative demand.

As GaAs PV configurations begin to gain momentum by 2030, a significant demand-supply gap is observed. It is projected that approximately 11 kt/year is required by 2030 in order to meet NZE projections, with a 1% market share of GaAs. CISG panels demand gallium as well, while to lesser extent, as is shown in Table 7. Based on historic data, gallium mining will be insufficient to meet demand as soon as 2030. A small drop is observed in 2050, reaching approximately 11 kt, in which it further decreases to 5 kt/year by 2075, due to limited PV capacity additions. Yet, no recycling of gallium is done.

Furthermore, demand for gallium outside clean energy technologies is going to surge as well, according to Watari et al. (2019), with 1 kt/year in 2030, increasing to 1.65 kt/year by 2050. This demand is driven by its use in medical application, optoelectronics and use in high-temperature processes. It might be that gallium will be used in other applications as well, due to its unique bandgap properties (Prata & Isabel, 2012; Zhao et al., 2021; Zhong et al., 2022).

As the worldwide gallium refining is dominated by China, this further enhances the ETM's criticality. The trajectory of the gallium supply chain will significantly depend on the preferred PV technology, as the choice of GaAs PV panels over other types will drive higher demand for gallium.

5.3 Germanium

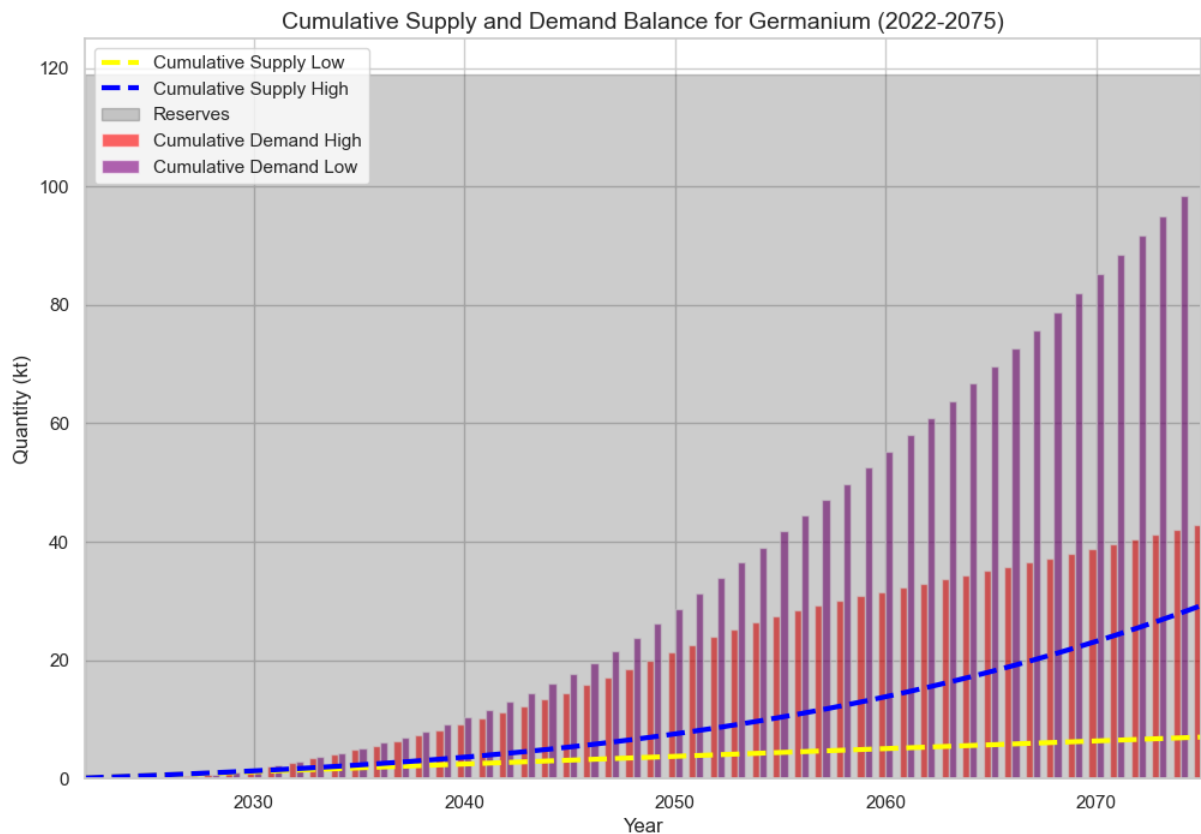


Figure 19: Cumulative Germanium Demand and Supply under NZE projections in kt, 2022–2075.

Germanium is expected to play a minor role in future clean energy technologies, with a projected demand of only 0.05 kilotons per year by 2050. This limited demand is partly due to the focus on amorphous silicon (a-Si) panels, which are anticipated to lose market momentum under NZE projections, despite their high efficiencies. However, germanium's future application in microelectronics is seen as inevitable, with its major use being in fiber-optic systems and high-brightness light-emitting diodes. Additionally, germanium is a critical semiconductor used in high-speed computer chips and other electronic components, which is expected to be a primary driver of future demand (USGS, 2024). The demand outside for these applications is estimated to reach 2.8 kt/year in 2050 (Watari et al., 2020).

The demand trajectory for clean energy technologies could shift due to the environmental concerns associated with current perovskite panels, which contain lead in their active layers. Azizman et al. (2023) propose a non-toxic tin-germanium (SnGe) perovskite PV panel that could achieve high efficiencies, although these are still in development.

Germanium is primarily co-mined from zinc deposits, and the yield observed in historic data shows fluctuations, yet increasing. If no improvements were to be made, the current extraction of germanium would not suffice with future demand. Nonetheless, with the significantly improved yields in terms of ore grades and growing importance of germanium, it might be that extraction may be improved over time. Henckens (2021) estimates that 2000 Mt of global germanium resources could be made available: with the incremental demand trend observed it safe to assume that new reserves will be exploited. Currently, germanium recycling is non-existent, but developing recycling processes is crucial for ensuring long-term availability, as a considerable difference between the two scenarios can be observed in Figure 19.

5.4 Indium

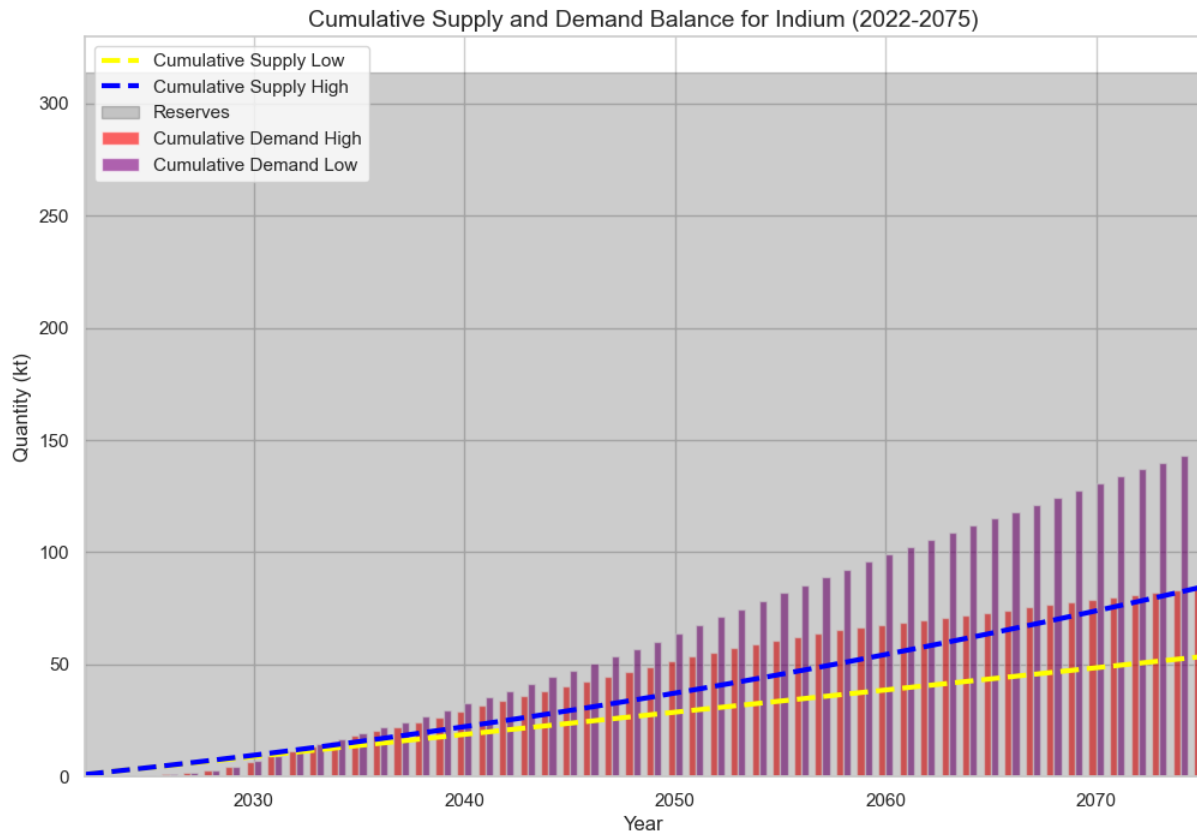


Figure 20: Cumulative Demand and Supply for indium under NZE projections in kt, 2022–2075.

Indium is demanded by both CISGS and GaAs PV configurations, reaching demand of 0.13, 1.9 and 0.96 kt/year by 2030, 2050 and 2075, respectively. This rapid increase can be observed in Figure 20, as both supply scenarios cannot meet the surging demand. A similar trend compared to gallium is observable, at the point that GaAs panels begin to gain momentum, which also contains significant amounts of indium. While demand for indium is already significant due to its application in electronics, based on historical data, a significant surge in refining needs to be done to align with future market developments.

Indium is increasingly critical to clean energy technologies, particularly within CISGS and GaAs PV configurations. The cumulative demand for indium is projected to reach 0.13 kt/year by 2030, rising sharply to 1.9 kt/year by 2050, after it stagnates to 0.96 kt/year by 2075. This steep increase is primarily driven by the expanding market share of GaAs PV panels, which begin to significantly influence demand post-2040. Indium is co-mined at electrolytic copper refining; therefore, indium supply is heavily dependent on future copper supply chains.

The demand from PV applications is expected to overtake traditional electronics by mid-century. Historically, indium has been extensively used in electronics, especially for manufacturing LCD screens, semiconductors, and other electronic components, with Watari et al. (2019) estimating that 3.3 kt/year is required by 2030 for these applications. However, the shift towards renewable energy, particularly in the PV sector, introduces a new and substantial demand stream for indium, further stressing its supply.

Similar to other thin-film ETMs, supply is dominated by China (Carrara et al., 2023). To decrease supply dependency and increase supply diversification, recycling efforts should be improved. Zhang et al. (2015) address the significant outflow of electronic materials, which could be used to ramp up recycling of indium. As indium has no primary ores, EoL flows might have higher concentrations than primary production, i.e., by vacuum carbonization, allowing high indium purity rates.

5.5 Tellurium & Selenium

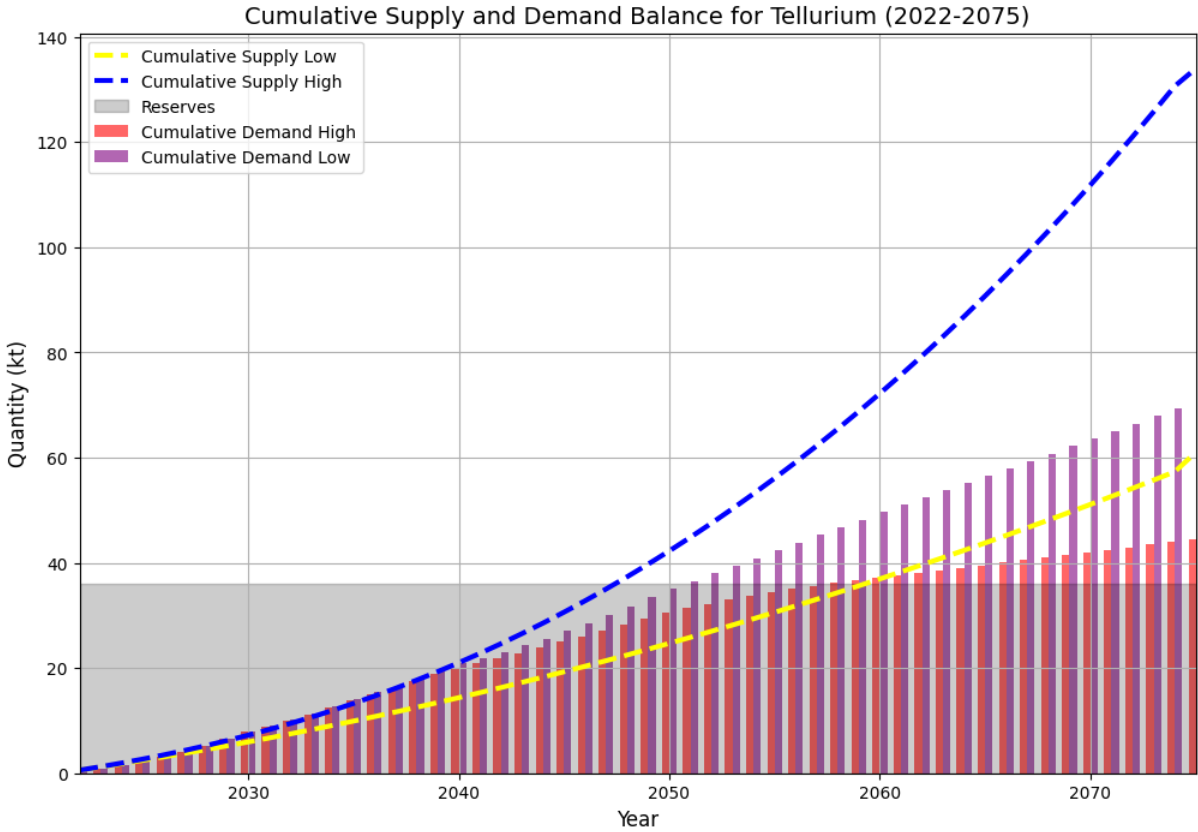


Figure 21: Cumulative Demand and Supply for tellurium under NZE projections in kt, 2022-2075.

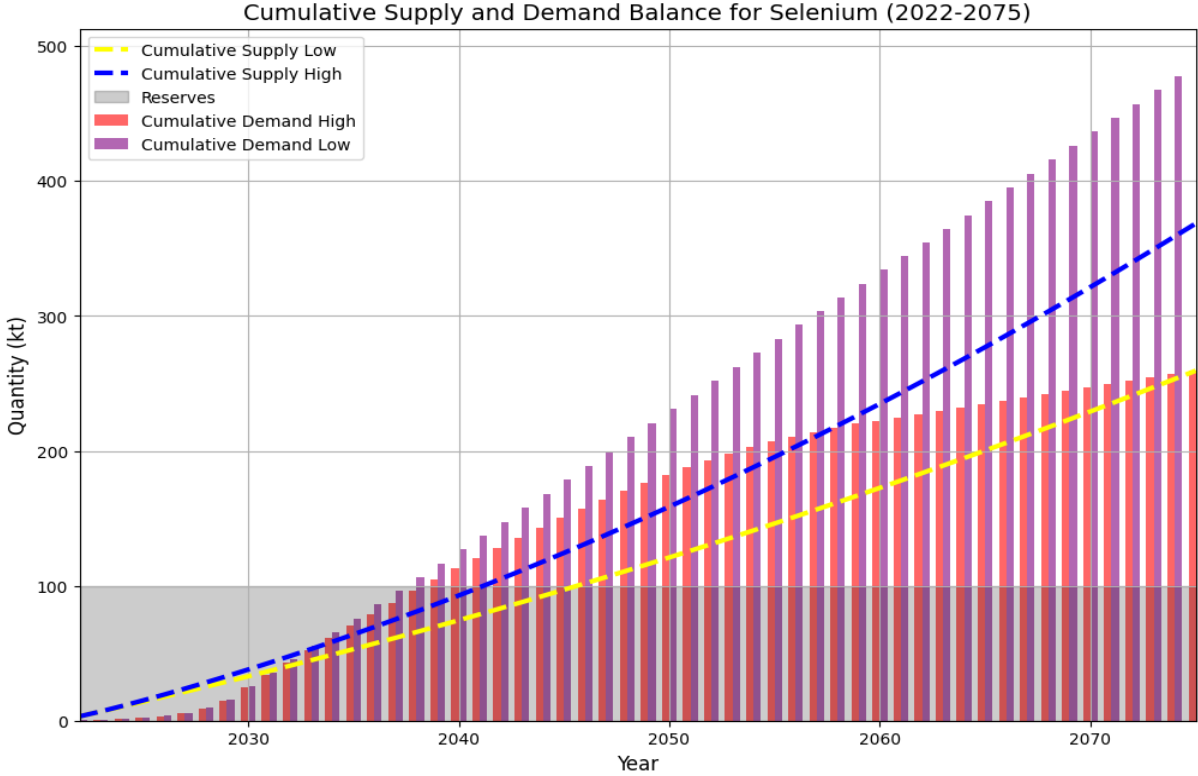


Figure 22: Cumulative Demand and Supply for selenium under NZE projections in kt, 2022-2075.

Figure 21 and Figure 22 show the supply demand trajectories for tellurium and selenium. Both ETMs are susceptible to supply risks, while both being primarily co-mined from copper extraction. Historical ore grades are low, with tellurium ore grades showing an increase. Contrarily, selenium shows a decreasing trend. Similar to other thin-film materials, a surge in refinery production is necessary. NZE projections show that CISGS panels are losing market momentum, only representing a 0.3% share in the total PV deployment. Only 0.04 kt/year is required by 2050, primarily driven by stock turnover. This trend is further extended to Therefore, it is uncertain whether this is necessary, due to the limited adoption of CISGS in the future. The share of CdTe panels is projected to be at 4%, with tellurium demand reaching 0.75 kt/year by 2050 and 0.38 kt/year by 2075.

Therefore, it could be that the demand by PV will be significantly less, and the selenium could be recovered for other purposes. Both tellurium and selenium have received increased interest in the medical applications, as an effective drug carrier, which might drive future demand (Wang et al., 2020; Ansari et al., 2024). Watari et al. (2019) estimates that approximately 10 kt/year for selenium and 0.3 kt/year for tellurium by 2030, which is further increased to approximately 12 kt/year and 1 kt/year by 2050. Current recycling rates for both ETMs are close to 0%, and no economically attractive recycling technologies have been commercialized, although in development (Li et al., 2022). Nevertheless, outflow of CISGS and CdTe will increase over time, which might enhance feasibility. For CdTe panels, it was found that cadmium has demand outside clean energy technologies as well, further raising uncertainty whether CdTe panels can achieve its market share projected in the NZE scenario.

In conclusion, it can be observed that historic supply rates for various ETMs used in PV have been low due to co-mining, and that a shift is required to more efficient extraction methods. Furthermore, these ETMs are currently mined as by-products, but with the incremental demand trends observed, the value of these ETMs will inevitably increase, making it much more attractive to focus on efficient extraction of these minerals. It is found that secondary materials which can be recovered from future outflow may provide more yield compared to primary production, therefore recycling of thin-film ETMs should be prioritized.

5.6 Cobalt

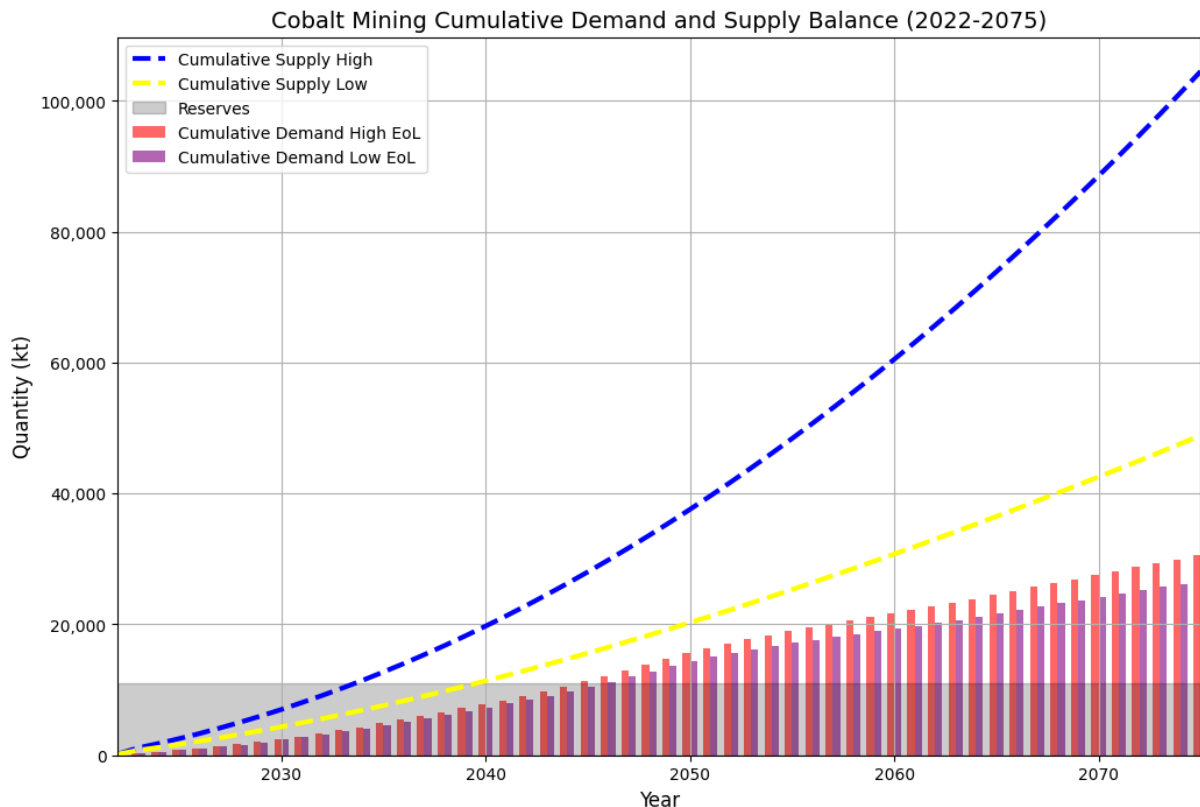


Figure 23: Cumulative supply demand balance of cobalt mining in the NZE scenario, 2022–2075.

According to the IEA (2024), 77% of global cobalt mining and 88% of refining are concentrated in just three countries, with the Democratic Republic of Congo (DRC) and China dominating these activities.

The demand for cobalt is rising rapidly, driven by its pivotal role in battery technologies. Figure 23 illustrates the cumulative demand and supply projections for cobalt, indicating that future refining trajectories will be sufficient to meet surging demand. Cobalt mining provided trends well above the projected demand, due to quick lead times of mines in Congo of 14.7 years (S&P Global, 2023). Therefore, refining trends were compared identically, which resulted in no observable supply bottlenecks. It should be noted that many EV manufacturers are trying to cut ties with Congo, due to increased interest for critical mineral passports, in response to consumer demand for environmental and ethical supply chains (S&P Global, 2024).

IEA (2024) claims that by 2050, 222 kt/year is required for catalysts, superalloys for jet engines, cemented carbides and diamond tools used in modern construction, mining and manufacturing (Gulley, 2022). With the highest demanding battery chemistry scenario, the NMC_x/Flow scenario, it was found that 1354 kt/year is required by 2050, a substantial increase from 2035, in which the projected demand was defined to be 690 kt. While current EoL RIR rates are relatively high (22%), the high recycling scenario exceeds the reserve base in 2046. Shifting to a less cobalt-intensive chemistry such as LFP, slices cobalt demand by half (641 kt/year by 2050). As car manufacturers primarily focus on NMC batteries due to its improved driving range compared to LFP batteries, the increasing costs of future cobalt extraction as reserves shrink might be a reason to shift to less cobalt-intensive batteries (Cusenza et al., 2021).

Despite ongoing efforts to reduce or eliminate cobalt usage in various technologies, it remains essential for the development of advanced battery chemistries. Low-Co options, such as the NMC₈₁₁ battery, still rely on cobalt to some extent. It was assumed that by 2050, the NMC₈₁₁ batteries gained market dominance, which still resulted in a significant demand of cobalt post-2050 (1045 kt/year including BESS applications). Additionally, NMC batteries are the preferred anode choice for ASSB indicating that cobalt will have a function in future battery technologies (Boaretto et al., 2021).

5.7 Graphite

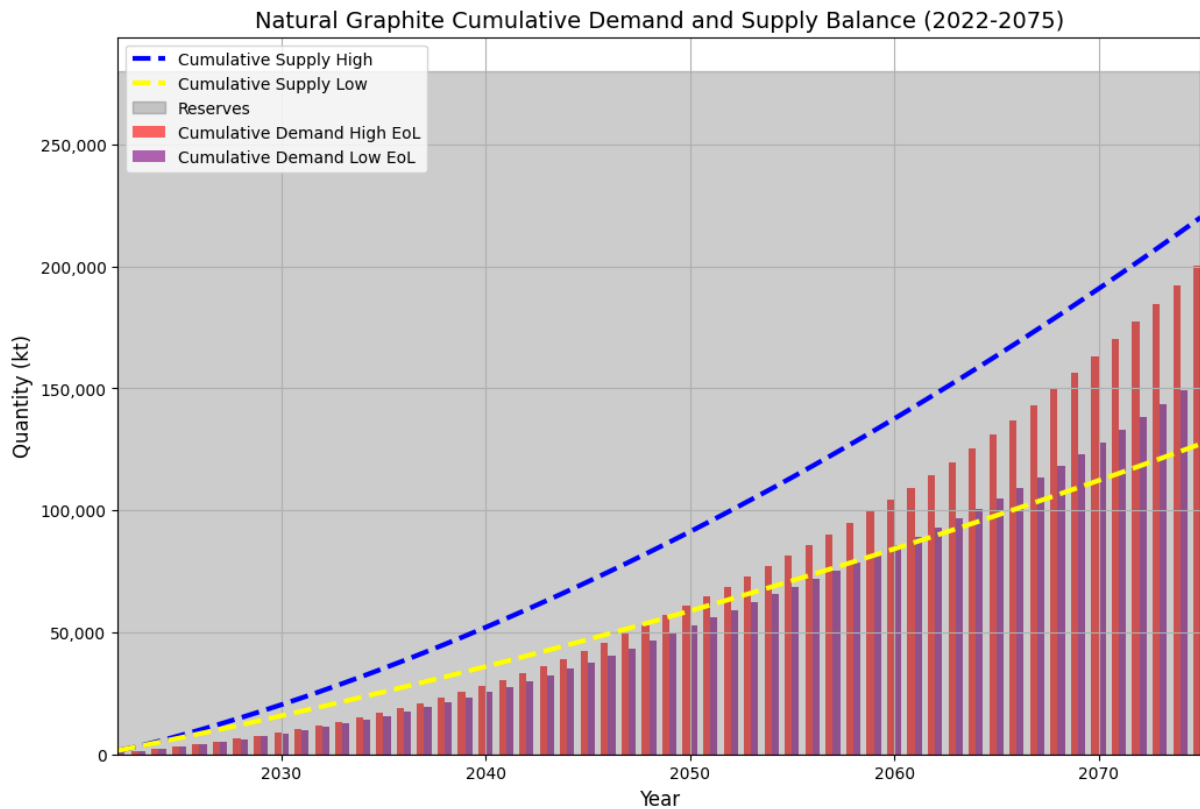


Figure 24: Cumulative supply demand balance for natural graphite mining in the NZE scenario, 2022-2075

Figure 24 provides the cumulative supply demand balance for natural graphite. It tested whether 25% of the demand could be met by natural graphite by 2075. While there is no risk for reserve depletion, it shows that a potential bottleneck for natural graphite may occur around 2050 in a scenario with low recycling. The primary demand for graphite, including the carbon-intensive synthetic graphite, reaches 14066 kt/year by 2050 in a NMC_x-Flow dominant market, which is more compared to a LIB-dominant market, which resulted in a demand of 12500 kt/year. Nonetheless, from the research it resulted that battery-grade graphite cannot be covered by natural graphite reserves. While current graphite recycling is still insignificant (around 3%), it could slice graphite demand by around 13% by 2050. It should be noted that natural graphite often has lower energy density compared to its synthetic counterpart (Barre et al., 2024).

Furthermore, battery-grade synthetic graphite refining is found to be centralized, with IEA (2024) claiming that 93% of refining is accounted for by China. Therefore, the global graphite market is centralized and short- and long-term availability might be disturbed due to geopolitical conditions. Thus, research has been done on how to decrease its dependency on graphite, for example by the development of silicon-graphite anodes, which show acceptable cost, desirable integrity and reliable lithium storage capacity (Li et al., 2020). Due to the observed production trends (Figure 40), this might be the preferred option for anodes in battery applications in the future.

Although synthetic graphite, using a by-product of petroleum production, may seem at odds with climate targets outlined in the NZE, ongoing research is focused on reducing the carbon intensity of its production. Abusueda and Fisher (2023) suggest using electricity generated from methane pyrolysis as a promising approach. This method not only produces both hydrogen and graphite with zero direct emissions but also yields high-purity hydrogen at competitive costs, which in turn causes lower demand of ETMs in electrolyzers. Finally, substitution options could be another approach in decreasing graphite demand, i.e., using an NMC-cathode, but the potential trade-off in ETM demand might be unfavorable.

5.8 Lithium

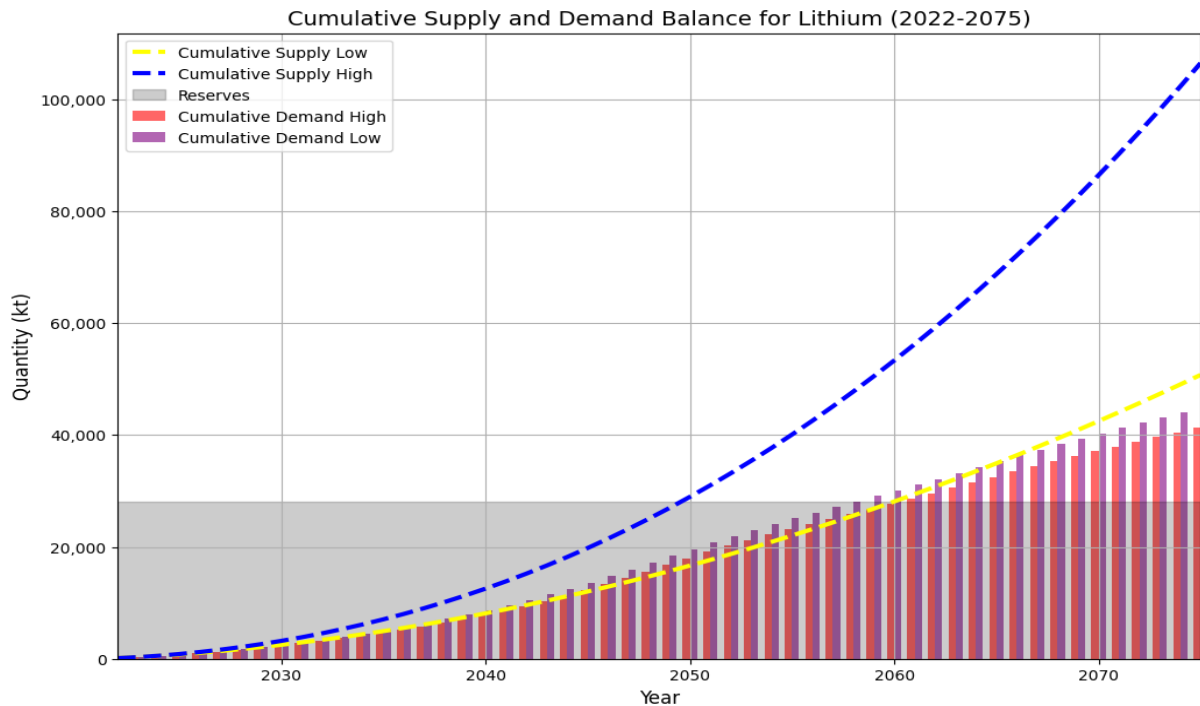


Figure 25: Cumulative Lithium Refining Demand and Supply under NZE projections in kt, 2022-2075.

Lithium demand is projected to surge in the investigated timespan, with minor differences between the investigated scenarios as depicted in Table 14. The only investigated battery chemistry not containing involved the VRFSBs, but due to the small demand in BESS compared to the vast amounts demanded by EVs, it is inevitable that lithium will dominate the global EV market. Since the future lithium demand of advanced LIBs such as Li-S and ASSBs remain uncertain due to limited data, the demand could significantly be improved by less lithium intensive batteries, or battery chemistries that eliminate lithium completely, such as sodium-ion (IEA, 2024a).

While the results show that mining is not the cause of future supply bottlenecks, Figure 25 indicates the two obtained trajectories for refining of battery-grade lithium. The low supply scenario only shows a minor supply demand gap. While the low recycling scenario does exceed supply quantities, it does recover to restore supply demand equilibrium. Strategic reserves could be an approach to avoid potential supply short term shortcomings.

Finally, lithium reserves will be exceeded in both recycling scenarios. Figure 25 provides the reserves in 2000 and 2023, equal to an increase of approximately 17000 kt. It is therefore likely that new deposits will be discovered, or that new techniques for extraction may become feasible. An example is Direct Lithium Extraction in geothermal energy production: at high temperature, lithium-rich fluid is pumped to the surface, heat is removed from the brine and used to drive a turbine, and lithium is extracted from the brine before the brine is injected into the ground, reaching high purity lithium. Through this synergy, geothermal energy is proven to become financially feasible (CEC, 2024).

Table 14: Lithium demand under NZE projections under the investigated scenarios for selected years in kt/year

kt/year	2035	2050	2075
Li-ion	455	1293	872
NMC_x	521	1262	894
Li-ion (BESS)	85	64	85
Flow	110	61	68

5.9 Manganese

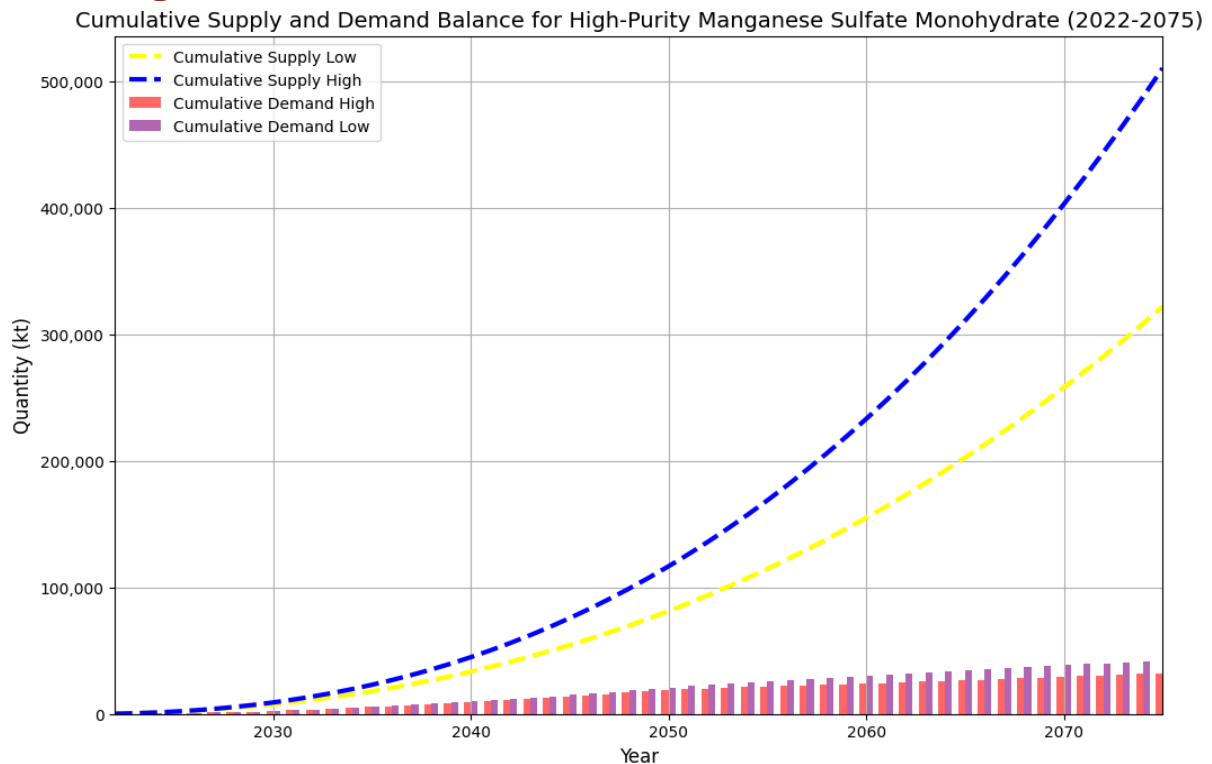


Figure 26: Cumulative demand and supply balance for HPMSM under NZE projections in kt, 2022-2075.

Although manganese reserves are vast (1.9 million kt), S&P Global (2024) addresses that manganese refining to HPMSM are lacking, claiming that only around 1% is currently refined to be used to battery-grade applications. As EV manufacturers are trying to cut their reliance from cobalt and Congo due to ethical and environmental implications, as well as that more manufacturers are adopting critical mineral passports, it is inevitable that manganese will be the preferred battery ETM in the future. However, it is hampered by the dominance of HPMSM refining by China. It is found that by 2050, HPMSM demand will reach 1220 kt/year, more than double compared to the 2030 value (529 kt/year) under the manganese intensive NMC_x-Flow scenario.

It seems that for HPMSM, short-term supply bottlenecks will occur for the deployment of battery chemistries containing HPMSM, as is shown in Figure 26. It was assumed that the total manganese suitable for battery applications would increase to 30% by 2075, following a linear increase. It can be observed that HPMSM will endure short-term bottlenecks, as new refineries have to emerge the coming decade. In other battery-grade materials such as lithium it was shown that refining can rapidly scale up, eventually allowing cost-efficient high-manganese battery chemistries. Cobalt has not only shown to have ethical implications but also a tense supply chain. Regardless, it is uncertain whether this can be achieved, due to centralization of refining in China and limited data availability.

A key consideration in this context is the feasibility of using recycled HPMSM for battery-grade applications. Research indicates that while recycling can reduce material demand, the quality and purity of recycled HPMSM must meet stringent standards for reuse in batteries (Zeng et al., 2018). Still, with the abundant amount of manganese that is extractable, as well as the amount of manganese that is could be refined, this should not be a major bottleneck from a resource perspective. Nonetheless, to decrease environmental impact of HPMSM refining and manganese extraction, it is still essential to advance recycling technologies and establish robust quality control measures to ensure that recycled HPMSM can fulfill the requirements for battery-grade materials.

Manganese is used in wind turbines as well for steel production, corrosion resistance and more some electronic components. It is projected that this demand will reach 300 kt/year by 2030, and this value will remain stable until 2050, with 313 kt/year. By 2075, due to limited wind capacity additions and primarily stock turnover having the most ETM demand, it will drop to 107 kt/year. It is found that each investigated wind turbine will need a significant amount of manganese, as is shown in Table 8. Therefore, wind turbines will prove a valuable source of manganese in the future. Outside power, manganese is had a wide array of applications, as it is essential in iron and steel production due to its sulfur-fixing, deoxidizing and alloying properties (USGS, n.d.). Watari et al. (2020) estimates that a total of 18000 kt/year of manganese is required for all these applications by 2050.

5.10 Nickel

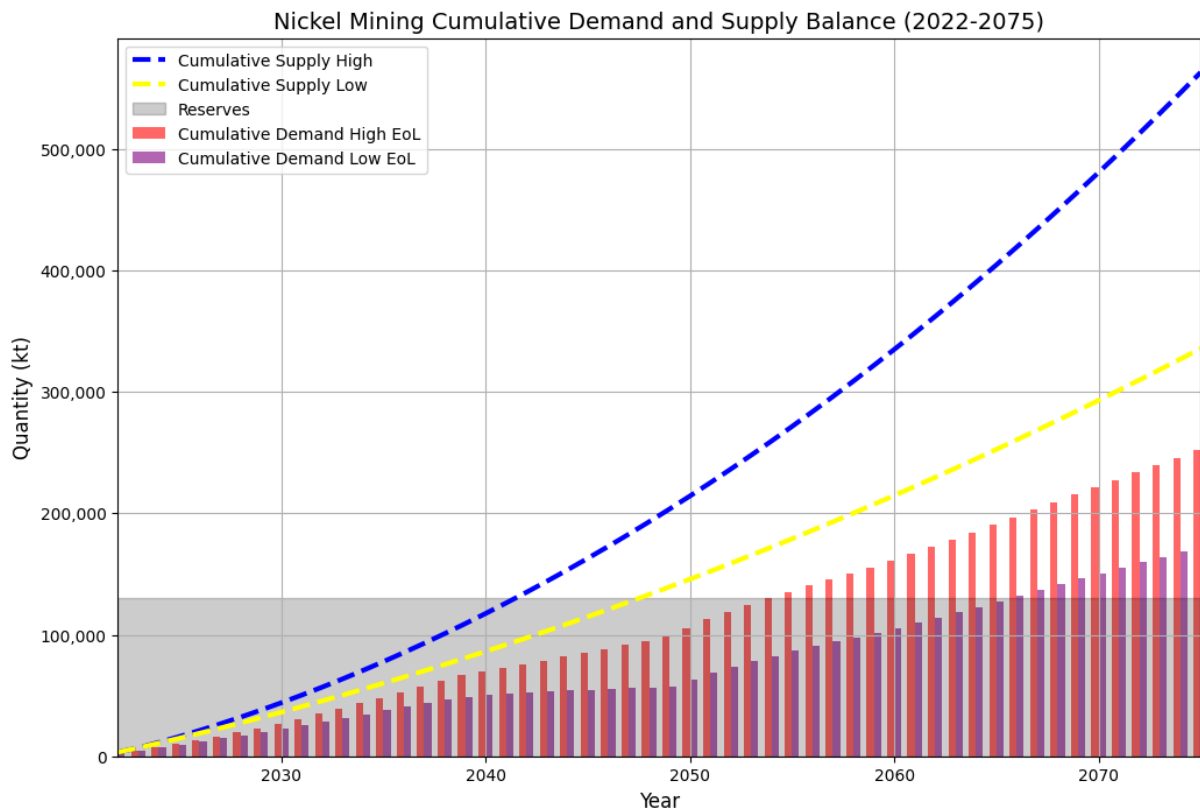


Figure 27: Nickel Supply Demand Balance under NZE projections in kt, 2022-2075.

Nickel was found to have a role in a wide variety of clean energy technologies. Table 15 provides the overview of demand for each investigated technology. For battery-applications, nickel demand is heavily dependent on the choice of dominant battery chemistry. With the introduction of market dominance by 2050 for the nickel-intensive NMC₈₁₁, a surge of demand is expected, which also explains the surging trend post-2050 in Figure 27. Complete elimination of nickel use in BESS applications is achievable with increased penetration of nickel-free VRFSBs. For wind applications in which nickel is used for its corrosion resistance and in the production of stainless steel, manganese could be used as a substitution material. For electrolyzers, nickel is used for its catalytic properties, and substitution with i.e., aluminum would decrease the energy capacity of the electrode (Filho et al., 2024). Therefore, it is uncertain whether substitution of nickel in some applications can be considered favorable.

Under the low recycling scenario, it is expected that risk of reserve depletion is high, while under a high recycling scenario, this risk is only postponed. No supply bottlenecks were observed. Furthermore, nickel refining is less centralized compared to other battery materials, as Indonesia is the dominant player in this market; most of the world's nickel is coming from Indonesia as well. Primarily, refined nickel is sold to produce steel, (super)alloys, catalysts and plating (USGS, n.d.)

Nonetheless, it is found that nickel recovery from batteries is already economically feasible. Unlike HPMSM, the grade of recycled nickel from recovered outflow is sufficient for re-use in batteries, and with matured technologies such as hydrometallurgy and pyrometallurgy as the main recycling processes for nickel, nickel EoL RIR rates are already at 17%. Therefore, it seems safe to assume that nickel recycling rates will be significantly improved over the short term, especially when outflow becomes more available. This recycling is required in order to mitigate potential risk of reserve depletions, as there are no significant new discoveries of nickel reserves (USGS, n.d.).

Table 15: Primary Demand for nickel in the NZE scenario for selected years, in kt/year. (*) is extrapolated based on observed growth rates.

Clean energy technology	2035	2050	2075
EV Li-ion	832	3026	2092
EV NMC _x	2422	8459	5848
BESS Li-ion	85	5	0
BESS Flow	262	181	302
Wind	142	140	50
Electrolyzers	16	123	236
Total Li-ion	1075	3294	2378
Total NMC _x /Flow	2842	8903	6436
Demand outside clean energy technologies (IEA, 2024)	2998	3354	3473 (*)

5.11 Copper

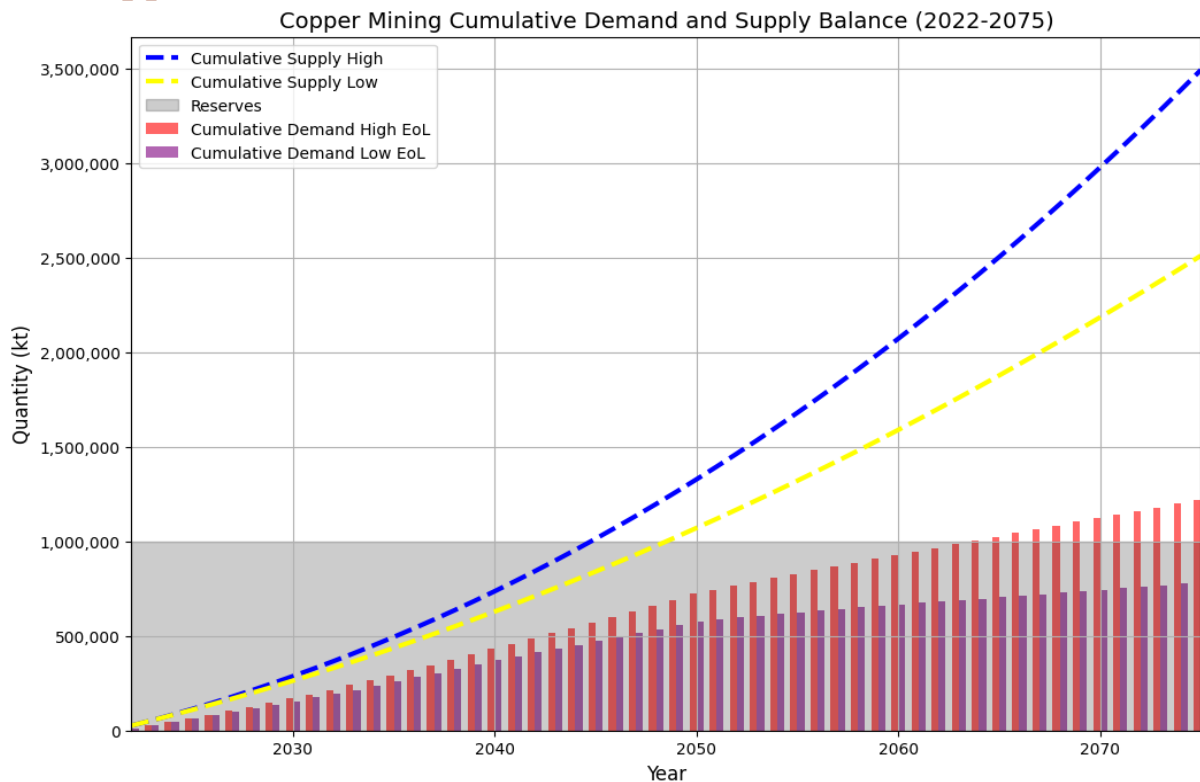


Figure 28: Cumulative Supply Demand Balance for Copper under NZE projections in kt, 2022–2075.

Copper is found to be pivotal in electrification, with a wide variety of applications, as shown in Table 16. According to the analysis, the most demanding element is found to be infrastructure, with a demand of 13916 kt/year by 2050. Transformers in high-voltage transmission grids were found to be very copper-intensive, as is observed in Figure 28. The demand for copper is found to be substantial in EV application but is very dependent on the dominant battery chemistry. NMC_x was found to be less copper-intensive compared to its LFP counterparts. This is also found in BESS applications. A small discrepancy can be observed in the 2075 value for BESS Li-ion, due to increased capacity additions of copper-intensive BESS configurations.

Wind energy deployment is expected to increase copper demand significantly by 2050, particularly due to the material-intensive nature of offshore configurations. Conversely, PV systems show a stable trend in copper demand, partially attributed to the limited adoption of CIGS technology. Due to a combination of material efficiency improvements and limited capacity additions, the copper demand for these renewables is expected to drop by 2075, primarily driven by stock turnover.

As shown in Figure 28, the cumulative supply-demand balance for copper suggests that while mining and refining capacity may meet incremental demand, the risk of reserve depletion remains a concern. IEA (2024) claims that copper demand outside of clean energy technologies is 21473 kt by 2050, leading to a potential risk of reserve depletion in the low recycling scenario by 2064. Nonetheless, this can be mitigated significantly through efficient EoL practices. By 2050, implementing high EoL efficiency could reduce primary copper demand by 36%, compared to a low EoL scenario. This impact is even more pronounced by 2075, with a potential 68% reduction in primary demand.

Despite the maturity of copper recycling—with EoL RIR currently at 55%, according to UNEP—there is considerable potential for improvement. Effective utilization and collection of in-use copper stock are crucial for ensuring long-term availability. Furthermore, is uncertain to what extent the IEA estimates the substitution of copper in future infrastructure by aluminum, which is found to be much more abundant (Figure 41). Nonetheless, according to Hoekstra (2023), it is feasible, although aluminum has only 60% of copper's conductivity. In contrast, aluminum wiring will have half the cost and weight of an identical copper cable. Therefore, a slight increase in copper costs could result in aluminum being the preferred option in cabling, significantly reducing copper demand in clean energy technologies. Additionally, a study published by Tost et al. (2020) highlights that primary aluminum has the greatest potential for replacing copper in energy infrastructure, further emphasizing the potential impact of material substitution.

Table 16: Primary Copper demand over all investigated technologies under the NZE, 2022-2075

[kt/year]	2035	2050	2075
EV Li-ion	3317	9723	6726
EV NMC_x	2295	6301	4356
BESS Li-ion	1087	697	859
BESS Flow	863	505	339
Wind	934	1119	440
PV	2599	2589	1297
Infrastructure	13072	13916	9933
Total [Li-ion]	21639	28044	19255
Total [NMC_x/ Flow]	20393	24430	16365

5.12 PGMs

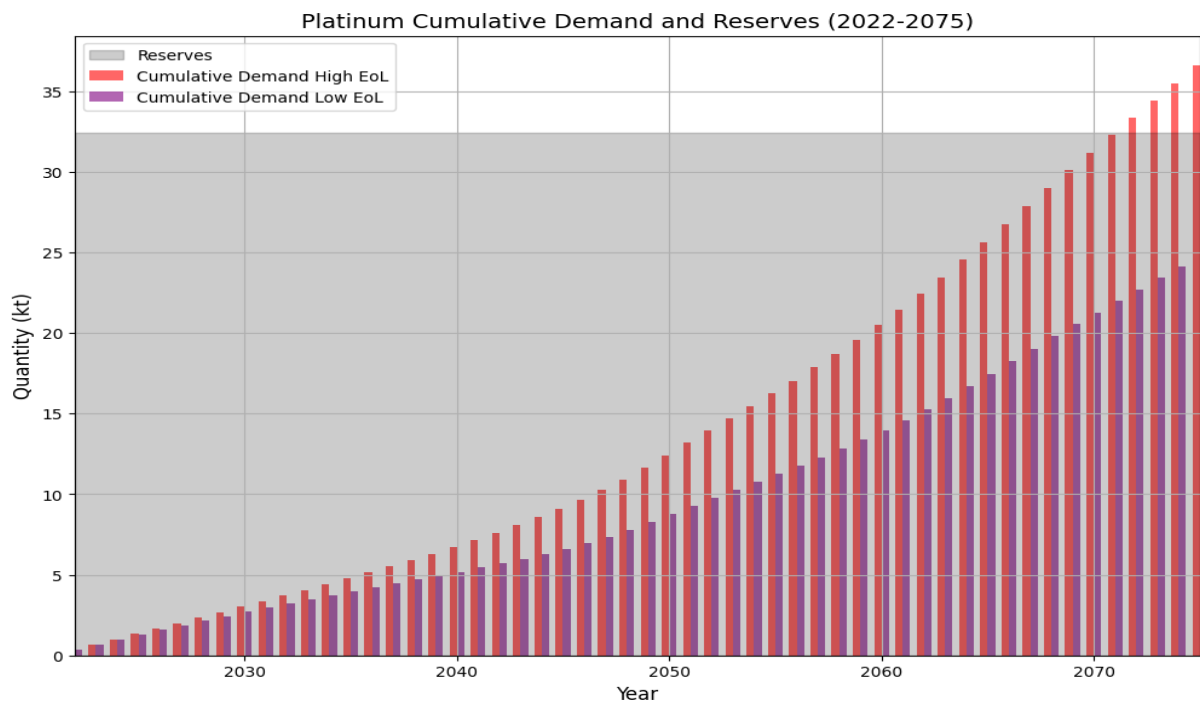


Figure 29: Platinum Cumulative Demand under NZE projections in kt, 2022-2075. Supply was found to be abundant.

Historically, the demand for PGMs has been significant due to their application in catalytic converters for fossil fuel vehicles. According to Grilli et al. (2023), currently, 80% of PGM demand is driven by the automotive industry to comply with stringent environmental standards. However, the role of PGMs in clean energy technologies, particularly in FC vehicles, is also noteworthy.

In the coming decades, the demand for PGMs in FCs is expected to surpass that in catalytic converters. By 2050, an estimated 0.4 kt/year of palladium and platinum will be required for FCs, assuming a 1:1 ratio in catalyst coating. Additionally, PEM fuel cells will necessitate another 0.009 kt/year, although advancements in material efficiency are projected to reduce this requirement over time (IRENA, 2020). Moreover, palladium is found to have tighter reserves as can be found in Figure 46.

Iridium, primarily used in solid oxide electrolyzers, has been excluded from this analysis due to limited reserves (1.53 kt) and the lack of market momentum for these electrolyzer (Hughes et al., 2021). Figure 29 indicates that reserve depletion risk is significant only in scenarios with low recycling rates. Thus, it is anticipated that alkaline and PEM electrolyzers will dominate the market. High recycling can alleviate supply chain tensions.

PGM demand beyond clean energy technologies remains substantial, with an estimated 0.46 kt/year required for various industrial applications. PGMs are extensively used as catalysts in the partial oxidation of ammonia to produce nitric oxide, a key component in fertilizers. Additionally, PGMs are prized in the jewelry industry due to their resistance to tarnishing and corrosion. In scientific research, PGMs facilitate the growth of single crystals, particularly oxides, which are essential in various advanced materials applications (USGS, n.d.).

The USGS provides aggregated data on PGM supply, indicating a potential mining capacity of 1700 kt based on extrapolation, suggesting no supply bottlenecks. However, the fluctuating and generally increasing prices of PGMs introduce uncertainty in future supply and demand dynamics (Bao, 2020).

Recycling rates for PGMs are significant, with the UNEP reporting an EoL RIR of 12%. The increasing outflow of automotive catalysts, coupled with rising PGM prices, enhances the feasibility of recycling. Incorporating the outflow of automotive catalysts into the analysis could substantially reduce the primary demand for PGMs, especially if high recycling rates are achieved (Tang et al. (2023).

PGM prices play a crucial role in determining the feasibility of their applications and the efficiency of recycling processes. Soaring prices can incentivize the development of more efficient recycling technologies and alternative materials, potentially reducing reliance on primary PGM sources. Conversely, lower prices might discourage recycling efforts and investment in alternative technologies, increasing dependence on primary PGM mining.

5.13 Rare Earth Elements

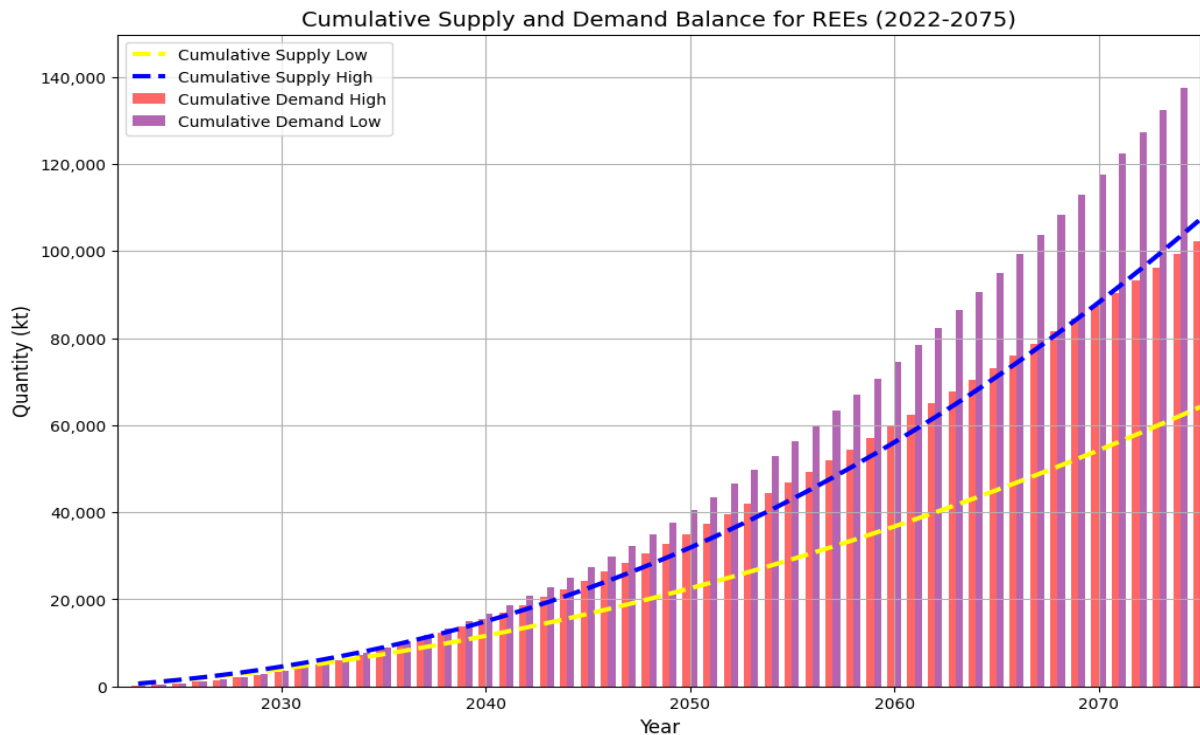


Figure 30: Cumulative REE Demand and Supply under NZE projections in kt, 2022–2075.

No risk of reserve depletion was found for the investigated REEs and can be found in chapter S4. As the market share of solid oxide electrolyzers is insignificant under NZE projections, yttrium and lanthanum have been excluded from the analysis. Yttrium and lanthanum (and cerium) are the cheapest and most abundant of all REEs according to Liu et al. (2023). As mentioned in 2.1.4 Co-mining, REEs are co-mined, meaning that an increase in production of one will result in an increase in another. Therefore, it was decided to analyze the aggregated supply curve for REEs with the individual minerals. It should be noted that, while literature exists for determining REE demand outside clean energy technologies, the range of applications for REEs including electronics, defense and industrial processes with each having different growth trajectories, making it complex to estimate. Moreover, companies and manufacturers often disclose any information about REE use.

This is shown in Figure 30. As the demand data only provides demand by the investigated REEs (Dyprosium, Neodymium, Praseodymium and Terbium, which analysis can be found in S.8 Supply Demand Analysis) the extrapolated supply data shows a minimal supply demand gap. Given that cerium and lanthanum are much more abundant in REE-oxide ores, it is uncertain whether sufficient REEs can be supplied to meet incremental demand. Industrial separation is complex due to similar physical and chemical properties of REEs, and the most common technique used is solvent extraction. The associated environmental impacts of this process are severe due to energy, water and chemical use (Zapp et al., 2022). New techniques are on the rise, such as membrane separation technology, which shows excellent potential for upscaling and is found to be more economical with easier operation (Bashiri et al., 2021). Therefore, new developments might accelerate REE extraction and refining in the future.

Despite the critical role of REEs, current recycling rates remain very low. Recycling of REEs offers various advantages compared to primary production, as recycling can avoid the costly extraction of the low-value REEs (lanthanum and cerium), and EoL products often have greater REE concentrations compared to primary sources. While recycling of REEs is complex, given the many process steps, it does provide unique opportunities, the yield in EoL can often be higher compared to primary ores (Fujita et al., 2022; Balaram, 2023). Substitution options, such as induction motors or HTS wind turbines, can cut the need for REEs in electric vehicles and wind turbines, therefore alleviating demand pressures.

6. Sensitivity Analysis

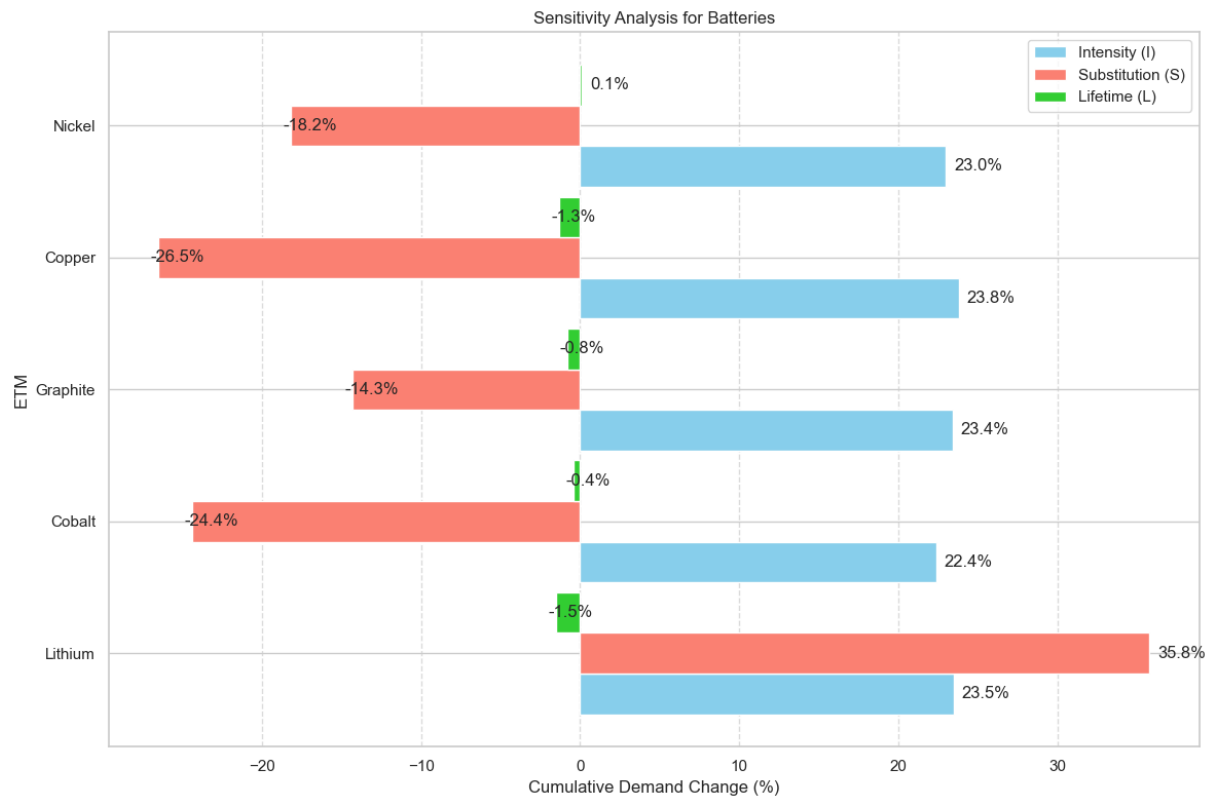


Figure 31: Sensitivity Analysis Batteries

Several factors have influenced the outcomes of this study, with two main variables emerging as pivotal, material intensity (I) which includes battery sized, and lifetime. Only the ETMs driven by demand in clean energy technologies which resulted in potential supply bottlenecks, will be explored here, as shown in Figure 31 for batteries.

The effect on ETM demand of ASSB application in EVs has been explored, which according to Liang et al. (2023), do not use any copper, cobalt, graphite. Although current lithium refining and supply trends show no immediate concerns, limited reserves of lithium could pose future challenges. ASSBs would only be feasible for widespread EV adoption.

Next is material intensity, in the case of batteries, battery size. For LDEVs, an battery capacity increase of 80 kWh was integrated, for HDEVs to 500 kWh and for 2/3 wheelers to 75 kWh. Etxandi-Santoloya et al. (2022) claims that it is unlikely that future battey size exceed 70 kWh for LDEVs as has been used in this research, however it is still interesting to see the impact of battery size to ETM demand, which is found to be significant for all materials, suggesting that future EV manufacturers might prefer smaller batteries to reduce material demand, and thereby reducing costs.

It can be noted that lifetime only has small impact on the total ETM demand of batteries. For both BESS and EV applications, lifetime has been extended with 5 years. While this extension slows the metabolic rate, it does not have significant impact on the obtained ETM demand. If the analysis timeframe was to be shortened to i.e. 2050, a future technological cycle might not be accounted for, potentially leading to surging ETM demand due to an increasing car stock, with outflows occurring beyond the scope of the research.

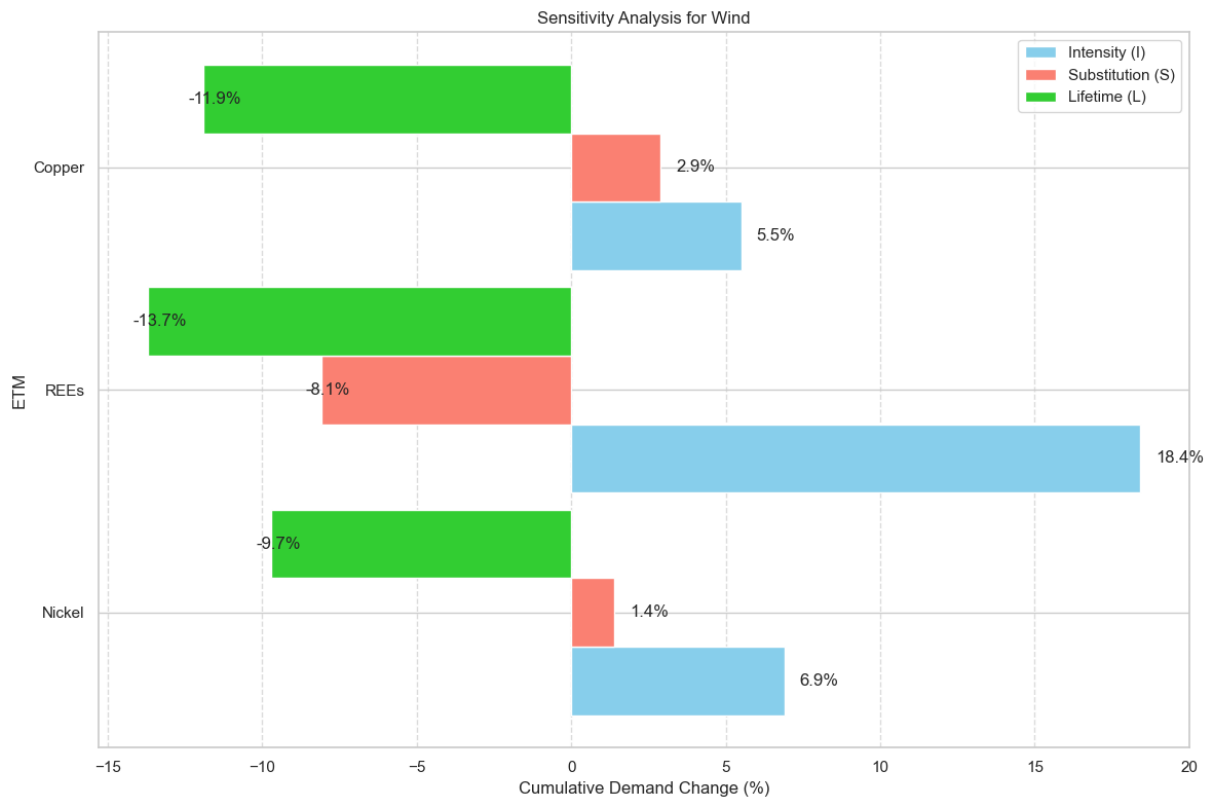


Figure 32: Sensitivity Analysis for Wind

Figure 32 provides the sensitivity analysis for wind. It reveals that lifetime has a significantly higher effect: less stock turnover is required within the investigated timespan. Regarding substitution, an increased share of non REE-intensive configurations, such as GB-SCIG and DD-EESG have been explored. While it significantly reduces the demand for REEs, it does increase the amount of copper needed, as these configurations are found to be more copper-intensive. Furthermore, keeping material intensity constant over time leads to a significant increase in REE demand. Material intensity needs to be prioritized, as it significantly reduces the amount of REEs required in wind configurations.

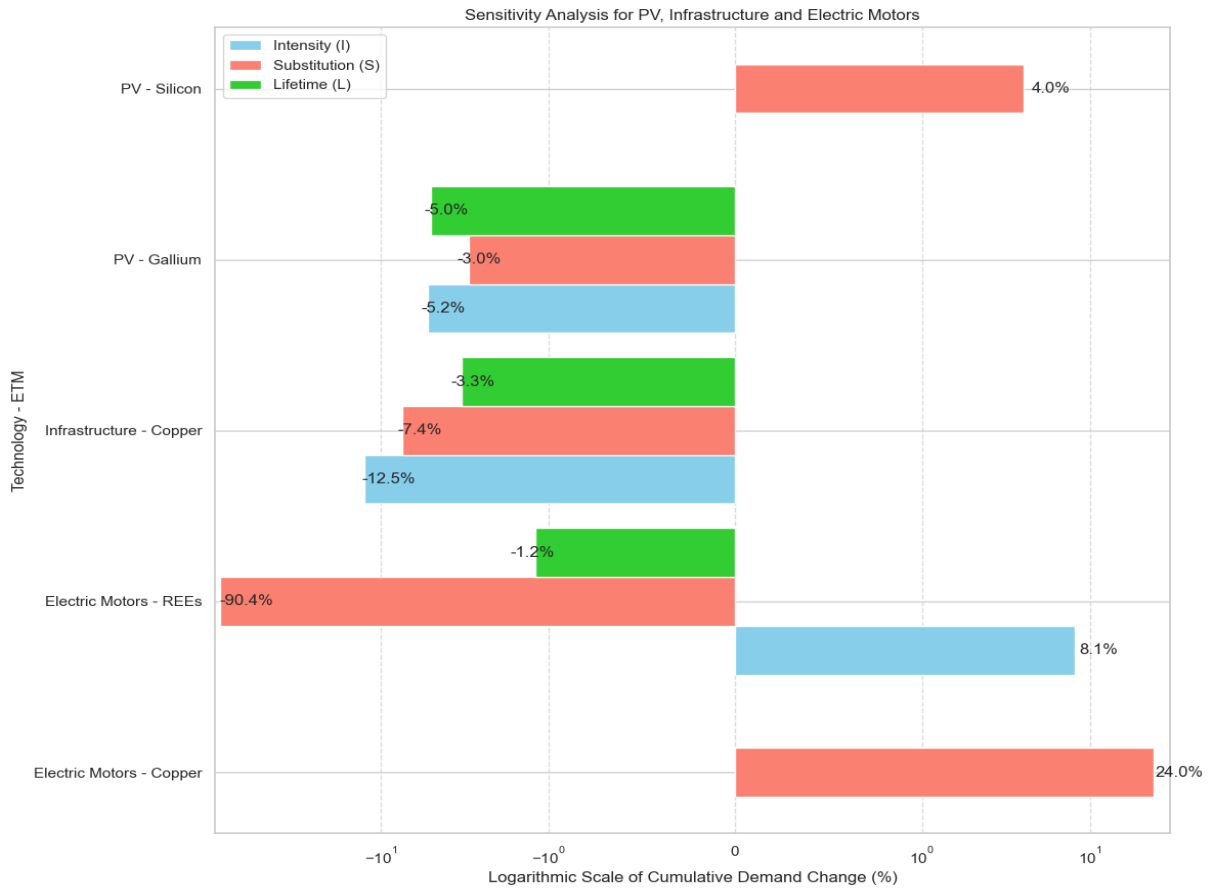


Figure 33: Sensitivity Analysis for PV, infrastructure and electric motors, with a logarithmic scale.

Finally, Figure 33 shows the sensitivity analysis on a logarithmic scale for PV, infrastructure and electric motors. For PV and infrastructure, with a lifetime extension of 5 and 10 years respectively, a cumulative demand change of 5% and 3.3% is observed, due to less stock turnover in the investigated timespan.

For PV, as it was assumed that GaAs only would enter the market around 2030 and no material efficiency improvements were included in this research,. A hypothetical 20% improvement based on other PV material intensities was tested, showing only minor effects. If GaAs remains a niche technology, and c-Si panels maintain their market share over time, silicon demand might be a material trade-off. For infrastructure, as it was unknown how much aluminium should be used in order to replace an identical copper cable, it was analyzed how HVDC lines would impact the overall material use of infrastructure.

After 2035, it was assumed that 10% of the lines would be HVDC, which according to IEA (2022b) has 79% less copper use compared to conventional transmission lines. Even this minor share has significant impact on the ETM demand of infrastructure. Additionally, a 20% reduction in material intensity would decrease cumulative demand by 12.5%

Finally, it was analyzed if 50% of the total EV fleet would benefit from the inclusion of a copper-intensive induction motor. While it significantly slices REE demand, the amount of copper used is significantly increased. Due to the wide array of applications that copper is utilized in, this might not be feasible. Moreover, compared to REE use in PSMSM applications in wind turbines, the cumulative demand change is neglectable.

A constant material intensity, as was found before, is also not feasible in electric motors. The sensitivity analysis highlights that material intensity is crucial in determining ETM demand for clean energy technologies, with lifetime effects being heavily affected by the timeframe. While strategies like substitution and efficiency improvements can mitigate demand for certain materials, trade-offs often arise, emphasizing the need for careful management of resources to ensure sustainable growth in these technologies.

7 Discussion

7.1 Demand comparison

Watari et al. (2020) addresses several key challenges in long-term material demand research. A significant issue highlighted is the lack of long-term demand outlooks for certain materials, as many projections, including the IEA, only extend to 2050. This limitation restricts comprehensive planning for materials expected to play pivotal roles in future energy deployment. Additionally, the research identifies a lack of detailed projections for specific ETMs, such as ETMs used in thin-film applications. Moreover, it emphasizes the importance of considering the growth of emerging technologies such as robotics and medical applications. These could significantly impact the availability and cost of essential materials to the energy transition, thereby influencing the feasibility and cost-effectiveness of clean energy technologies.

Table 17 compares demand projections found to have supply implications including lithium, gallium, copper, battery-grade manganese HPMSM, and nickel across various scenarios, highlighting significant differences and trends. For example, lithium demand projections vary notably between the STEPS and NZE scenarios, with NZE projecting 616 kt/year by 2030 and 1573 kt/year by 2050, compared to 381 kt/year and 964 kt/year in the STEPS. When compared to other studies, these differences become more pronounced, indicating the need for more consistent and detailed modeling approaches.

Copper projections provide an even broader range of estimates. The obtained value in this research is significantly higher than the ones obtained in the NZE projections, with 26175 kt/year expected in 2050 in this research, while NZE projections demand 19239 kt/year. This might have to do with the assumption of constant material efficiency over time for infrastructure. It is also unknown to what extent HVDC lines and substitution with aluminum were considered in the deployment of infrastructure. Comparing to other literature, even less copper is demanded, but this could be due to the adoption of outdated climate scenarios, as is the case in Deetman et al. (2020) and Watari et al. (2020).

Gallium demand presents a significant point of divergence. The NZE scenario predicts substantial growth in gallium in the coming decades, which has also been quantified in this research. Although current developments under STEPS suggest a more moderate increase, yet notable. Literature indicates that while GaAs will play a role in PV deployment, it may not be as dominant as the IEA projections.

Battery-grade manganese, HPMSM, is projected to see increasing demand in both the NZE and STEPS scenarios, largely due to a shift from cobalt-intensive battery chemistries towards more ethical alternatives. Discrepancies arise due to the IEA's focus on lithium-manganese-iron-phosphate (LMFP) batteries, which have a similar range to their NMC counterparts. As these were outside the scope of this study and limited data was available, it helps explain the differences observed between the obtained value and other literature, which focuses on nickel-intensive battery chemistries such as NMC₈₁₁. Furthermore, sodium-ion batteries were not considered in this research, which only uses some copper and aluminum, but IEA (2024a) claims that due to price developments of lithium, LIBs are the preferred choice.

The demand projections after 2050 are primarily driven by conservative assumptions, as it was observed that most growth rates (apart from electrolyzer capacity and BESS) were less significant in the 2040-2050 period compared to the initial phase. Nonetheless, stock turnover will play a significant role from this point on, which has resulted in lower material demand, but still considerable. Moreover, uncertainties remain regarding growth trajectories for other sectors, and the confidentiality of material compositions of high-end technology complicates accurate prediction of future demand.

Technology choice appears to be a crucial factor in future ETM demand development. For instance, while tellurium refining capacity is currently mined as a by-product, the NZE projections indicate a higher penetration of CdTe. If this capacity is not enhanced in the short term this will have disadvantageous effects on the costs and feasibility of CdTe panels. Other tradeoffs should be considered as well, for example perovskite PV panels. While using fewer ETMs and comparable or higher efficiencies, lead-based perovskite are highly toxic (O'Connor & Hou, 2021). Similarly, while the IEA suggests that LMFP batteries will be dominant battery chemistry, current HPMSM refining is not in line with the projections made by the NZE. Another example is the substitution of PMSMs with induction motors, which have shown to have a significant material tradeoff, thereby eliminating REE demand, but in turn are very copper-intensive, all at the cost of efficiency (de Almeida & Greenberg, 2004). HTS technologies are promising technologies as well, with potentially higher efficiency compared to conventional wind configurations, but still use various CRMs such as copper.

Concluding that there is a need for more robust and detailed approaches in long-term material demand research, particularly for emerging technologies. Addressing the highlighted gaps is crucial for ensuring resource availability at a reasonable price. Collaboration across sectors will be essential to develop resilient supply chains and invest in alternative technologies that can support a sustainable future.

Table 17: Comparison of Lithium, Copper, Gallium, HPMSM and nickel demand across various sources in kt/year for selected years

Author	2030	2050
Lithium		
IEA, STEPS	381	964
IEA, NZE	616	1573
Computed Value	630	1354
Liang et al. (2023)	400	1750
Watari et al. (2020)	350	1330
Copper		
IEA, STEPS	10542	12967
IEA, NZE	15046	19239
Computed Value	26853	26175
Watari et al. (2020)	3823	12492
Deetman et al. (2018)	9000	17200
Gallium		
IEA, STEPS	0.2	5.0
IEA, NZE	13.25	18.8
Computed Value	11.1	12.8
Lovik et al. (2016)	2.8	5.3
Watari et al. (2019)	1.0	1.7
HPMSM		
IEA, STEPS	328	1854
IEA, NZE	524	2258
Computed Value	834	1220
Liang et al. (2023)	410	600
Watari et al. (2019)	272	1048
Nickel		
IEA, STEPS	1585	2074
IEA, NZE	2794	3094
Computed Value	2862	3166
Liang et al. (2023)	3000	4500
Watari et al. (2019)	1100	4500

7.2 Supply comparison

This research underscores the distinction between 'reserves'—the portion of global resources that can be economically extracted under current technological and market conditions—and resources,' which encompass all known and potential material sources, regardless of their present economic feasibility. Technological advancements, exploration, and upscaling may reduce extraction and refining costs, which will convert global resources into economically viable resources. Nonetheless, even if resources are abundant, their extraction is hampered by logistical, economic and environmental challenges. For instance, marine deposits, while abundant in certain minerals, are difficult to access and have the potential for severe environmental implications. The environmental impact of extraction and refining processes remains a critical concern, especially in the light of climate pathways such as the one in the NZE projections. A balance should be found between future advancements, economic viability with sustainability.

Henckens (2021) provides a comprehensive estimation of the extractable global resources, as shown in Table 18. These estimations suggest that while reserves of certain ETMs may be exhausted within a few decades, the total extractable resources could sustain society for centuries if technological and recycling advancements are realized. For example, nickel resources are projected to remain for more than 2000 years under 2050 projected demand, while the current reserves would already be depleted around 2044 (Figure 23). These projections underscore the importance of exploring new deposits and improving extraction technologies.

Table 18: Reserves as defined by USGS and literature, as well as total extractable global resources based on Henckens (2021). Only ETMs have been included that resources were provided for. Years to depletion is based on highest obtained 2050 value.

Unit: Mt	Reserves	Extractable Global Resources (Henckens, 2021)	Demand 2050 [Mt/year]	Years to Resource Depletion
Aluminium	30000	10000000	33.5	298960
Cadmium	66	40000	17.7	2260
Cobalt	11	3000	1.19	2521
Copper	1000	35131	45.501	772
Gallium	11	2000	0.01	200000
Germanium	1.19	200	0.0014	138889
Indium	0.312	30	0.002	14851
Lithium	28	2000	0.911	2195
Manganese	1900	100000	1.47	68027
Nickel	130	8000	6.197	1291
Platinum	0.071	3	0.0005	5769
REEs	110	20000	2.25	8875

Co-mining, in which an ETM is mined as a by-product of lesser value compared to its primary ore, adds complexity to resource and reserve estimates. Gallium is extracted as a byproduct of bauxite and zinc extraction. This interdependence can lead to supply bottlenecks if the production of the primary ore decreases. As a result, co-mining introduces an additional layer of uncertainty in resource estimation and necessitates more sophisticated modeling approaches. As new markets emerge, it may be found that these co-mined products eventually may become more valuable compared to their current primary ore, as has been the case before in lithium mining from iron (IEA, 2023e).

ARIMA has been used as the primary method for extrapolating production data, capturing historical trends to project future data points. Whilst effective in certain contexts, ARIMA has limitations, particularly in its inability to account for evolving geopolitical, environmental and economic drivers. One example being that lead times for mines have been increased over time according to S&P global (2023), which may have resulted in overexaggerated results. This limitation is particularly relevant in co-mined products, where production can be highly volatile and dependent on the production dynamics of other commodities.

To address these limitations, a multi-model approach should be employed, as demonstrated by Mutele & Carranza (2024), who utilized ARIMA, Vector Autoregressive (VAR) and Autoregressive Neural Network (ARNN) models. VAR are particularly useful for analyzing multivariate time series data, making them suitable for co-mined products especially. ARNN are specifically designed for time series data and can provide better estimate future data points based on fluctuations. Regardless, ARIMA remains a strong method for univariate data such as supply over time but incorporating a multi-model approach would further substantiate the obtained results.

In conclusion, improving the accuracy of reserve estimates and future projections requires access to more detailed, aggregated data on deposits and mining operations. The current lack of international reporting standards hampers these efforts. Therefore, establishing resilient and transparent supply chains for ETMs is imperative for sustainable resource management (Alonso et al., 2012).

7.3 EoL

EoL RIR indicators were derived from the UNEP (2011) analysis. Given that this data is over a decade old, there is uncertainty regarding how the recycling chain has developed. Linear interpolation was used to project the development over the investigated timespan. Nonetheless, this approach may not fully capture the nuances of recycling infrastructure evolution, particularly for materials which have surging demand post-2030. Even with limited outflow, it was assumed that recycling rates would develop, which typically evolves in response to the available stock. Moreover, it was assumed that the stock turnover was equal to the outflow.

Nonetheless, urban mining potential should not be neglected: it is found that electronic waste, while difficult to separate, has higher ETM yields (such as gallium, REEs, germanium) compared to that of natural ores (de Oliveira, 2021). UNEP (2011) acknowledges, when there is an economic incentive, recovery will happen, which is a possibility with the surging demand for ETMs. Complementary, the impacts of future primary extraction may far exceed the costs of recycling.

Recycling is not just a fallback option but a necessary component of a resilient supply chain. As has been shown in the results, it allows supply diversification, domestic production, and less import dependence on dominant suppliers. In the NZE projections, it is found that significant outflow of the in-use stock may occur as early as 2030. These outflow streams, including PMSMs from wind turbines with significant quantities of critical REEs, could be an even more significant source of ETMs in the future, and this extraction potential is only found to be increasing over time.

Nonetheless, several challenges remain. Battery-grade materials require stringent quality standards, and it is uncertain whether recycling can consistently recover these materials to be used in similar applications (Zeng et al., 2018). Nevertheless, other circular strategies could be investigated, i.e., the repurposing of LIB batteries in BESS applications. While not having the sufficient capacity for automotive applications, these could be repurposed for stationary applications, which would also slow down costs and accelerate BESS development, while also decreasing pressure on ETM supply chains (Colarullo & Thakur, 2022).

The effectiveness of recycling practices is affected by the design of the products themselves. Future policies will need to promote design for recycling, such as minimizing the use of difficult-to-separate metal alloys, or a threshold to the amount of primary material used in the production of the technology. A recent example is the EU's battery directive (2023/1542), which targets recovery, recycling efficiency and recycling content. For example, by the end of 2031, 95% of all copper used in batteries needs to be recovered and recycled. It should be made clear that perfect recycling does not exist: Henckens (2021) defines that copper dissipation currently reaches 2% (i.e., due to corrosion), something that only can be avoided by material substitution. This implies that primary extraction will be necessary even with recycling infrastructure in place.

The importance of recycling and recovery for the energy transition cannot be overstated. By reducing reliance on primary extraction, recycling can help stabilize the supply of critical ETMs, reduce environmental impacts associated with mining, and create a circular economy that supports sustainable development, while minimizing import dependence. It is found that efficient EoL practices have the potential to alleviate short- and long-term supply bottlenecks and criticality risks, although more effort must be made to enable this.

8. Conclusion

The global shift towards is driving a significant increase in demand for ETMs. Nonetheless, this demand is influenced not only by clean energy technologies but also the rapid growth of emerging sectors. It is essential to consider whether the NZE projections, aimed at limiting global warming to 1.5 °C, can be realized in light with growth trajectories in these other industries. Based on this study, ETM availability should not impede NZE projections, but careful resource management is crucial

Post-2050, after peak demand driven by major capacity additions from renewables, ETM demand will remain substantial, which can largely be attributed to stock turnover. Hydrogen and BESS are expected to grow even further. The growing needs of emerging industries will further stress supply chains. The analysis defines that certain ETMs used in thin-film PV are currently refined insufficient to meet NZE projections.

It was found that the accelerating adoption of EVs is not aligned with historic car sales trends, but future ETM demand will be highly affected by the dominant battery chemistry. Given the ethical concerns surrounding cobalt, it is likely that nickel- or manganese intensive chemistries will dominate the market. For BESS, critical ETM demand can be mitigated by the introduction of flow batteries, such as VRFBs.

While hydrogen production is expected to play a pivotal role in decarbonizing heavy industry, the prohibitive costs of PGMs necessitates material efficiency improvements to reduce reliance on iridium and minimize PGM use in electrolyzers and FCs. Recycling, especially the recovery of PGMs of catalytic converters, should be prioritized to alleviate supply bottlenecks.

Copper, a pivotal material in electrification, is extensively used across various applications, leading to significant supply bottlenecks. Given the importance of copper in infrastructure, improving material efficiency and exploring substitution options are essential. Nickel remains a challenging material to substitute due to its unique characteristics, underscoring the need for enhanced recycling practices to meet growing demand. Wind turbines, identified as valuable urban mines for nickel, REEs, copper and manganese, present an opportunity for supply diversification.

While current demand trajectories suggest that reserves of several ETMs may not be sufficient, it is uncertain how these reserves may expand in the future. The growing importance of ETMs will likely drive advances in extraction technologies, increased refining capacity and more resilient supply chains. Nonetheless, the environmental, social and economic impacts of expanded extraction and refining must be carefully monitored.

It is identified that data availability remains a core concern. The USGS provides limited and aggregated data on refined minerals, making it difficult to make accurate global estimates. Inconsistent international reporting standards further complicate long-term material projections. Additionally, the lack of transparency regarding ETM content in high-end applications and the uncertainty of future developments add to the complexity of forecasting ETM demand. On the demand side, it was found in literature that there was great difference in the scope and climate scenarios of long-term material demand analyses.

The analysis reveals that the yield of ETMs from EoL products is substantial, and for some ETMs, recycling yields could surpass those of primary extraction, for example for gallium and PGMs. As the outflow of clean energy technologies will increase over the coming decades, effective EoL practices will be pivotal in mitigating both short- and long-term supply bottlenecks. Although recycling for some ETMs is currently non-existent, the analysis highlights the importance of establishing efficient EoL practices to reduce import dependency and enhance supply diversification.

In conclusion, enabling NZE projections while ensuring long-term resource availability for future generations requires a multifaceted approach. This includes effective resource management, technological innovation and policy support. Only by addressing these challenges comprehensively sustainable resource management and resource availability can be assured for current and future generations.

9. Recommendations

Given the pivotal role of ETMs in the global energy transition, a multifaceted approach to ensure a resilient, secure, sustainable and ethically responsible supply chain. Policy makers must take a proactive stance by implementing a range of strategies that address both short-term and long-term challenges in ETM supply chains.

9.1 Policy recommendations

First, diversifying supply sources is essential to mitigate geopolitical risks associated with the centralization of extraction and refining. The EU should not only prioritize domestic extraction and refining but also the development of urban mining initiatives. On the short-term, outflow of electronic waste may prove to be a valuable source of ETMs, often having higher ETM yields compared to primary extraction. This will eventually decrease import dependency. For short-term supply bottlenecks, strategic reserves could be introduced to buffer against market disruptions and supply-demand gaps. Orchard & Son (2012) address that this is an effective policy measure, on the condition that the costs for storage are minimized, and that the reserves come at a fixed cost, making it easier to budget and plan their use.

While the EU's CRM directive and Battery directive, aimed at the year 2035, is a step in the right direction, it lacks a long-term perspective. This directive should continuously be developed to include long-term targets for domestic extraction, processing beyond 2035, ensuring alignment with the EU's 2050 climate goals to limit global warming to 1.5 °C. Additionally, the directive should incorporate stronger incentives for manufacturers to design technologies that are less reliant on ETMs or design it in a way that facilitates recycling. For example, policy measures could reward the development of alternative technologies that minimize ETM use or substitute with more abundant materials, such as the use of silicon in graphite anodes. For recycling this could be to promote extended producer responsibility (EPR), which ensures that manufacturers design their products with recyclability in mind. Tong et al. (2024) addresses that EPR is a necessity in acquiring long term sustainability and incentivizing sustainable production approaches.

The adoption of material passports is a promising strategy to increase transparency in the supply chain and raise consumer awareness of the environmental and ethical implications of a certain product. While already addressed in the building sector according to Cetin et al (2023), S&P Global (2024) that there is increased interest in clean energy technologies. This would empower consumers to make more informed and sustainable choices, potentially driving demand for products with lower ETM content and better sustainability considerations. The EU could introduce regulations mandating the use of material passports for certain high-impact products, like existing energy labelling.

Furthermore, this could also prove a valuable data source for effectively monitoring mineral supply chains across the globe. Unlike the US, the EU does not have a dedicated entity for the monitoring of mineral supply chains. Although initiatives like Mine4EU were intended to serve this role, the lack of active functioning highlights the need for a more robust and operational framework. Such an agency could provide comprehensive data on mineral resources, track global supply chains, and assess impacts of geopolitical developments. This in turn could help to inform policy makers on long-term sustainability from a European perspective.

9.2 Further research

Material analyses should adopt longer timeframes, as most current projections, such as those from the IEA, typically only extend to 2050. This limitation restricts the understanding of long-term resource availability, especially considering that IPCC climate scenarios often project until 2100 (and some even beyond). Although extending the timeframe introduces greater uncertainties, it also provides more comprehensive insights into the effects of additional technological cycles and the long-term sustainability of critical material supplies. In addition, the IEA's methodology could benefit from greater transparency and comprehensiveness. The key assumptions underlying important projections – such as market share and handling of stock turnover - remain uncertain. A clearer articulation of these factors would enhance the credibility and utility of such analyses, particularly for policymakers and stakeholders along the supply chain.

As innovative technologies emerge, their material requirements and environmental impacts require thorough examination. While many of this data is highly confidential, a comprehensive life cycle assessment of emerging ETM-intensive technologies could be done, to estimate their long-term sustainability. This includes evaluating the impact of extraction and refining, its criticality in the supply chain, feasibility of recycling and potential of material substitution. Given the major influence of geopolitical dynamics, this should be addressed complementarily. This includes analyzing the impact of trade policies, international agreements, and regional conflicts on the global distribution and pricing of ETMs. Furthermore, potential trade-offs by substitution should not be unaddressed. Understanding these dynamics, in combination with aggregated insights into its environmental impacts, can support in formulating strategies to mitigate risks and ensure a stable supply chain for essential ETMs.

While there have been significant advancements in material efficiency for some technologies, there is a surging need to place greater emphasis on efficient circular practices. For example, while the EU currently incentivizes the discovery of domestic ETM deposits, the yields and specific materials derived from these sources remain uncertain. In contrast, multiple studies (i.e., UNEP 2011; de Oliveira, 2021) have demonstrated that recycling is the most effective mechanism for increasing supply diversity, reducing import dependency, and ensuring resource availability at an affordable price for current and future generations. Focused research on the interplay between long-term resource availability and circular strategies would provide valuable insights. This makes even more sense as the outflow from automotive and electronics, and later clean energy technologies, become more abundant over the coming decades. This presents a unique opportunity to become market leader in efficient EoL practices in future sustainable supply chain of CRMs.

10. References

- Abuseada, M., & Fisher, T. S. (2023). Continuous solar-thermal methane pyrolysis for hydrogen and graphite production by roll-to-roll processing. *Applied Energy*, 352, 121872. <https://doi.org/10.1016/j.apenergy.2023.121872>
- Alhousni, F. K., Ismail, F. B., Okonkwo, P. C., Mohamed, H., Okonkwo, B. O., & Al-Shahri, O. A. (2022). A review of PV solar energy system operations and applications in Dhofar Oman. *AIMS Energy*, 10(4), 858–884. <https://doi.org/10.3934/energy.2022039>
- Alonso, E., Sherman, A. M., Wallington, T. J., Everson, M. P., Field, F. R., Roth, R., & Kirchain, R. E. (2012). Evaluating Rare Earth Element Availability: A Case with Revolutionary Demand from Clean Technologies. *Environmental Science & Technology*, 46(6), 3406–3414. <https://doi.org/10.1021/es203518d>
- Alves Dias, Patrícia & Bobba, Silvia & Carrara, Samuel & Plazzotta, Beatrice. (2021). THE ROLE OF RARE EARTH ELEMENTS IN WIND ENERGY AND ELECTRIC MOBILITY An analysis of future supply/demand balances. 10.2760/303258.
- Ansari, J. A., Malik, J. A., Ahmed, S., Manzoor, M., Ahemad, N., & Anwar, S. (2024). Recent advances in the therapeutic applications of selenium nanoparticles. *Molecular Biology Reports*, 51(1), 688. <https://doi.org/10.1007/s11033-024-09598-z>
- Azizman, M. S. A., Azhari, A. W., Halin, D. S. C., Ibrahim, N., Sepeai, S., Ludin, N. A., Nor, M. N. M., & Ho, L. N. (2023). Progress in tin-germanium perovskite solar cells: A review. *Synthetic Metals*, 299, 117475. <https://doi.org/10.1016/j.synthmet.2023.117475>
- Balaram, V. (2023). Potential Future Alternative Resources for Rare Earth Elements: Opportunities and Challenges. *Minerals*, 13(3), 425. <https://doi.org/10.3390/min13030425>
- Bandyopadhyay, S., & Nandan, B. (2023). A review on design of cathode, anode and solid electrolyte for true all-solid-state lithium sulfur batteries. *Materials Today Energy*, 31, 101201. <https://doi.org/10.1016/j.mtener.2022.101201>
- Barei, K., de la Rua, C., Mckl, M., & Hamacher, T. (2019). Life cycle assessment of hydrogen from proton exchange membrane water electrolysis in future energy systems. *Applied Energy*, 237, 862–872. <https://doi.org/10.1016/j.apenergy.2019.01.001>
- Barre, F. I., Billy, R. G., Lopez, F. A., & Mller, D. B. (2024). Limits to graphite supply in a transition to a post-fossil society. *Resources, Conservation and Recycling*, 208, 107709. <https://doi.org/10.1016/j.resconrec.2024.107709>
- Bilgin, B., Liang, J., Terzic, M. v., Dong, J., Rodriguez, R., Trickett, E., & Emadi, A. (2019). Modeling and Analysis of Electric Motors: State-of-the-Art Review. *IEEE Transactions on Transportation Electrification*, 5(3), 602–617. <https://doi.org/10.1109/TTE.2019.2931123>
- Boaretto, N., Garbayo, I., Valiyaveetil-SobhanRaj, S., Quintela, A., Li, C., Casas-Cabanas, M., & Aguesse, F. (2021). Lithium solid-state batteries: State-of-the-art and challenges for materials, interfaces and processing. *Journal of Power Sources*, 502, 229919. <https://doi.org/10.1016/j.jpowsour.2021.229919>
- Bonjakovi, Mladen & Santa, Robert & Crnac, Zoran & Bonjakovi, Tomislav. (2023). Environmental Impact of Pv Power Systems. 10.20944/preprints202306.1734.v1.
- Bruce, P. G., Freunberger, S. A., Hardwick, L. J., & Tarascon, J.-M. (2012). Li-O₂ and Li-S batteries with high energy storage. *Nature Materials*, 11(1), 19–29. <https://doi.org/10.1038/nmat3191>
- California Energy Commission. (2024). *Pilot Scale Recovery of Lithium from Geothermal Brines (CEC-500-2024-020)*. <https://www.energy.ca.gov/sites/default/files/2024-03/CEC-500-2024-020.pdf>
- Calvo, G., Mudd, G., Valero, A., & Valero, A. (2016). Decreasing Ore Grades in Global Metallic Mining: A Theoretical Issue or a Global Reality? *Resources*, 5(4), 36. <https://doi.org/10.3390/resources5040036>
- Carrara, S., Bobba, S., Blagoeva, D., Alves Dias, P., Cavalli, A., Georgitzikis, K., Grohol, M., Itul, A., Kuzov, T., Latunussa, C., Lyons, L., Malano, G., Maury, T., Prior Arce, A., Somers, J., Telsnig, T., Veeh, C., Wittmer, D., Black, C., Pennington, D., Christou, M., Supply chain analysis and material demand forecast in strategic technologies and sectors in the EU – A foresight study, Publications Office of the European Union, Luxembourg, 2023, doi:10.2760/386650, JRC132889.

- Castillo-Villagra, R., & Thoben, K.-D. (2022). Towards Supply Chain Resilience in Mining Industry: A Literature Analysis (pp. 92–103). https://doi.org/10.1007/978-3-031-05359-7_8
- Cavaliere, P. (2023). Fundamentals of Water Electrolysis. In *Water Electrolysis for Hydrogen Production* (pp. 1–60). Springer International Publishing. https://doi.org/10.1007/978-3-031-37780-8_1
- Çetin, S., Raghu, D., Honic, M., Straub, A., & Gruis, V. (2023). Data requirements and availabilities for material passports: A digitally enabled framework for improving the circularity of existing buildings. *Sustainable Production and Consumption*, 40, 422–437. <https://doi.org/10.1016/j.spc.2023.07.011>
- Chehreh Chelgani, S., Rudolph, M., Kratzsch, R., Sandmann, D., & Gutzmer, J. (2016). A Review of Graphite Beneficiation Techniques. *Mineral Processing and Extractive Metallurgy Review*, 37(1), 58–68. <https://doi.org/10.1080/08827508.2015.1115992>
- Chen, Y., Kang, Y., Zhao, Y., Wang, L., Liu, J., Li, Y., Liang, Z., He, X., Li, X., Tavajohi, N., & Li, B. (2021). A review of lithium-ion battery safety concerns: The issues, strategies, and testing standards. *Journal of Energy Chemistry*, 59, 83–99. <https://doi.org/10.1016/j.jechem.2020.10.017>
- Cheng, D., & Gao, Y. (2024). A critical review on the fracture of ultra-thin photovoltaics silicon wafers. *Solar Energy Materials and Solar Cells*, 274, 112999. <https://doi.org/10.1016/j.solmat.2024.112999>
- Choi, C., Kim, S., Kim, R., Choi, Y., Kim, S., Jung, H., Yang, J. H., & Kim, H.-T. (2017). A review of vanadium electrolytes for vanadium redox flow batteries. *Renewable and Sustainable Energy Reviews*, 69, 263–274. <https://doi.org/10.1016/j.rser.2016.11.188>
- Colarullo, L., & Thakur, J. (2022). Second-life EV batteries for stationary storage applications in Local Energy Communities. *Renewable and Sustainable Energy Reviews*, 169, 112913. <https://doi.org/10.1016/j.rser.2022.112913>
- Cusenza, M. A., Bobba, S., Ardente, F., Cellura, M., & di Persio, F. (2019). Energy and environmental assessment of a traction lithium-ion battery pack for plug-in hybrid electric vehicles. *Journal of Cleaner Production*, 215, 634–649. <https://doi.org/10.1016/j.jclepro.2019.01.056>
- Dalvi, A. D., Bacon, W. G., & Osborne, R. C. (2004). The past and the future of nickel laterites. PDAC International Convention, Trade Show & Investors Exchange.
- de Almeida, A., & Greenberg, S. (2004). Electric Motors. In *Encyclopedia of Energy* (pp. 191–201). Elsevier. <https://doi.org/10.1016/B0-12-176480-X/00096-6>
- de Oliveira, R. P., Benvenuti, J., & Espinosa, D. C. R. (2021). A review of the current progress in recycling technologies for gallium and rare earth elements from light-emitting diodes. *Renewable and Sustainable Energy Reviews*, 145, 111090. <https://doi.org/10.1016/j.rser.2021.111090>
- Deetman, S., de Boer, H. S., van Engelenburg, M., van der Voet, E., & van Vuuren, D. P. (2021). Projected material requirements for the global electricity infrastructure – generation, transmission and storage. *Resources, Conservation and Recycling*, 164, 105200. <https://doi.org/10.1016/j.resconrec.2020.105200>
- Derwent, R., Simmonds, P., O'Doherty, S., Manning, A., Collins, W., & Stevenson, D. (2006). Global environmental impacts of the hydrogen economy. *International Journal of Nuclear Hydrogen Production and Applications*, 1(1), 57. <https://doi.org/10.1504/IJNHPA.2006.009869>
- Desalegn, B., Gebeyehu, D., Tamrat, B., Tadiwose, T., & Lata, A. (2023). Onshore versus offshore wind power trends and recent study practices in modeling of wind turbines' life-cycle impact assessments. *Cleaner Engineering and Technology*, 17, 100691. <https://doi.org/10.1016/j.clet.2023.100691>
- Devashish, & Thakur, A. (2017). A comprehensive review on wind energy system for electric power generation: Current situation and improved technologies to realize future development. *International Journal of Renewable Energy Research*, 7(4),
- Dincer, I., & AlZahrani, A. A. (2018). 4.25 Electrolyzers. In *Comprehensive Energy Systems* (pp. 985–1025). Elsevier. <https://doi.org/10.1016/B978-0-12-809597-3.00442-9>
- Dunn, J. B., Gaines, L., Kelly, J. C., James, C., & Gallagher, K. G. (2015). The significance of Li-ion batteries in electric vehicle life-cycle energy and emissions and recycling's role in its reduction. *Energy & Environmental Science*, 8(1), 158–168. <https://doi.org/10.1039/C4EE03029J>
- El-Shafie, M. (2023). Hydrogen production by water electrolysis technologies: A review. *Results in Engineering*, 20, 101426. <https://doi.org/10.1016/j.rineng.2023.101426>
- European Commission, Study on the Critical Raw Materials for the EU 2023 – Final Report

- Fan, L., Tu, Z., & Chan, S. H. (2021). Recent development of hydrogen and fuel cell technologies: A review. *Energy Reports*, 7, 8421–8446. <https://doi.org/10.1016/j.egy.2021.08.003>
- Fujita, Y., McCall, S. K., & Ginosar, D. (2022). Recycling rare earths: Perspectives and recent advances. *MRS Bulletin*, 47(3), 283–288. <https://doi.org/10.1557/s43577-022-00301-w>
- Gielen, D. (2021), Critical minerals for the energy transition, International Renewable Energy Agency, Abu Dhabi.
- Giurco, D., Dominish, E., Florin, N., Watari, T., & McLellan, B. (2019). Requirements for Minerals and Metals for 100% Renewable Scenarios. In *Achieving the Paris Climate Agreement Goals* (pp. 437–457). Springer International Publishing. https://doi.org/10.1007/978-3-030-05843-2_11
- Goodenough, J. B., & Kim, Y. (2010). Challenges for rechargeable Li batteries. *Chemistry of Materials*, 22(3), 587–603. Link Nitta, N., Wu, F., Lee, J. T., & Yushin, G. (2015). Li-ion battery materials: present and future. *Materials Today*, 18(5), 252–264.
- Greenwald, J. E., Zhao, M., & Wicks, D. A. (2024). Critical mineral demands may limit scaling of green hydrogen production. *Frontiers in Geochemistry*, 1. <https://doi.org/10.3389/fgeoc.2023.1328384>
- Grilli, M. L., Slobozeanu, A. E., Larosa, C., Paneva, D., Yakoumis, I., & Cherkezova-Zheleva, Z. (2023). Platinum Group Metals: Green Recovery from Spent Auto-Catalysts and Reuse in New Catalysts—A Review. *Crystals*, 13(4), 550. <https://doi.org/10.3390/cryst13040550>
- Henckens, M. L. C. M., & Worrell, E. (2020). Reviewing the availability of copper and nickel for future generations. The balance between production growth, sustainability, and recycling rates. *Journal of Cleaner Production*, 264, 121460. <https://doi.org/10.1016/j.jclepro.2020.121460>
- Henckens, M. L. C. M., van Ierland, E. C., Driessen, P. P. J., & Worrell, E. (2016). Mineral resources: Geological scarcity, market price trends, and future generations. *Resources Policy*, 49, 102–111. <https://doi.org/10.1016/j.resourpol.2016.04.012>
- Henckens, T. (2021). Scarce mineral resources: Extraction, consumption and limits of sustainability. *Resources, Conservation and Recycling*, 169, 105511. <https://doi.org/10.1016/j.resconrec.2021.105511>
- Hernández-Callejo, L., Gallardo-Saavedra, S., & Alonso-Gómez, V. (2019). A review of photovoltaic systems: Design, operation and maintenance. *Solar Energy*, 188, 426–440. <https://doi.org/10.1016/j.solener.2019.06.017>
- Hodson, T. O. (2022). Root-mean-square error (RMSE) or mean absolute error (MAE): when to use them or not. *Geoscientific Model Development*, 15(14), 5481–5487. <https://doi.org/10.5194/gmd-15-5481-2022>
- Hoekstra (NEON Research). (2023, July 24). *Copper scarcity will not materially slow down the energy transition*. <https://neonresearch.nl/copper-scarcity-will-not-materially-slow-down-the-energy-transition/>
- Hughes, A. E., Haque, N., Northey, S. A., & Giddey, S. (2021). Platinum Group Metals: A Review of Resources, Production and Usage with a Focus on Catalysts. *Resources*, 10(9), 93. <https://doi.org/10.3390/resources10090093>
- Hyndman, R.J., & Athanasopoulos, G. (2018) *Forecasting: principles and practice*, 2nd edition, OTexts: Melbourne, Australia. [OTexts.com/fpp2](https://otexts.com/fpp2).
- IEA (2022), *Global Hydrogen Review 2022*, IEA, Paris <https://www.iea.org/reports/global-hydrogen-review-2022>, Licence: CC BY 4.0
- IEA (2023a), *Net Zero Roadmap: A Global Pathway to Keep the 1.5 °C Goal in Reach*, IEA, Paris <https://www.iea.org/reports/net-zero-roadmap-a-global-pathway-to-keep-the-15-oc-goal-in-reach>, Licence: CC BY 4.0
- IEA (2023b), *Electricity Grids and Secure Energy Transitions*, IEA, Paris <https://www.iea.org/reports/electricity-grids-and-secure-energy-transitions>, Licence: CC BY 4.0
- IEA (2023c), *World Energy Outlook 2023*, IEA, Paris <https://www.iea.org/reports/world-energy-outlook-2023>, Licence: CC BY 4.0 (report); CC BY NC SA 4.0 (Annex A)
- IEA (2023d), *Global Energy and Climate Model*, IEA, Paris <https://www.iea.org/reports/global-energy-and-climate-model>, Licence: CC BY 4.0

- IEA (2023e), *Global Hydrogen Review 2023*, IEA, Paris <https://www.iea.org/reports/global-hydrogen-review-2023>, Licence: CC BY 4.0
- IEA (2024a), *Global Critical Minerals Outlook 2024*, IEA, Paris <https://www.iea.org/reports/global-critical-minerals-outlook-2024>, Licence: CC BY 4.0
- IEA (2024b), *Global EV Outlook 2024*, IEA, Paris <https://www.iea.org/reports/global-ev-outlook-2024>, Licence: CC BY 4.0
- IPCC, 2022: Annex II: Glossary [Möller, V., R. van Diemen, J.B.R. Matthews, C. Méndez, S. Semenov, J.S. Fuglestvedt, A. Reisinger (eds.)]. In: *Climate Change 2022: Impacts, Adaptation and Vulnerability*. Contribution of Working Group II to the Sixth Assessment Report of the Intergovernmental Panel on Climate Change [H.-O. Pörtner, D.C. Roberts, M. Tignor, E.S. Poloczanska, K. Mintenbeck, A. Alegría, M. Craig, S. Langsdorf, S. Lösschke, V. Möller, A. Okem, B. Rama (eds.)]. Cambridge University Press, Cambridge, UK and New York, NY, USA, pp. 2897–2930, doi:10.1017/9781009325844.029.
- IRENA (2020), *Green Hydrogen Cost Reduction: Scaling up Electrolysers to Meet the 1.5°C Climate Goal*, International Renewable Energy Agency, Abu Dhabi.
- Isabel M. Prata, M. (2012). Gallium–68: A New Trend in PET Radiopharmacy. *Current Radiopharmaceuticalse*, 5(2), 142–149. <https://doi.org/10.2174/1874471011205020142>
- Itani, K., & de Bernardinis, A. (2023). Review on New-Generation Batteries Technologies: Trends and Future Directions. *Energies*, 16(22), 7530. <https://doi.org/10.3390/en16227530>
- Janek, J., & Zeier, W. G. (2016). A solid future for battery development. *Nature Energy*, 1(9), 16141. <https://doi.org/10.1038/nenergy.2016.141>
- Jordens, A., Cheng, Y. P., & Waters, K. E. (2013). A review of the beneficiation of rare earth element bearing minerals. *Minerals Engineering*, 41, 97–114. <https://doi.org/10.1016/j.mineng.2012.10.017>
- Junne, T., Wulff, N., Breyer, C., & Naegler, T. (2020). Critical materials in global low-carbon energy scenarios: The case for neodymium, dysprosium, lithium, and cobalt. *Energy*, 211, 118532. <https://doi.org/10.1016/j.energy.2020.118532>
- Kgoete, F. M., Uyor, U. O., Popoola, A. P., & Popoola, O. (2024). Insight on the recent materials advances for manufacturing of high-voltage transmission conductors. *The International Journal of Advanced Manufacturing Technology*, 130(9–10), 4123–4136. <https://doi.org/10.1007/s00170-023-12890-0>
- Kim, H.-J., Krishna, T., Zeb, K., Rajangam, V., Gopi, C. V. V. M., Sambasivam, S., Raghavendra, K. V. G., & Obaidat, I. M. (2020). A Comprehensive Review of Li-Ion Battery Materials and Their Recycling Techniques. *Electronics*, 9(7), 1161. <https://doi.org/10.3390/electronics9071161>
- Li, P., Kim, H., Myung, S.-T., & Sun, Y.-K. (2021). Diverting Exploration of Silicon Anode into Practical Way: A Review Focused on Silicon-Graphite Composite for Lithium Ion Batteries. *Energy Storage Materials*, 35, 550–576. <https://doi.org/10.1016/j.ensm.2020.11.028>
- Li, Z., Qiu, F., Tian, Q., Yue, X., & Zhang, T. (2022). Production and recovery of tellurium from metallurgical intermediates and electronic waste—A comprehensive review. *Journal of Cleaner Production*, 366, 132796. <https://doi.org/10.1016/j.jclepro.2022.132796>
- Liang, Y., Kleijn, R., & van der Voet, E. (2023). Increase in demand for critical materials under IEA Net-Zero emission by 2050 scenario. *Applied Energy*, 346, 121400. <https://doi.org/10.1016/j.apenergy.2023.121400>
- Liu, S.-L., Fan, H.-R., Liu, X., Meng, J., Butcher, A. R., Yann, L., Yang, K.-F., & Li, X.-C. (2023). Global rare earth elements projects: New developments and supply chains. *Ore Geology Reviews*, 157, 105428. <https://doi.org/10.1016/j.oregeorev.2023.105428>
- Liu, T., Vivek, J. P., Zhao, E. W., Lei, J., Garcia-Araez, N., & Grey, C. P. (2020). Current Challenges and Routes Forward for Nonaqueous Lithium–Air Batteries. *Chemical Reviews*, 120(14), 6558–6625. <https://doi.org/10.1021/acs.chemrev.9b00545>
- Lokanc, M., Eggert, R., & Redlinger, M. (2015). *The Availability of Indium: The Present, Medium Term, and Long Term*. <https://doi.org/10.2172/1327212>

- Lourenssen, K., Williams, J., Ahmadpour, F., Clemmer, R., & Tasnim, S. (2019). Vanadium redox flow batteries: A comprehensive review. *Journal of Energy Storage*, 25, 100844. <https://doi.org/10.1016/j.est.2019.100844>
- Lu, F., Xiao, T., Lin, J., Ning, Z., Long, Q., Xiao, L., Huang, F., Wang, W., Xiao, Q., Lan, X., & Chen, H. (2017). Resources and extraction of gallium: A review. *Hydrometallurgy*, 174, 105–115. <https://doi.org/10.1016/j.hydromet.2017.10.010>
- Luboń, W., Pełka, G., Marszałek, K., & Małek, A. (2017). Performance Analysis of Crystalline Silicon and CIGS Photovoltaic Modules in Outdoor Measurement. *Ecological Chemistry and Engineering S*, 24(4), 539–549. <https://doi.org/10.1515/eces-2017-0035>
- Mishra, G., Jha, R., Meshram, A., & Singh, K. K. (2022). A review on recycling of lithium-ion batteries to recover critical metals. *Journal of Environmental Chemical Engineering*, 10(6), 108534. <https://doi.org/10.1016/j.jece.2022.108534>
- Mo, S., Du, L., Huang, Z., Chen, J., Zhou, Y., Wu, P., Meng, L., Wang, N., Xing, L., Zhao, M., Yang, Y., Tang, J., Zou, Y., & Ye, S. (2023). Recent Advances on PEM Fuel Cells: From Key Materials to Membrane Electrode Assembly. *Electrochemical Energy Reviews*, 6(1), 28. <https://doi.org/10.1007/s41918-023-00190-w>
- Moats, M., Alagha, L., & Awuah-Offei, K. (2021). Towards resilient and sustainable supply of critical elements from the copper supply chain: A review. *Journal of Cleaner Production*, 307, 127207. <https://doi.org/10.1016/j.jclepro.2021.127207>
- Modaresi, R., Pauliuk, S., Løvik, A. N., & Müller, D. B. (2014). Global Carbon Benefits of Material Substitution in Passenger Cars until 2050 and the Impact on the Steel and Aluminum Industries. *Environmental Science & Technology*, 48(18), 10776–10784. <https://doi.org/10.1021/es502930w>
- Mutele, L., & Carranza, E. J. M. (2024). Statistical analysis of gold production in South Africa using ARIMA, VAR and ARNN modelling techniques: Extrapolating future gold production, Resources – Reserves depletion, and Implication on South Africa’s gold exploration. *Resources Policy*, 93, 105076. <https://doi.org/10.1016/j.resourpol.2024.105076>
- Nitta, N., Wu, F., Lee, J. T., & Yushin, G. (2015). Li-ion battery materials: present and future. *Materials Today*, 18(5), 252–264.
- O’Connor, D., & Hou, D. (2021). Manage the environmental risks of perovskites. *One Earth*, 4(11), 1534–1537. <https://doi.org/10.1016/j.oneear.2021.11.002>
- Oliveira Filho, H. R., Zanin, H., Monteiro, R. S., Barbosa, M. H. P., & Teófilo, R. F. (2024). High-nickel cathodes for lithium-ion batteries: From synthesis to electricity. *Journal of Energy Storage*, 82, 110536. <https://doi.org/10.1016/j.est.2024.110536>
- Mgaya, J. F. (2019). Application of ARIMA models in forecasting livestock products consumption in Tanzania. *Cogent Food & Agriculture*, 5(1), 1607430. <https://doi.org/10.1080/23311932.2019.1607430>
- Olivetti, E. A., Ceder, G., Gaustad, G. G., & Fu, X. (2017). Lithium-Ion Battery Supply Chain Considerations: Analysis of Potential Bottlenecks in Critical Metals. *Joule*, 1(2), 229–243. <https://doi.org/10.1016/j.joule.2017.08.019>
- Pan, Y., & Gu, D. (2016). Superconducting Wind Turbine Generators. *Transactions on Environment and Electrical Engineering*, 1(3), 9–15. <https://doi.org/10.22149/tee.v1i3.19>
- Patel, M., & Karamalidis, A. K. (2021). Germanium: A review of its US demand, uses, resources, chemistry, and separation technologies. *Separation and Purification Technology*, 275, 118981. <https://doi.org/10.1016/j.seppur.2021.118981>
- Prabhakaran, S. (2023, May 15). ARIMA Model – Complete Guide to Time Series Forecasting in Python. *Machine Learning Plus*. <https://www.machinelearningplus.com/time-series/arima-model-time-series-forecasting>
- Preet, S., & Smith, S. T. (2024). A comprehensive review on the recycling technology of silicon based photovoltaic solar panels: Challenges and future outlook. *Journal of Cleaner Production*, 448, 141661. <https://doi.org/10.1016/j.jclepro.2024.141661>
- R. Firschnknect, R. Itten, P. Sinha, M. de Wild-Scholten, J. Zhang, V. Fthenakis, H. C. Kim, M. Raugel, M. Stucki, 2015, Life Cycle Inventories and Life Cycle Assessment of Photovoltaic Systems, International Energy Agency (IEA) PVPS Task 12, Report T12-04:2015

- Rachidi, N. R., Nwaila, G. T., Zhang, S. E., Bourdeau, J. E., & Ghorbani, Y. (2021). Assessing cobalt supply sustainability through production forecasting and implications for green energy policies. *Resources Policy*, 74, 102423. <https://doi.org/10.1016/j.resourpol.2021.102423>
- Rimpas, D., Kaminaris, S. D., Piromalis, D. D., Vokas, G., Arvanitis, K. G., & Karavas, C.-S. (2023). Comparative Review of Motor Technologies for Electric Vehicles Powered by a Hybrid Energy Storage System Based on Multi-Criteria Analysis. *Energies*, 16(6), 2555. <https://doi.org/10.3390/en16062555>
- Rizwan, M., Alstad, V., & Jäschke, J. (2021). Design considerations for industrial water electrolyzer plants. *International Journal of Hydrogen Energy*, 46(75), 37120–37136. <https://doi.org/10.1016/j.ijhydene.2021.09.018>
- S&P Global Market Intelligence. (2023, June 21). Average lead time almost 18 years for mines started in 2020–23. S&P Global Market Intelligence. <https://www.spglobal.com/marketintelligence/en/news-insights/research/average-lead-time-almost-18-years-for-mines-started-in-2020-23>
- Saadat, S., Hussain, I., & Faisal, M. (2021). Modeling and forecasting of principal minerals production. *Arabian Journal of Geosciences*, 14(9), 797. <https://doi.org/10.1007/s12517-021-07135-x>
- Shah, N., Shah, A. A., Leung, P. K., Khan, S., Sun, K., Zhu, X., & Liao, Q. (2023). A Review of Third Generation Solar Cells. *Processes*, 11(6), 1852. <https://doi.org/10.3390/pr11061852>
- Shaked, D., & Holdengreber, E. (2022). Efficiency Improvement of an Electric-Grid Transformer Using the Diamagnetism Characteristics of a Bulk Superconductor. *Energies*, 15(19), 7146. <https://doi.org/10.3390/en15197146>
- Son, Y.S., Orchard, R.K. (2013). *Effectiveness of Policy for mitigating supply disruptions* [PDF]. MacEwan University Repository. <https://roam.macewan.ca:8443/server/api/core/bitstreams/66f4ad33-68fb-4258-87bo-9e35756bae33/content>
- Sreevalsan-Nair, J. (2023). *Normal Distribution* (pp. 999–1002). https://doi.org/10.1007/978-3-030-85040-1_228
- Stavrakakis, G. S. (2012). Electrical Parts of Wind Turbines. In *Comprehensive Renewable Energy* (pp. 269–328). Elsevier. <https://doi.org/10.1016/B978-0-08-087872-0.00211-0>
- Sverdrup, H. U., van Allen, O., & Haraldsson, H. V. (2024). Modeling Indium Extraction, Supply, Price, Use and Recycling 1930–2200 Using the WORLD7 Model: Implication for the Imaginaries of Sustainable Europe 2050. *Natural Resources Research*, 33(2), 539–570. <https://doi.org/10.1007/s11053-023-10296-z>
- The Institute of Electrical and Electronics Engineers, IEEE (2007), Std 575, IEEE Guide for the Application of Sheath-Bonding Methods for Single-Conductor Cables and the Calculation of Induced Voltages and Currents in Cable Sheaths.
- Tolcin, A. C. (2012). Indium. U.S. Geological Survey Minerals Yearbook. <https://www.usgs.gov/publications/mineral-resource-month-indium>
- Tong, X., Wang, T., Li, J., & Wang, X. (2024). Extended producer responsibility to reconstruct the circular value chain. *Circular Economy*, 3(1), 100076. <https://doi.org/10.1016/j.cec.2024.100076>
- Tost, M., Murguia, D., Hitch, M., Lutter, S., Luckeneder, S., Feiel, S., & Moser, P. (2020). Ecosystem services costs of metal mining and pressures on biomes. *The Extractive Industries and Society*, 7(1), 79–86. <https://doi.org/10.1016/j.exis.2019.11.013>
- Tsiropoulos, I., Tarvydas, D., Lebedeva, N., Li-ion batteries for mobility and stationary storage applications – Scenarios for costs and market growth, EUR 29440 EN, Publications Office of the European Union, Luxembourg, 2018, ISBN 978-92-79-97254-6, doi:10.2760/87175, JRC113360
- U.S. Geological Survey (USGS). (n.d.).** Historical statistics (Data Series 140). U.S. Department of the Interior. Retrieved from <https://www.usgs.gov/centers/national-minerals-information-center/historical-statistics-mineral-and-material-commodities>
- U.S. Geological Survey (USGS).** Mineral commodity summaries 2024. (2024). <https://doi.org/10.3133/mcs2024>
- UNEP (2011) Recycling Rates of Metals – A Status Report. A Report of the Working Group on the Global Metal Flows to the International Resource Panel. Graedel, T.E.; Allwood, J; Birat, J; P, J.P; Reck, B.K; Sibley, S.F; Sonneman, G; Buchert, M; Hagelücken, C.

- United States Geographical Survey, USGS. *Mineral commodity summaries 2024*. (2024). <https://doi.org/10.3133/mcs2023>
- Usman, Z., Tah, J., Abanda, H., & Nche, C. (2020). A Critical Appraisal of PV-Systems' Performance. *Buildings*, 10(11), 192. <https://doi.org/10.3390/buildings10110192>
- van de Kaa, G., van Ek, M., Kamp, L. M., & Rezaei, J. (2020). Wind turbine technology battles: Gearbox versus direct drive - opening up the black box of technology characteristics. *Technological Forecasting and Social Change*, 153, 119933. <https://doi.org/10.1016/j.techfore.2020.119933>
- Vikström, H., Davidsson, S., & Höök, M. (2013). Lithium availability and future production outlooks. *Applied Energy*, 110, 252-266.
- Wang, H., Chai, L., Xie, Z., & Zhang, H. (2020). Recent Advance of Tellurium for Biomedical Applications. *Chemical Research in Chinese Universities*, 36(4), 551-559. <https://doi.org/10.1007/s40242-020-0193-0>
- Watari, T., McLellan, B. C., Giurco, D., Dominish, E., Yamasue, E., & Nansai, K. (2019). Total material requirement for the global energy transition to 2050: A focus on transport and electricity. *Resources, Conservation and Recycling*, 148, 91-103. <https://doi.org/10.1016/j.resconrec.2019.05.015>
- Watari, T., Nansai, K., & Nakajima, K. (2020). Review of critical metal dynamics to 2050 for 48 elements. *Resources, Conservation and Recycling*, 155, 104669. <https://doi.org/10.1016/j.resconrec.2019.104669>
- Widmer, J. D., Martin, R., & Kimiabeigi, M. (2015). Electric vehicle traction motors without rare earth magnets. *Sustainable Materials and Technologies*, 3, 7-13. <https://doi.org/10.1016/j.susmat.2015.02.001>
- Yazdani-Asrami, M., Fang, L., Pei, X., & Song, W. (2023). Smart fault detection of HTS coils using artificial intelligence techniques for large-scale superconducting electric transport applications. *Superconductor Science and Technology*, 36(8), 085021. <https://doi.org/10.1088/1361-6668/ace3fb>
- Zapp, P., Schreiber, A., Marx, J., & Kuckshinrichs, W. (2022). Environmental impacts of rare earth production. *MRS Bulletin*, 47(3), 267-275. <https://doi.org/10.1557/s43577-022-00286-6>
- Zeng, A., Chen, W., Rasmussen, K. D., Zhu, X., Lundhaug, M., Müller, D. B., Tan, J., Keiding, J. K., Liu, L., Dai, T., Wang, A., & Liu, G. (2022). Battery technology and recycling alone will not save the electric mobility transition from future cobalt shortages. *Nature Communications*, 13(1), 1341. <https://doi.org/10.1038/s41467-022-29022-z>
- Zeng, X., Li, J., & Singh, N. (2014). Recycling of Spent Lithium-Ion Battery: A Critical Review. *Critical Reviews in Environmental Science and Technology*, 44(10), 1129-1165. <https://doi.org/10.1080/10643389.2013.763578>
- Zhao, X., Ding, M., Sun, H., & Long, S. (2021). *Controlling distinct phases of gallium oxide for solar-blind photodetector application* (pp. 101-151). <https://doi.org/10.1016/bs.semsem.2021.04.003>
- Zhong, Y., Zhang, J., Wu, S., Jia, L., Yang, X., Liu, Y., Zhang, Y., & Sun, Q. (2022). A review on the GaN-on-Si power electronic devices. *Fundamental Research*, 2(3), 462-475. <https://doi.org/10.1016/j.fmre.2021.11.0>

Supplementary Document

For all data involving the computations done in this research, please consult the provided datasheet.

S.1 Compound Annual Growth Rate

The fundament of this research is found in the scenario projections by the IEA, which include aggregated data on two modelled scenarios (NZE & STEPS) for the clean energy technologies investigated. Energy data on capacity, electricity production and total final consumption were provided over a 5-year interval.

To transform the data, values were interpolated using the compound annual growth rate (CAGR), which is computed as follows:

$$CAGR_{i,t} = \left(\frac{ED_{i,target\ yr}}{ED_{i,baseline\ yr}} \right)^{\frac{1}{target\ yr - baseline\ yr}} - 1 \quad (1)$$

In which $ED_{i,yr\ t}$ is the energy data for technology i in year t . The interpolated energy data for year t was then calculated by:

$$ED_{i,yr\ t} = ED_{i,baseline\ yr} * (1 + CAGR)^{target\ yr - baseline\ yr} \quad (2)$$

Finally, the annual additions to the energy system for each technology i was determined by:

$$\Delta Cap_{i,t} = Cap_{i,t} - Cap_{i,t-1} \quad (3)$$

The CAGR provides a stable measure of growth over time, accommodating fluctuations, and is commonly used in LTES (Bogdanov et al., 2021, IEA 2023a).

S.2 Rare Earth Elements abundancy and conversion factor

Table 19: REE in the first 5 km of the Earth's crust based on Taylor, Earlam and Seethamaram (2024)

Rare Earth Element	Oxide	Conversion factor to metal
Yttrium	Y ₂ O ₃	1.2699
Lanthanum	La ₂ O ₃	1.1728
Praseodymium	Pr ₂ O ₃	1.1703
Neodymium	Nd ₂ O ₃	1.1664
Terbium	Tb ₂ O ₃	1.151
Dyprosium	Dy ₂ O ₃	1.1477

S.3 Survival Functions

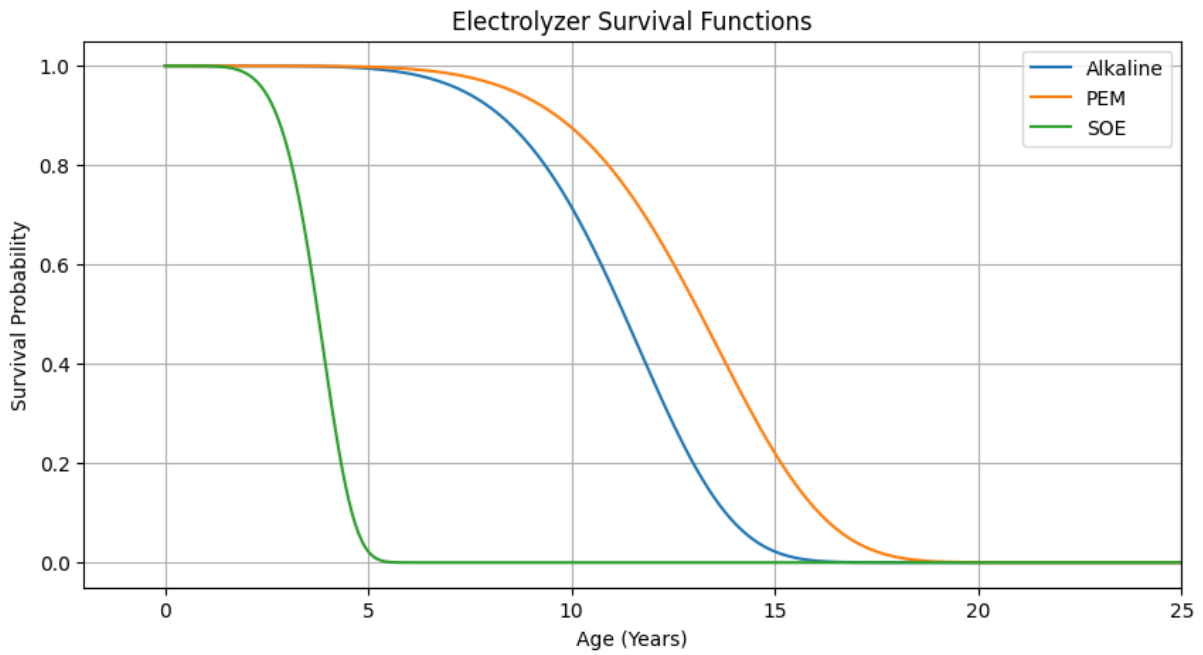


Figure 34: Weibull survival function Electrolyzers, based on a scale parameter of 6.2 and a lifetime of 12, 14 and 4 years for Alkaline, PEM and SOE, based on Gielen (2019).

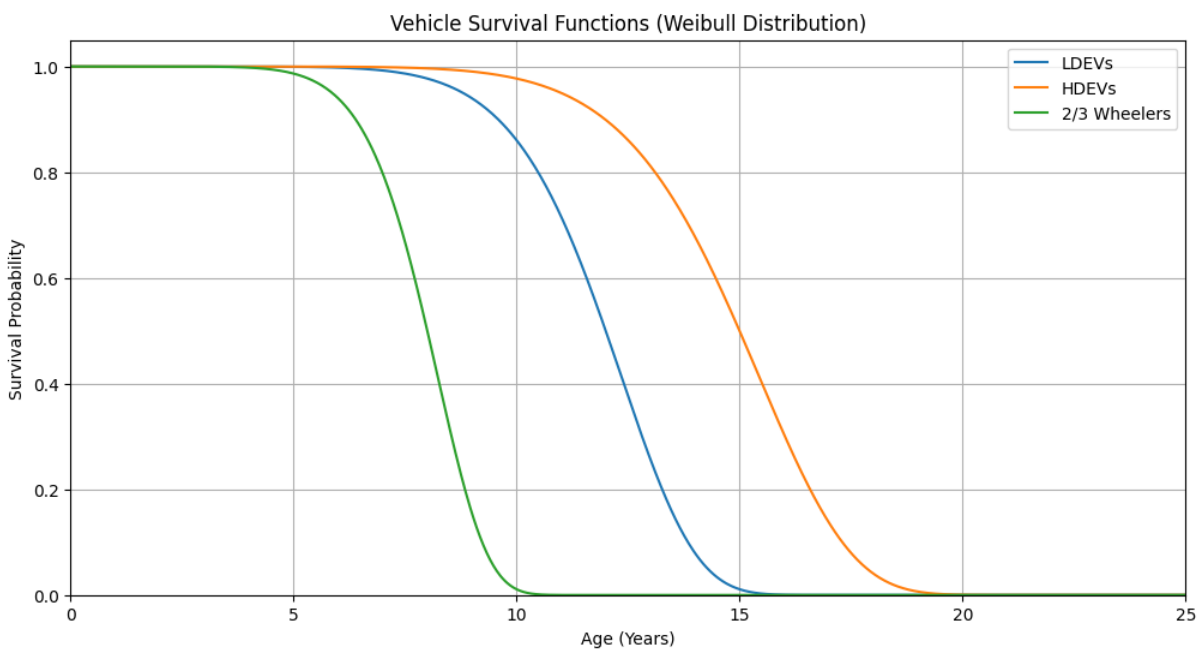


Figure 35: Weibull survival function based on a shape parameter of 8.4, based on Junne et al. (2020) with scale parameter of 12, 15 and 8 years for LDEVs, HDEVs and 2/3 wheelers respectively.

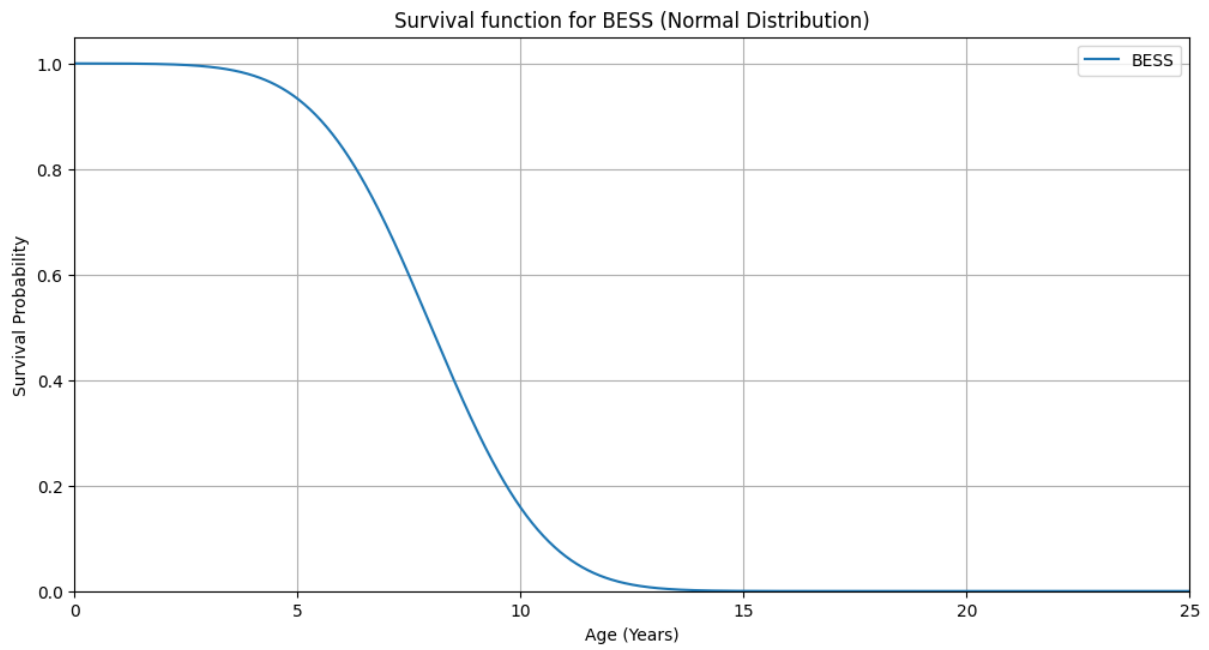


Figure 36: Normal distribution survival function for BESS applications based on 8 years lifetime, based on Junne et al. (2020)

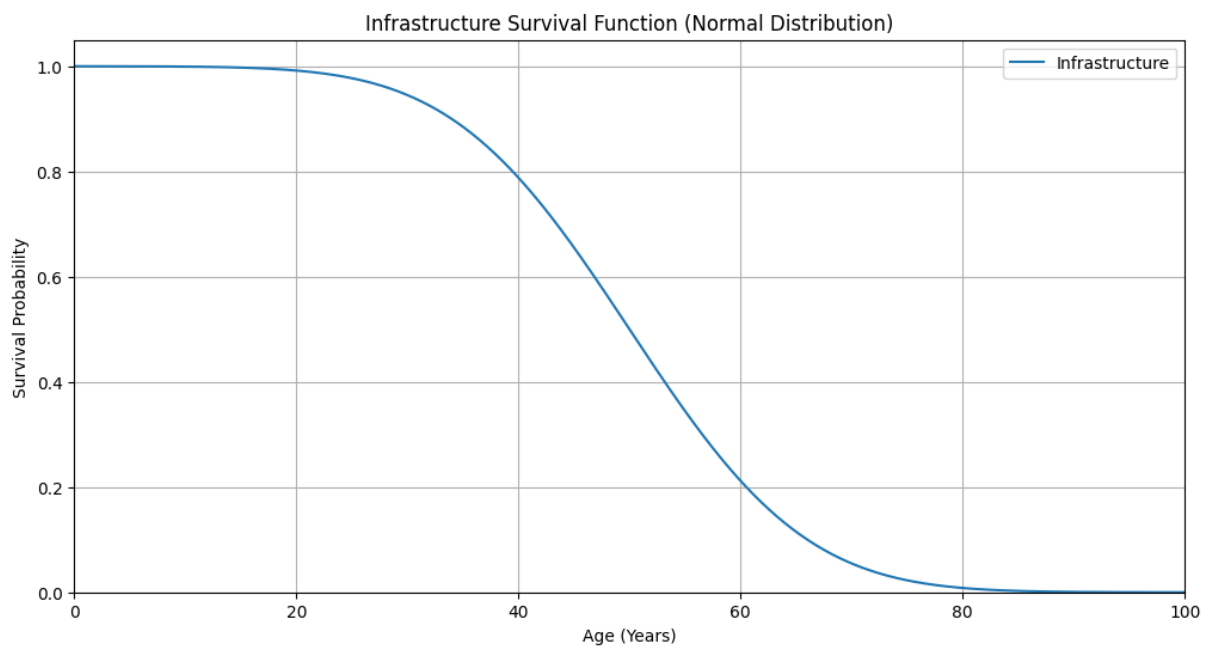


Figure 37: Normal distribution survival function for infrastructure based on a lifetime of 50 years IEA (2022b).

S.4 ARIMA Model

Defining ARIMA Parameters

The values of p, d and q were found based on statistical analysis. The d parameter ensured that the time series data was stationary — a prerequisite for dependable ARIMA forecasting. Stationarity is assessed using the Augmented Dickey-Fuller (ADF) test, which checks for a unit root in the data. The dataset can be defined stationary if the p value is less than 0.05, allowing to reject the null hypothesis that a unit root was present.

If the time series is found to be non-stationary, differencing was performed:

$$Y'_t = Y_t - Y_{t-1} \quad (1, \text{Mgaya, 2019})$$

where Y'_t is the differenced series, Y_t is the original series, and Y_{t-1} is the lagged series.

A second differentiation was applied whenever the p-value, after the first differentiation, still exceeded the confidence interval. This was done with a logarithmic differentiation (Eq. 2), which can be denoted as:

$$\Delta \log Y_t = \log(Y_t) - \log(Y_{t-1}) \quad (2, \text{Hyndman \& Athanaspoulos, 2018})$$

If only the first differentiation was performed, $d = 1$; if the logarithmic differentiation was performed as well, $d = 2$.

Utilizing a combination of these transformations allowed ARIMA to better capture underlying patterns and provide more exact forecasts. ARIMA captured the proportional changes rather than the absolute changes, leading to more reliable predictions.

Once stationarity is achieved, the next step is to define the (p) and (q) parameters using the Autocorrelation Function (ACF, Eq. 4) and Partial Autocorrelation Function (PACF, Eq. 5). The ACF (Eq. 4) measures the correlation between Y_t and Y_{t-k} over the pairs in the dataset, while the PACF assesses the linear correlation between (Y_t) and (Y_{t-k}), controlling for intermediate lags. The values for (p) and (q) are visually determined from the point where the ACF and PACF values are within the upper confidence interval.

$$ACF = \frac{\sum(Y_t - \mu)(Y_{t-k} - \mu)}{\sum(Y_t - \mu)^2} = \frac{\text{Covariance}(Y_t, Y_{t-k})}{\text{Variance}(Y_t)}$$

$$PACF = \frac{\text{Covariance}\left(Y_t, \frac{Y_t Y_{t-2}}{Y_{t-1}}\right)}{\sqrt{\left(\frac{\text{Variance } Y_t}{Y_{t-1}}\right)\left(\frac{\text{Variance } Y_{t-2}}{Y_{t-1}}\right)}} \quad (4 \& 5, \text{Mgaya, 2019})$$

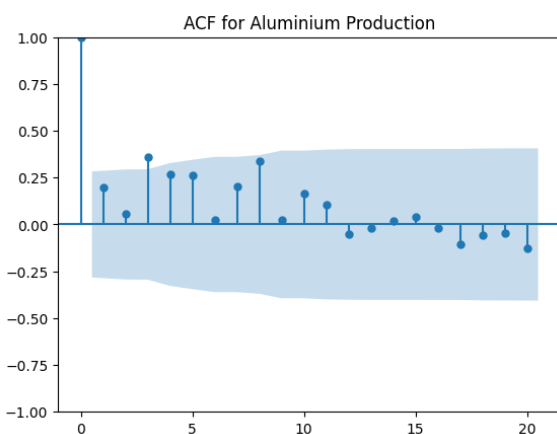


Figure 38: Autocorrelation function

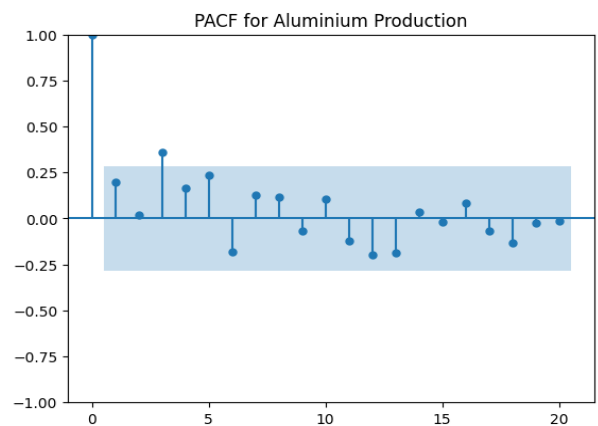


Figure 39: Partial Autocorrelation function

Model output

ARIMA will provide, based on the defined parameters, the extrapolated production data from 2023-2075. The model will also provide both a higher and a lower confidence interval. The lower confidence interval was set to the last point in the dataset to avoid negative values. The output will be used to plot against the computed demand scenarios for NZE and STEPS for the investigated commodities in the final supply demand analysis. Moreover, it will be defined whether current reserves are sufficient to cover this extrapolated production.

Table 20: ARIMA Parameters

	DF (1)	p-value (1)	DF (2)	p-value (2)	log_dif DF	p_value (3)	RMSE	ARIMA	unit
Aluminium production	2.82	1	-5.51	0.0000019	x	x	2261	(2,1,2)	(kt)
Copper mining	1.93	0.99	-0.05	0.95	-7.7	8.85E-12	1336	(1,2,1)	(kt)
Lithium refining	-2.4	0.13	1.74	0.99	-5.8	4.23E-07	12.2	(1,2,1)	(kt)
Lithium mining	0.25	0.97	-1.31	0.61	-3.6	0.004	65.5	(1,2,1)	(kt)
Cobalt refining	3.5	1	0.43	0.98	-3.3	0.014	7.4	(2,2,2)	(kt)
Cobalt mining	3.6	1	-4.4	0.003	-6.99	7.4E-10	9.9	(1,2,1)	(kt)
Nickel refining	0.78	0.99	0.78	0.99	-5.49	0.00002	157.2	(1,2,1)	(kt)
Nickel mining	3.57	1	-1.33	0.61	-4.87	0.000038	209	(1,2,1)	(kt)
Gallium	4.8	1	-0.46	0.89	-7.71	1.23E-07	58.1	(1,2,1)	(t)
Germanium	-1.63	0.43	-5.85	0.000000343	-	-	23.3	(1,2,1)	(t)
Graphite	-0.96	0.77	-1.3	0.5677	-6.25	4.3E-08	171.1	(1,2,1)	(kt)
Indium	0.88	0.99	-1.2	0.123	-6.04	1.34E-07	44.4	(1,2,1)	(t)
Cadmium	-1.53	0.51	-9.6	1.24	-	-	2884	(2,1,2)	(t)
PGMs	-1.3	0.62	-10.6	3.9E-19	-	-	36.3	(2,1,2)	(t)
Manganese	0.12	0.96	-1.23	0.89	-7.3	1.23E-10	2046	(1,2,1)	(kt)
REEs	4.25	1	-0.6	0.86	-6.8	2.32E-09	13.1	(1,2,1)	(kt)
Tellurium	-1.81	0.355	-1.1	0.7	-4.7	0.00059	37.2	(1,2,1)	(kt)
Selenium	0.37	0.98	-8.81	1.9E-14	-	-	290.2	(1,1,1)	(t)

S.5 Market shares for technologies

Table 21: PV market shares based on IEA (2022f).

Year	c-Si	Cd Te	CIGS	a-si	GaAas
2021	95%	2%	2%	0.30%	0%
2030	95%	4%	1%	0.30%	1%
2040	91%	4%	1%	0.30%	4.5%
2050	85%	4%	0.30%	0.30%	10%

Table 22: Wind configuration market share based on Carrara et al. (2020) & Liang et al. (2023).

Year	GB-SCIG		GB-DFIG		GB-PSMG		DD-PSMG		DD-EESG	
	On	Off								
2022	7%	NA	54%	NA	12%	10%	17%	80%	10%	10%
2030	8%	NA	52%	NA	14%	10%	20%	80%	6%	10%
2040	9%	NA	45%	NA	19%	5%	26%	85%	1%	10%
2050	10%	NA	41%	NA	21%	5%	28%	80%	0%	5%

Table 23: Electrolyzer share, based on IEA (2022h).

	Alkaline	PEM	SOFC
2022	69%	30%	1%
2030	64%	35%	1%
2040	60%	40%	1%
2050	50%	50%	0%

Table 24: Battery chemistry based on Xu et al. (2020) and own assumptions.

		NCA	NCM111	NCM532	NCM622	NCM811	LFP
2022	LFP	8%	7%	19%	19%	19%	27%
	NMCx	8%	7%	19%	19%	19%	27%
2030	LFP	7%	1%	3%	3%	19%	61%
	NMCx	7%	6%	20%	10%	47%	10%
2040	LFP	4%	2%	2%	6%	23%	63%
	NMCx	0%	4%	4%	10%	72%	10%
2050	LFP	0%	0%	2%	2%	31%	65%
	NMCx	0%	0%	0%	6%	89%	5%

Table 25: BESS chemistry shares based on Tsiropoulos et al. (2018) and own assumption.

Market Share	2010		2020		2030		2050	
	Li-ion	Flow	Li-ion	Flow	Li-ion	Flow	Li-ion	Flow
NCA	10%		10%	10%	0%	0%	0%	0%
NCM111	40%		15%	10%	0%	0%	0%	0%
NCM532	0%		5%	5%	0%	0%	0%	0%
NCM622	0%		5%	5%	0%	5%	0%	0%
NCM811	0%		0%	15%	15%	30%	0%	35%
LFP	50%		65%	55%	70%	45%	65%	30%
ASSB	0%		0%	0%	15%	0%	35%	0%
VRFB	0%		0%	0%	0%	20%	0%	35%

S.6 Recycling Scenarios

Table 26: Current Recycling Rates and Scenarios based on UNEP (2011) and European Commission (2023)

ETM	Current EoL RIR	Low Recycling Scenario	High Recycling Scenario	Source
Aluminum	32%	52%	95%	
Cadmium	25%	45%	85%	
Cobalt	22%	40%	95%	
Copper	55%	75%	95%	UNEP (2011)
Gallium	0%	16%	80%	
Germanium	0%	16%	80%	
Graphite	3%	23%	85%	European Commission (2023)
Indium	0%	16%	80%	UNEP (2011)
Lithium	1%	35%	85%	
Manganese	9%	30%	85%	
Nickel	18%	40%	95%	
PGMs	12%	32%	95%	
REEs	0%	21%	80%	
Selenium	0%	16%	80%	
Silicon	0%	16%	80%	European Commission (2023)
Tellurium	0%	16%	80%	UNEP (2011)

S.7 ETM demand for selected years

Table 27: Primary ETM demand, without recycling, for selected years under NZE projections for PV, in kt/year

kt/year	2035	2050	2060	2075
Aluminium	8468.8	8546.2	6034.4	4315.7
Cadmium	0.99	0.94	0.57	0.39
Copper	2599.3	2589.2	1834.4	1297.1
Gallium	12.01	12.24	7.33	5.07
Germanium	0.10	0.08	0.04	0.03
Indium	0.15	1.91	1.35	0.96
Selenium	0.12	0.10	0.03	0.02
Silicon	3359.3	2197.6	1209.7	837.3
Tellurium	1.11	0.94	0.53	0.38

Table 28: Primary ETM demand, without recycling, for selected years under NZE projections for wind, in kt/year

kt/year	2035	2050	2060	2075
Copper	934.4	1119.3	840.6	496.5
Dyprosium	3.13	2.69	1.53	0.87
Manganese	305.0	340.4	271.3	126.3
Neodymium	28.6	35.5	13.1	7.4
Nickel	139.6	147.1	115.6	50.2
Praseodymium	5.09	6.43	2.02	1.08
Terbium	1.17	1.58	0.60	0.34

Table 29: Primary ETM demand, without recycling, for selected years under NZE projections for EVs, for a LFP dominant market and a NMC dominant market, in kt/year

EV	2035	2050	2060	2075
Aluminium Li-ion	4109.5	13014.6	11144.6	7001.7
Aluminium NMCx	11199.3	35222.6	30160.8	18946.6
Cobalt Li-ion	165.6	418.6	357.1	289.4
Cobalt NMCx	462.5	1102.8	940.8	762.4
Copper Li-ion	3317.3	9727.9	8298.9	6725.6
Copper NMCx	2294.7	6300.9	5375.3	4356.3
Graphite Li-ion	1393.6	4042.7	3449.0	2795.2
Graphite NMCx	2294.7	6300.9	5375.3	4356.3
Lithium Li-ion	454.7	1293.3	1103.3	894.1
Lithium NMCx	520.8	1262.0	1076.6	872.5
Manganese Li-ion	163.8	469.3	400.4	324.5
Manganese NMCx	22.2	227.1	288.8	162.2
Nickel Li-ion	988.5	3026.1	2581.6	2092.2
Nickel NMCx	2422.0	8459.0	7216.4	5848.3

Table 30: Primary ETM demand for electric motors under NZE projections, in t/year

ETM	2035	2050	2060	2075
Dyprosium	14.2	27.9	26.7	19.4
Neodymium	41.4	81.7	78.0	56.7
Praseodymium	12.7	25.0	23.8	17.3
Terbium	1.7	3.4	3.3	2.4

Table 31: Primary ETM demand for BESS applications under NZE projections for a LFP- and Flow-dominant market, in kt/year

ETM	2035	2050	2060	2075
Aluminium Li-ion	3128.5	1976.8	994.6	1257.4
Aluminium Flow	2675.7	1522.3	679.6	724.7
Copper Li-ion	1087.7	697.4	600.9	859.8
Copper Flow	863.6	505.6	407.3	339.9
Cobalt Li-ion	15.5	0.0	0.0	0.0
Cobalt Flow	42.8	28.4	28.7	47.0
Graphite Li-ion	999.0	609.4	497.0	668.7
Graphite Flow	949.1	609.4	497.0	389.8
Lithium Li-ion	85.1	64.2	56.4	85.3
Lithium Flow	110.2	60.9	50.1	68.3
Manganese Li-ion	34.0	157.1	104.7	158.4
Manganese Flow	34.0	21.2	21.4	35.3
Nickel Li-ion	98.7	0.0	0.0	0.0
Nickel Flow	34.0	181.5	183.2	302.5

Table 32: Primary ETM demand for hydrogen technologies for selected years under NZE projections, in t/year. Iridium, yttrium and lanthanum were assumed to be eliminated in future electrolyzer types and have been excluded.

	2035	2050	2060	2075
PGMs Fuel cell	43.14	806.88	790.18	632.38
PGMs Electrolyzers	9.06	19.39	23.98	27.88

Table 33: Primary ETM demand for infrastructure for selected years under NZE projections, in t/year

	2035	2050	2060	2075
Aluminium	7540.3	9823.5	5407.4	6792.5
Copper	13072.7	14349.3	9070.3	9933.3

S.8 Supply Demand Analysis

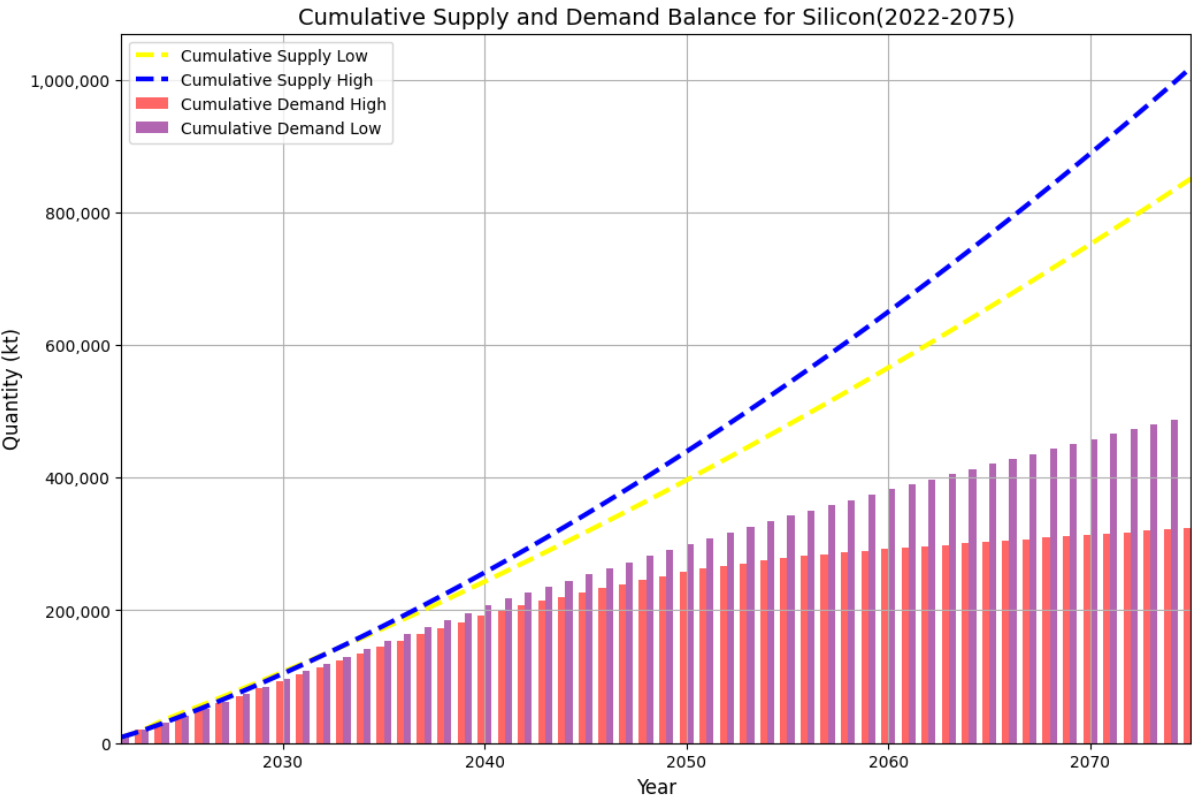


Figure 40: Cumulative Demand for and Supply for silicon mining under NZE projections, 2022-2075.

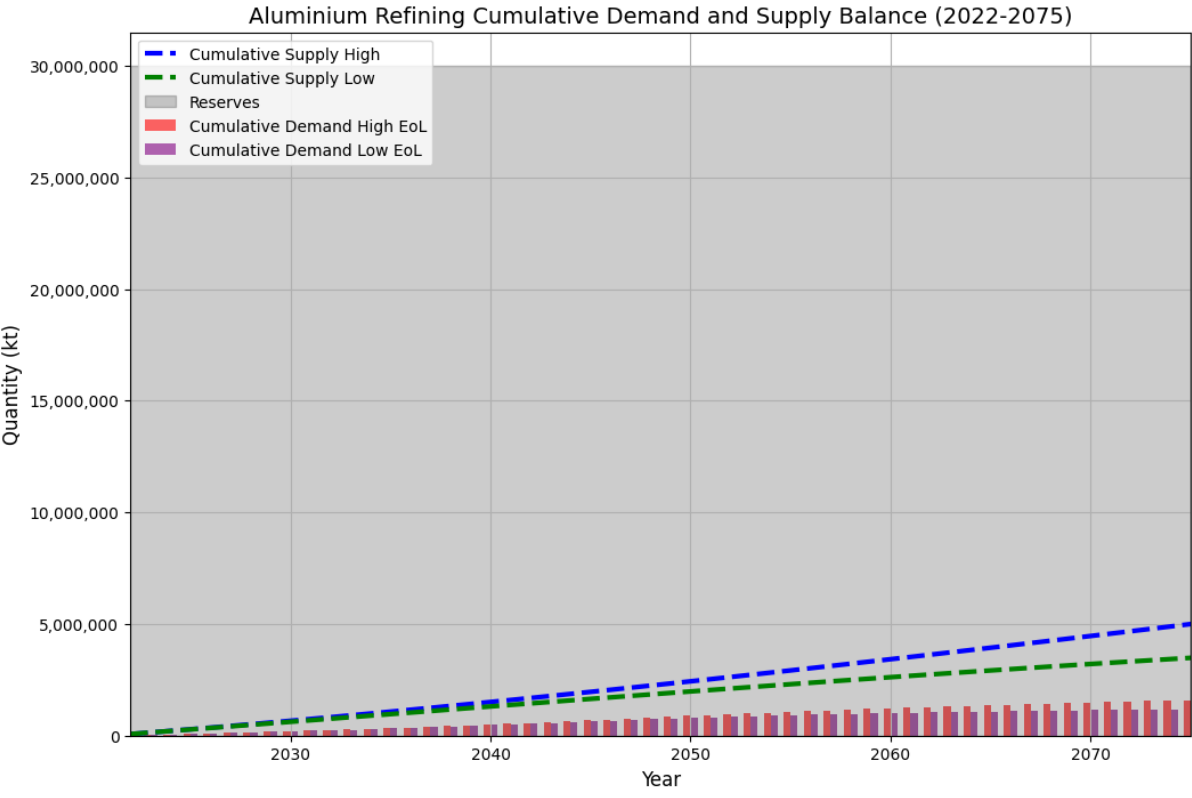


Figure 41: Cumulative Demand for and Supply for aluminium refining under NZE projections, 2022-2075.

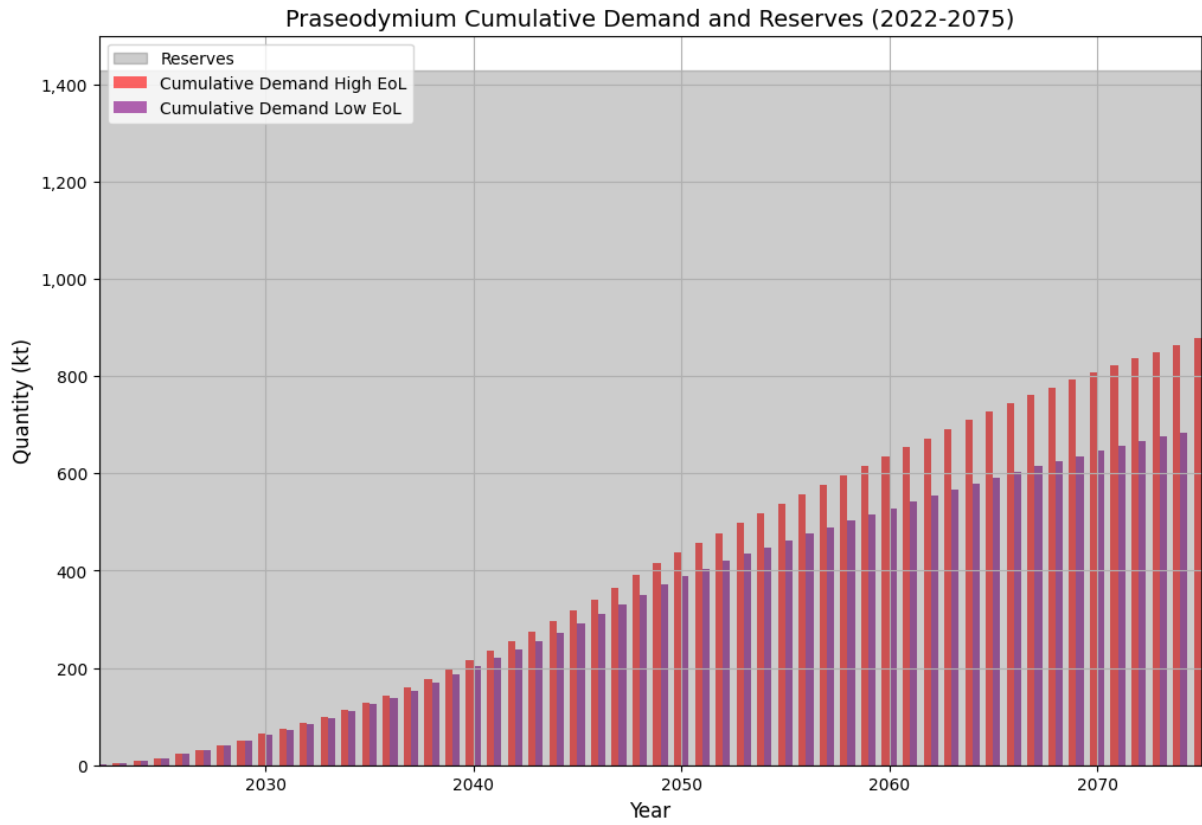


Figure 42: Cumulative Demand for praseodymium under NZE projections 2022-2075, in kt.

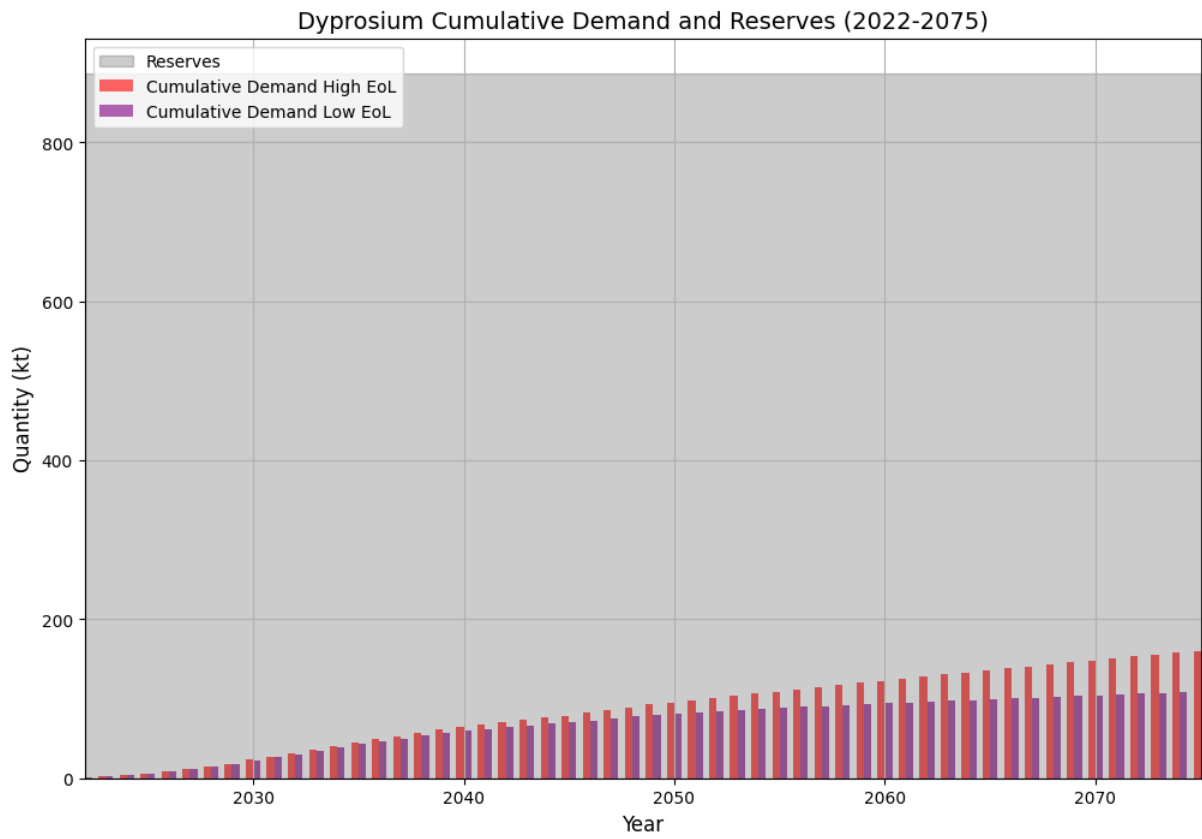


Figure 43: Cumulative Demand for dyprosium under NZE projections 2022-2075, in kt.

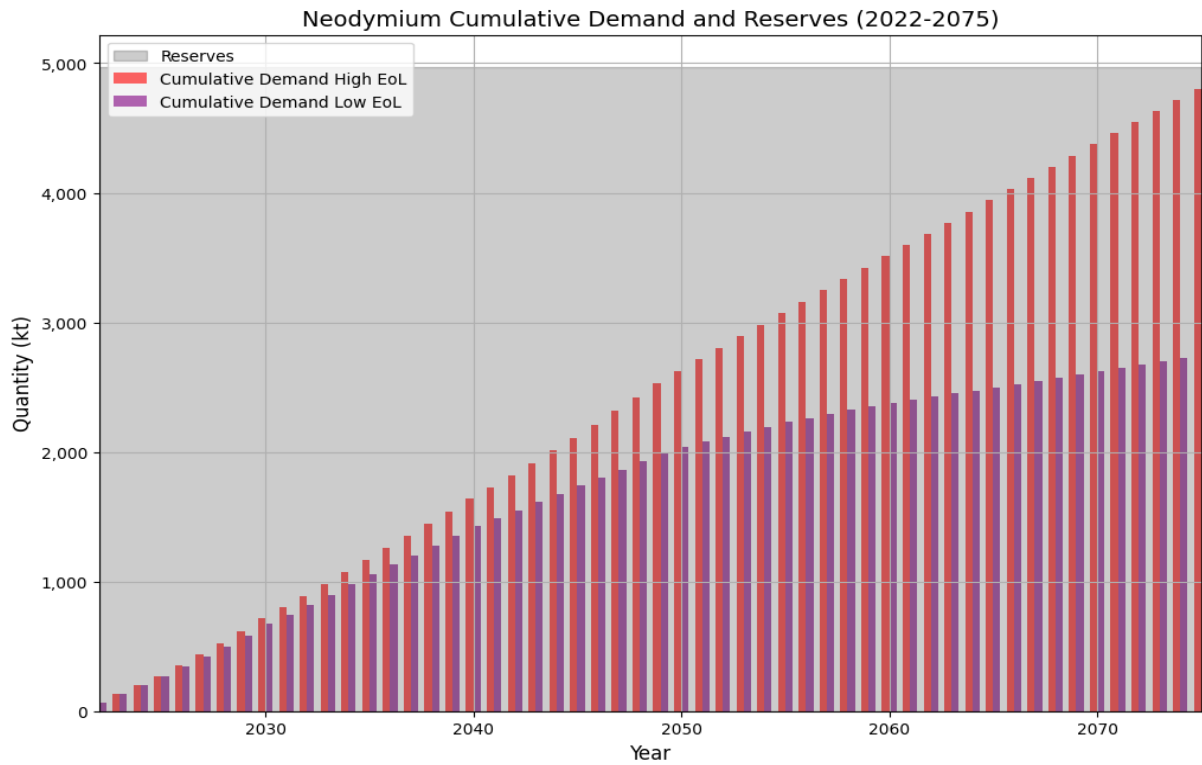


Figure 44: Cumulative Demand for neodymium under NZE projections 2022-2075, in kt.

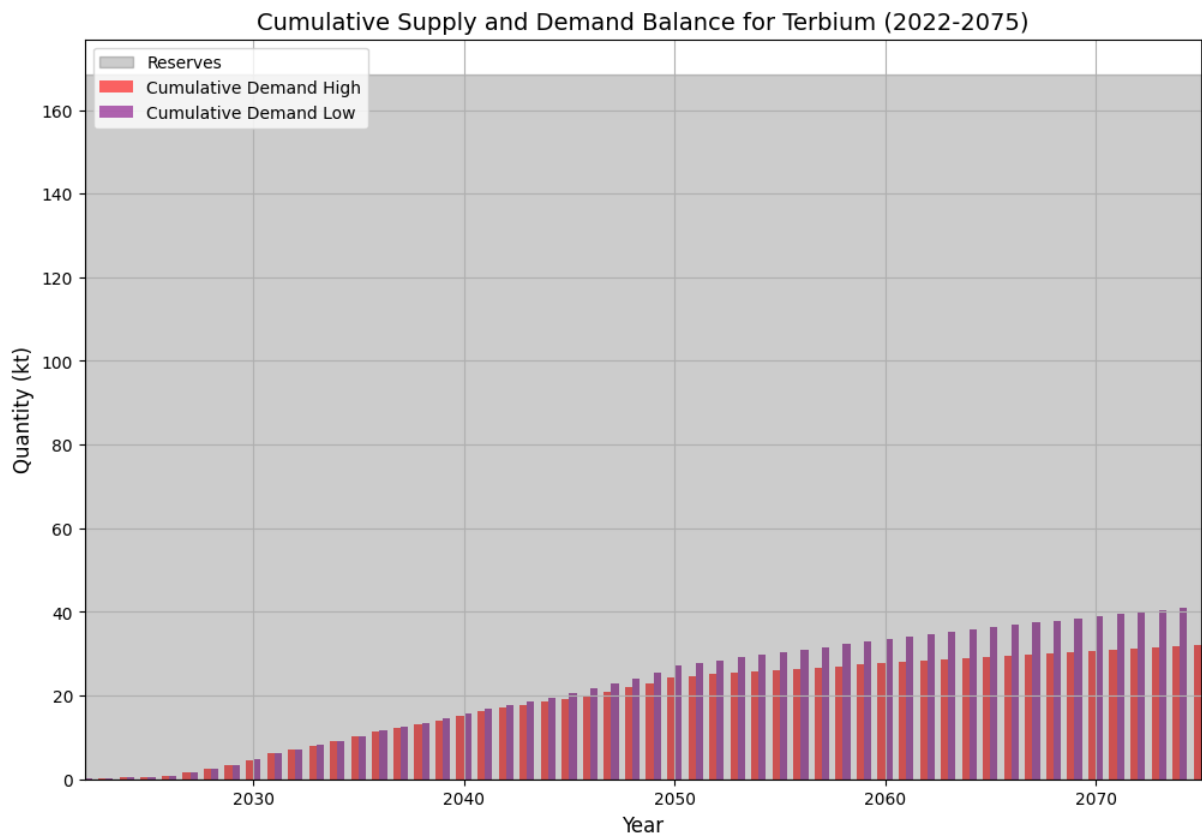


Figure 45: Cumulative Demand for terbium under NZE projections 2022-2075, in kt.

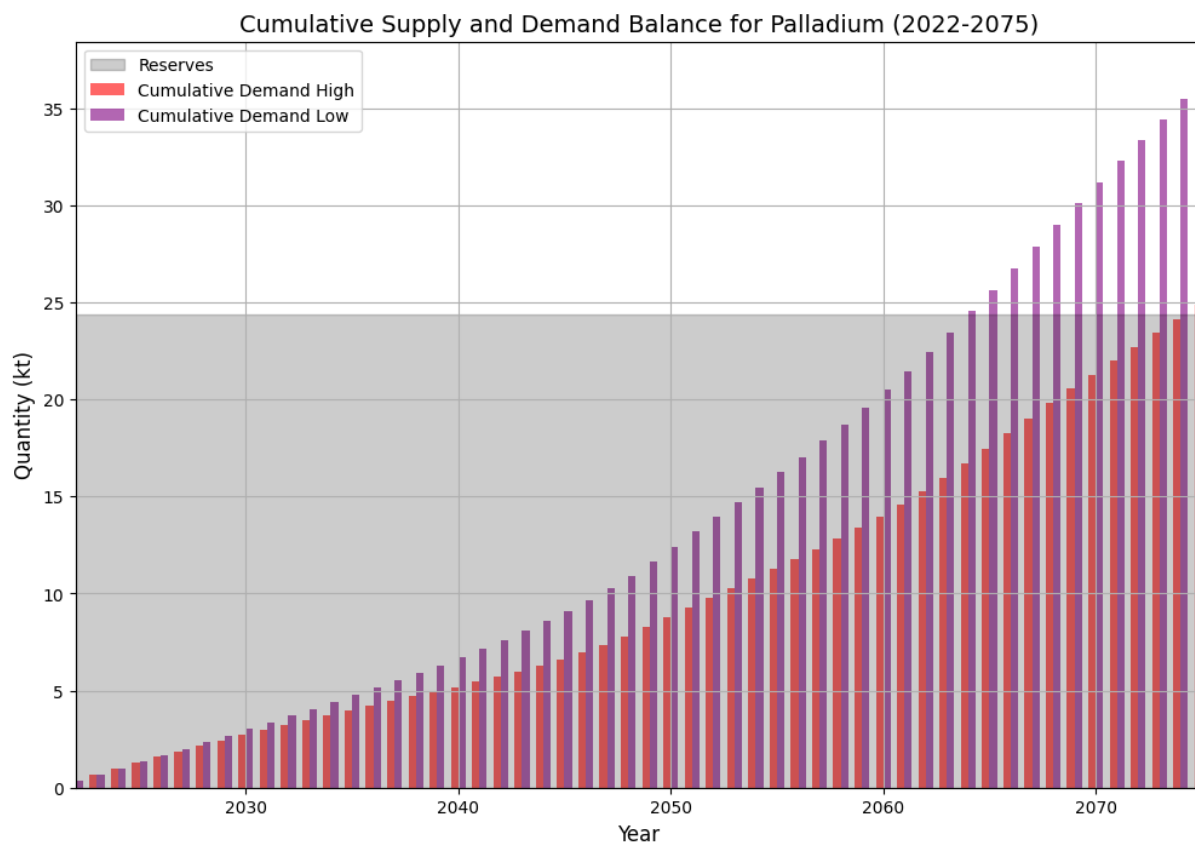


Figure 46: Cumulative supply and demand for palladium under NZE projections 2022-2075, in kt.